Bio-engineering of porcine lacrimal gland tissue with secretory capacity

Inaugural-Dissertation

zur Erlangung des Doktorgrades
der Mathematisch-Naturwissenschaftlichen Fakultät
der Heinrich-Heine-Universität Düsseldorf

vorgelegt von

Dr. med. Kristina Spaniol
aus Münster

Düsseldorf, April 2017

aus dem Institut für Experimentelle Ophthalmologie der Augenklinik
der Heinrich-Heine-Universität Düsseldorf

Gedruckt mit der Genehmigung der
Mathematisch-Naturwissenschaftlichen Fakultät der
Heinrich-Heine-Universität Düsseldorf

Referent: Prof. Dr. Gerd Geerling

Koreferent: Prof. Dr. Ulrich Rüther

Tag der mündlichen Prüfung: 11.09.2017

Parts of this work were published previously by the author (Spaniol et al., 2015).

Danksagung

Mein Dank gilt Herrn Prof. Dr. Gerd Geerling und Herrn Prof. Dr. Stefan Schrader für die Möglichkeit dieses spannende Projekt durchzuführen und für die Unterstützung auf dem Weg zum Ziel.

Ein großer Dank auch Herrn Prof. Dr. Ulrich Rüther für die Betreuung und seine wertvollen Korrekturen.

Besonders beansprucht habe ich meine liebe Familie und meine Zwillingsschwester Judith, denen ich für ihre offenen Ohren und stärkende Worte dankbar bin.

Danken möchte ich auch allen Kollegen im Labor für interessante Gespräche und methodische Tipps.

Widmen möchte ich diese Arbeit meinem Mann Tobias, der alle Höhen und Tiefen gemeinsam mit mir durchlebt und mich immer positiv bestärkt hat.

Eidesstattliche Erklärung

Ich versichere an Eides Statt, dass die Dissertation „Bio-engineering of porcine lacrimal gland tissue with secretory capacity" von mir selbständig und ohne unzulässige fremde Hilfe unter Beachtung der „Grundsätze zur Sicherung guter wissenschaftlicher Praxis" an der Heinrich-Heine-Universität Düsseldorf erstellt worden ist. Die Arbeit ist zuvor keiner anderen Fakultät vorgelegt worden. Es wurden bisher keine Promotionsversuche an einer Mathematisch-Naturwissenschaftlichen Fakultät unternommen. Ich habe am 12. Oktober 2011 an der Medizinischen Fakultät der Westfälischen Wilhems-Universität Münster den Titel doctor medicinae (Dr. med.) erworben.

Düsseldorf, den Kristina Spaniol

Zusammenfassung

Das trockene Auge ist eine weltweit verbreitete Erkrankung und stellt eine persönliche sowie volkswirtschaftliche Belastung dar. Die Tränendrüseninsuffizienz, die nach Traumata, Bestrahlung im Kopf-Hals-Bereich, bei Autoimmunerkrankungen und kongenitaler Alacrimie auftreten kann, ist eine Hauptursache für ein schweres trockenes Auge und führt zu schmerzhaften Augenoberflächenstörungen bis hin zum Verlust der Sehkraft. Heutzutage gibt es keine kurative Therapie für diese Erkrankung.

In-vitro und *in-vivo* Studien zur Tränendrüsenregeneration wurden hauptsächlich an Nagern durchgeführt, deren Tränendrüsen sich in Bezug auf Anatomie, Physiologie und Histologie zum Teil deutlich vom Menschen unterscheiden. Einige Autoren haben Ergebnisse aus Arbeiten an Primaten publiziert. Diese Spezies wird aber aus ethischen Gründen in Europa selten für Tierversuche eingesetzt. Das Hausschwein (*Sus Scrofa*) ähnelt dem Menschen in Bezug auf Größe, Anatomie und Genetik. Arbeiten zur Kultur von sekretorisch aktiven azinären Tränendrüsenepithelzellen des Schweines liegen aber bisher nicht vor. Bis heute wurden azinäre Tränendrüsenepithelzellen mit Hilfe einer sogenannten Suspensionskultur isoliert, welche mehrere enzymatische Verdau- und Filtrationsschritte beinhaltet. Diese Methode ist zeitaufwendig, kostspielig und benötigt große Gewebemengen, was ihre klinische Anwendbarkeit deutlich einschränkt. Der einzige bisher erfolgreiche Versuch dreidimensionales Tränendrüsengewebe *in-vitro* zu rekonstruieren ist an embryonalem Gewebe von Mäusen erfolgt und daher aus ethischer Sicht in dieser Form nicht auf die Klinik übertragbar.

Das Ziel dieser Arbeit war zunächst die Kultur und Charakterisierung sekretorisch aktiver Schweinetränendrüsenepithelzellen um das Hausschwein als mögliches neues Tiermodel für Tränendrüsenstudien zu etablieren. Weiterhin wurde eine technisch einfache Explantkultur mit der etablierten Suspensionskultur verglichen um ein klinisch anwendbares Kultursystem für Tränendrüsenepithelzellen verfügbar zu machen. Schließlich wurde die dezellularisierte Schweinetränendrüse als Matrix für die Kultur von Tränendrüsenepithelzellen untersucht, um ein dreidimensionales, sekretorisch aktives Tränendrüsengewebe *in-vitro* zu rekonstruieren.

Primäre, azinäre Tränendrüsenepithelzellen konnten mittels der Suspensions- und Explantkultur erfolgreich aus Tränendrüsen des Schweines isoliert werden, wobei mit

Hilfe der Explantkultur aus einer 3,4 mm^3 Biopsie ebenso viele Zellen gewonnen wurden wie aus einer 100 mm^3 Biopsie durch die Suspensionskultur. Zellen aus beiden Isolationsmethoden wurden bis zu 30 Tage *in-vitro* kultiviert und zeigten keine signifikanten Unterschiede in Bezug auf epithelialen Phänotyp, proliferative Kapazität und sekretorische Kompetenz, was mit Hilfe von Immunfärbungen, Elektronenmikroskopie, Durchflusszytometrie und funktioneller Testung mittels ß-Hexosaminidase-Assay untersucht wurde. Schweinetränendrüsengewebe konnte dezellularisiert werden, während die histologische Struktur und wichtige Extrazellulärmatrixproteine erhalten blieben und sich *in-vitro* keine Zytotoxizität der dezellularisierten Gewebe zeigte. Tränendrüsenepithelzellen aus Suspensions- und Explantkultur wurden unter Erhalt ihres epithelialen Phänotyps in diese Matrix zurückbesiedelt. Sie bildeten Azinus-ähnliche Strukturen und behielten ihre sekretorische Fähigkeit für bis zu eine Woche. Eine Langzeitkultur über 28 Tage führte zu einer Re-Besiedlung und einem Umbau tiefer liegender Gewebestrukturen im Zentrum der Matrices. Ebenso war die allogene Kultur von Kaninchentränendrüsenzellen in der dezellularisierten Schweinetränendrüsenmatrix unter passagerem Erhalt der sekretorischen Kapazität möglich.

Zusammenfassend zeigt diese Arbeit, dass das Hausschwein ein geeignetes Tiermodel für laborexperimentelle Tränendrüsenstudien ist. Die Explantkultur stellt eine Gewebe- und Zeit-sparende und somit möglicherweise klinisch anwendbare Methode zur Isolation von sekretorisch aktiven Tränendrüsenzellen dar. Die dezellularisierte Schweinetränendrüse ist eine supportive Matrix für die Re-Besiedlung mit adulten (allogenen) Tränendrüsenepithelzellen für die Rekonstruktion von dreidimensionalem, sekretorisch aktivem Tränendrüsengewebe *in-vitro*. *In-vivo* Studien und die Kultur von humanen Tränendrüsenepithelzellen sind erforderlich um die Anwendbarkeit der Explantkultur auf menschliches Tränendrüsengewebe und Eignung der dezellularisierten Schweinetränendrüse als mögliche Matrix für Transplantationsstudien weiter evaluieren zu können.

Abstract

Dry eye is a worldwide disease and a personal as well as economic burden. Lacrimal gland deficiency can occur after trauma, radiation therapy of head and neck, due to autoimmune diseases or congenital alacrimia and is a main cause for severe dry eye leading to painful ocular surface disease and potentially loss of vision. Today, no causative treatment is available.

In-vitro and *in-vivo* studies on lacrimal gland regeneration mainly use rodent tissue, which differs from the human in terms of anatomy, physiology, and histological ultrastructure. Some authors worked with primate tissue but the availability of primates for animal testing in Europe is restricted due to ethic concerns. The domestic pig (*Sus Scrofa*) is similar to humans with regard to size, anatomy, and genetic background but studies on secretory porcine lacrimal gland epithelial cells have not been performed until today. So far, secretory competent lacrimal gland cells were cultured by a suspension culture method, which includes several enzymatic digestion and filtration steps. It is therefore time consuming, expensive, and requires large amounts of tissue, which impedes its clinical applicability. Until today, the only successful approach to engineer three-dimensional lacrimal gland matrix utilized embryonic mouse tissue and can therefore not be transferred into clinic in the current form.

This work first aimed to culture and characterize secretory competent porcine lacrimal gland cells to establish the domestic pig as a potential new animal model for lacrimal gland studies. Second, a simple explant culture method was compared to the suspension culture to establish a clinically usable culture system for lacrimal gland cells. Third, decellularized lacrimal gland tissue was characterized and evaluated as a matrix for the culture of lacrimal gland epithelial cells to bioengineer three-dimensional, secretory competent lacrimal gland tissue.

Primary porcine lacrimal gland acinar epithelial cells were successfully isolated from fresh porcine lacrimal glands by suspension and explant culture, while in terms of explant culture a 3.4 mm^3 biopsy obtained as many cells as a 100 mm^3 biopsy treated by suspension culture. Cells from both isolation methods were maintained *in-vitro* for about 30 days without significant differences regarding epithelial phenotype, proliferative capacity, and secretory competence as proofed by immunostaining, electron microscopy, flow cytometry, and functional testing by ß-hexosaminidase

assay. Lacrimal gland tissue was decellularized under preservation of the histological structure and main extracellular matrix proteins and this tissue did not convey cytotoxicity *in-vitro*. Lacrimal gland epithelial cells from suspension and explant culture were successfully reseeded into this matrix. They maintained their epithelial phenotype, formed acinus-like structures, and were secretory competent for up to one week. Long-term culture for 28 days induced deeper cell growth into and remodeling of the matrix. Further, rabbit lacrimal gland epithelial cells were cultured in the decellularized porcine lacrimal gland matrix under temporary maintenance of their secretory capacity.

In conclusion, this work introduces the domestic pig as an easily available animal model for lacrimal gland studies. Explant culture proofed to be a time saving method to isolate secretory competent lacrimal gland epithelial cells. It is tissue sparing and might therefore be a clinically applicable culture method for this vulnerable cell type. Decellularized porcine lacrimal gland proofed to be a supportive, three-dimensional matrix for the engineering of secretory competent, bioartificial lacrimal gland tissue *in-vitro* applying adult (allogeneic) lacrimal gland epithelial cells. *In-vivo* studies and work on human lacrimal gland cells are clearly needed to further validate the applicability of the explant culture method for human lacrimal gland cells and the decellularized porcine lacrimal gland as a potential matrix for transplantation studies.

1 Introduction 1
1.1 Dry eye disease and lacrimal gland insufficiency 1
1.2 Therapeutic options 1
1.3 Tissue engineering using decellularized matrices 2
1.4 The pig as an animal model 3
1.5 Anatomy and ultrastructure of the human and porcine lacrimal gland 3
1.6 Histological structure 6
1.7 Culture of lacrimal gland cells 9
1.7.1 Secretory cells 9
1.7.2 Progenitor cells 12
1.8 Tissue engineering of the lacrimal gland 13
2 Aim of this work 15
3 Material and Methods 17
3.1 Localization and removal of the porcine lacrimal gland 17
3.2 Tissue harvesting and decellularization 17
3.3 Proof of decellularization 18
3.3.1 Collagen quantification 18
3.3.2 DNA quantification 19
3.3.3 Cytotoxicity measurement 19
3.3.4 Western blotting 20
3.4 Cell culture 20
3.4.1 Cell culture medium 20
3.4.2 3T3/J2 feeder cells 20
3.4.3 Epithelial cell suspension culture 21
3.4.4 Epithelial cell explant culture 21
3.5 Recellularization of the decellularized matrices 22
3.5.1 Testing for secretory capacity (ß-hexosaminidase assay) 22
3.6 Protein detection 23
3.6.1 Hematoxylin and Eosin staining 23
3.6.2 Periodic acid Schiff reaction 23
3.6.3 Immunohistochemistry and Immunocytochemistry 23
3.6.4 Flow cytometry 24
3.7 Cell population doublings and colony forming assay 25

3.8 Electron microscopy 25
3.9 Statistical analysis 25
4 Results 27
4.1 Main cell types of the porcine lacrimal gland 27
4.2 Decellularized porcine lacrimal gland 29
4.2.1 Basement membrane components 33
4.2.2 Removal of the cellular components 36
4.3 Cell isolation and characterization - comparison of explant and suspension culture cells 39
4.3.1 Cell gain and phenotype 39
4.4 Functional capacity 42
4.4.1 Proliferative capacity and stem cell character 47
4.4.2 Recellularization of the decellularized porcine lacrimal gland 53
4.5 Culture of rabbit lacrimal gland acinar cells 60
5 Discussion 62
5.1 Comparison of suspension and explant culture 62
5.2 Proliferative capacity 65
5.3 Decellularized porcine lacrimal gland for lacrimal gland bioengineering 68
5.4 Recellularization of the decellularized lacrimal gland 70
5.5 Limitations of this work 72
5.6 Conclusion 73
6 Appendix 74
6.1 List of abbreviations 74
6.2 References 76
6.3 Declaration 86

1 Introduction

1.1 Dry eye disease and lacrimal gland insufficiency

Today, dry eye disease has a prevalence of about 14 % and affects approximately 3.2 million women and 1.04 million men in the United States (Moss et al., 2000) (Schaumberg et al., 2003) (Schaumberg et al., 2009). Dry eye disease is a multifactorial, complex ocular disorder, which is caused by decreased tear production (= aqueous deficient dry eye disease) and / or increased tear evaporation (= evaporative dry eye disease) (Schaumberg et al., 2009). Clinically, aqueous deficient dry eye disease occurs less frequently but can harm the ocular surface severely. As the lacrimal gland (LG) normally produces 90 % of the stimulated tear secretion, a primary cause for severe aqueous deficient dry eye disease is LG insufficiency with failure of lacrimal tear secretion (Perry, 2008). The resulting alterations of the tear film lead to visual impairment, pain, and potentially progressive damage of the ocular surface (Schaumberg et al., 2009). This can cause conjunctival and corneal inflammation, corneal ulceration, and corneal perforation eventually causing loss of vision (Pflugfelder et al., 1999). LG insufficiency results either from a primary LG dysfunction (congenital alacrima, familial dysautonomia, aging) or, more frequently, from secondary causes; such are auto-immunological processes with or without accompanying systemic diseases (secondary or primary Sjögren Syndrome), cicatrizing changes of the ocular surface, radiation therapy of the head and neck region, age and/or systemic medication (e.g. anti-androgens, anti-histamines, ß-blockers, diuretics) leading to progressive fibrosis and secretory dysfunction of the LG tissue (Pflugfelder et al., 1999).

1.2 Therapeutic options

The therapy of severe dry eye includes the treatment of underlying diseases but it predominantly consists of topical artificial tears, eye drops made from different blood components (autologous/allogeneic serum, fibronectin, plasma rich in platelets, albumin) and anti-inflammatory eye drops such as corticosteroids or cyclosporine A (Gayton, 2009) (Geerling et al., 2004). However, fibrosis of the LG is irreversible and in severe cases, the available therapies are not sufficient to relieve the patients´ symptoms and preserve the ocular surface (Borrelli et al., 2010). LG transplantation

has not been performed so far due to the short ischemia time of this organ. The transfer of salivary glands (submandibular, sublingual) for replacement of the LG function was successful as the transplants were secretory active after a five-year follow-up (Jacobsen et al., 2008) (Borrelli et al., 2010). Significant drawbacks of this approach are hypersecretion of the transplants and the secretory composition as it is a hypotonic secretion resulting in corneal edema and loss of vision (Borrelli et al., 2010).

1.3 Tissue engineering using decellularized matrices

Tissue engineering renders the ability to reconstruct tissues and organs *in-vitro* for *in-vivo* application. As the population grows and ages and medical skills increase, a severe shortage of donor organs strengthens the significance of tissue engineering (Atala, 2009). The goal is to create a matrix, which supports proliferation and differentiation of functionally competent, organ-specific cells, is immunologically compatible, and surgically manageable (Atala, 2009). One method to produce such a matrix is decellularization, which describes the process of removing all cellular components by preserving the extracellular matrix as a tissue to be recellularized with the host´s cells *in-vivo* after the transplantation or *in-vitro* prior to the transplantation (reviewed in (Arenas-Herrera et al., 2013)). Reasons for using the target-organ as a matrix are the organ-specific properties of the extracellular matrix. The extracellular matrix provides stability but also a particular protein structure and growth factor- and cytokine composition, which can be preserved by organ decellularization (reviewed in (Badylak, 2002) and (Arenas-Herrera et al., 2013)). The combination of these factors creates a “guidance” for the cells to initiate an organ-specific differentiation (Arenas-Herrera et al., 2013). It has been shown that decellularized allogeneic and xenogeneic tissues do only provoke minimal immunologic reactions and that the risk of infections (bacteria, viruses, prions) is low depending on the decellularization process (Moza et al., 2001). The use of these matrices would increase the number of transplantable organs significantly and diminish the need for immunosuppression (reviewed in (Badylak, 2002)).

Tissue engineering based on decellularized organs has been successfully applied to construct bladder-, urinary tract-, skin-, intestine, liver-, heart-tissue, and vessels *in-vitro* (El-Kassaby et al., 2003) (Chen et al., 2000) (Priya et al., 2008) (Linke et al., 2007) (Bitar and Raghavan, 2012) (Radisic and Christman, 2013) (Black et al., 1998)

(Bourget et al., 2012). Tissue engineered bladder was successfully tested in animal models and tissue engineered urethras were applied for urethral stricture repair in a clinical study (Jayo et al., 2008) (el-Kassaby et al., 2008) (Raya-Rivera et al., 2011). However, organ engineering requires recellularization of a decellularized organ scaffold, which brings up the question of a suitable cell source. Potential cell sources are embryonic stem cells, induced pluripotent stem cells, placenta- or amnion-derived stem cells, umbilical cord blood cells, and adult stem cells (reviewed in (Murphy and Atala, 2012)). Autologous cells from the organ to be engineered do not carry the risk of immunoreactions or disease transmission, are ethically unproblematic and have so far been most successfully used in translating bio-engineered tissues into the clinic (Atala et al., 2006) (Zhang et al., 2008).

1.4 The pig as an animal model

Between 79 and 97 million years ago, pig (*Sus scrofa*) and humans had at least one common ancestor and belong genetically to the same descent community (Kumar and Hedges, 1998). Regarding size, physiology, and anatomy, the pig is similar to humans (Walters et al., 2012). It provides an easily available cell and tissue source as it is sexually mature by the age of six to eight month, has a short gestation length of four month, gives birth to about ten to fourteen piglets and breads perennially (Walters et al., 2012). There also seem to be pathophysiological overlaps to humans as both share protein sequences predicted to be involved in obesity, diabetes, Alzheimer´s or Parkinson´s disease (Groenen et al., 2012). Further, for surgical approaches as transplantation studies large animal models are required and although non-human primates are most similar to humans there are ethical concerns about utilizing them in large quantities (Dehoux and Gianello, 2007). The pig is increasingly used for transplantation research and the fact that size and localization of the porcine LG mimic the human make the pig a valuable animal model for LG studies (Henker et al., 2013).

1.5 Anatomy and ultrastructure of the human and porcine lacrimal gland

The main human LG resides in the lacrimal fossa, which is a shallow cavity of the frontal bone in the superotemporal orbit (Tasman and Jaeger, 2010). It is a modified salivary gland that develops from invaginations of the embryonic ectoderm (Kivela, 1992). The LG of an adult human measures about 20 mm by 25 mm and the orbital and palpebral lobe have a height of five mm and three mm, respectively (Obata,

2006). The LG is divided by the aponeurosis of the levator palpebrae muscle into a smaller palpebral and larger orbital lobe. There are six to twelve secretory ducts, which drain into the superotemporal conjunctival fornix while the ducts of the orbital lobe pass through the palpebral lobe or lie on its surface before terminating at the conjunctiva (Obata, 2006). Although there are small accessory LGs (glands of Krause in the superior and inferior fornix and glands of Wolfring above the tarsus), removal of or damage to the main LG causes severe disturbances of the ocular surface (Tasman and Jaeger, 2010).

The arterial blood supply reaches the main human LG by a lacrimal branch of the ophthalmic artery, which passes through the LG and receives contributions by branches of the recurrent meningeal and infraorbital artery (Erdogmus and Govsa, 2005). The lacrimal vein follows the artery and both vessels communicate with the posterior surface of the gland (Erdogmus and Govsa, 2005).

Few publications describe the anatomy and ultrastructure of the porcine LG. As the human LG, the porcine LG lies in the superotemporal margin of the orbit (Henker et al., 2013). The LG of an adult domestic pig up to one year of age measures 34 mm by 22 mm and has a height of 12 mm (Henker et al., 2013). Henker et al. describe seven main excretory ducts, which drain into the conjunctival fornix in the lateral angle of the eye (Henker et al., 2013). The porcine LG receives its arterial blood supply by a lacrimal artery, which originates from an external ophthalmic artery and enters the LG after passing by the lateral rectus muscle (Henker et al., 2013). The lacrimal veins run with the lacrimal artery (Henker et al., 2013).

In comparison to the human LG, the porcine LG is about 50 % larger in the dorso-ventral diameter and 50 % thicker. The secretory system (number of ducts, termination in the temporal fornical conjunctiva) and the vascular supply (main supply by a single-trunk lacrimal artery and vein) are similar (Table 1) (Henker et al., 2013).

The human and porcine LG are tubuloalveolar glands in which acini – the secretory endpieces – drain into ducts, which open at a mucosal surface (conjunctiva of the upper lid) (Schechter et al., 2010). Many acini and the duct they drain into form a lobule and many lobules compose a lobe (Schechter et al., 2010). The acinar cells are pyramid shaped epithelial cells, which produce the LG secretions and open into the central lumen of an acinus (Obata, 2006). Acinar cells can be mucinous, serous or mucoserous depending on the secret they produce, while serous secretions are rich in water and electrolytes, mucinous secretions contain a higher amount of

glycoproteins (Schechter et al., 2010). For the human LG it is described that acini and ducts are surrounded by a basement membrane and that extracellular matrix molecules form a supportive tissue between acini and ducts, which increases in density the larger the ducts are (Schechter et al., 2010).

Table 1: Comparison of human and porcine lacrimal gland.

	human	**porcine**
localization	temporal superior margin of the orbit	
size	20 mm x 25 mm x 5 mm	34 mm x 22 mm x 15 mm
histology	• tubuloalveolar gland • single trunk lacrimal lacrimal artery and vein • delivery of secretion: upper conjunctival fornix	
type of secretion	predominantly serous	muco-serous

1.6 Histological structure

Histological descriptions of the porcine LG were published in 1979 by Kühnel and verified in this work (Kühnel and Scheele, 1979). The hematoxylin and eosin (H&E) staining of the porcine LG reveals a structure similar to the human LG. As described for the human gland, the porcine LG consists of several secretory acini, which build lobules that than form a lobe (Schechter et al., 2010). Lobules and lobes are divided by connective tissue and contain ducts (Figure 1) (Schechter et al., 2010) (Kühnel and Scheele, 1979).

Similar to the human LG, the acini consist of pyramid-shaped cells arranged around a central lumen with basally located nuclei (Obata, 2006). The Periodic acid Schiff (PAS) / alcian blue reaction indicates evidence of secretions containing glycosylated proteins and mucopolysaccharids as it stains neutral mucins intensely pink and acid mucins light blue and a positive PAS reaction is evident in several acinar cells of the porcine LG (Figure 2). Evidence of PAS positive secretions has also been described for the human LG previously, which indicates similarity between the species (Obata, 2006). However, the human LG has been found to be a predominantly serous gland comprising more non- or lightly glycosylated proteins while the porcine LG is a mucoserous gland with predominance of mucinous secretions (Schechter et al., 2010) (Kühnel and Scheele, 1979). According to the PAS / alcian blue reaction, the electron microscopy of the porcine LG reveals mucinous and serous acinar cells, while the mucinous cells can be identified by less electron-dense (“light”) vesicles compared to the dark (=electron dense) serous vesicles (Kühnel and Scheele, 1979). However, as described previously one can not strictly distinguish between “mucinous” or “serous” acini as many of them contain mixed, mucinoserous or seromucinous granula (Figure 3) (Schechter et al., 2010).

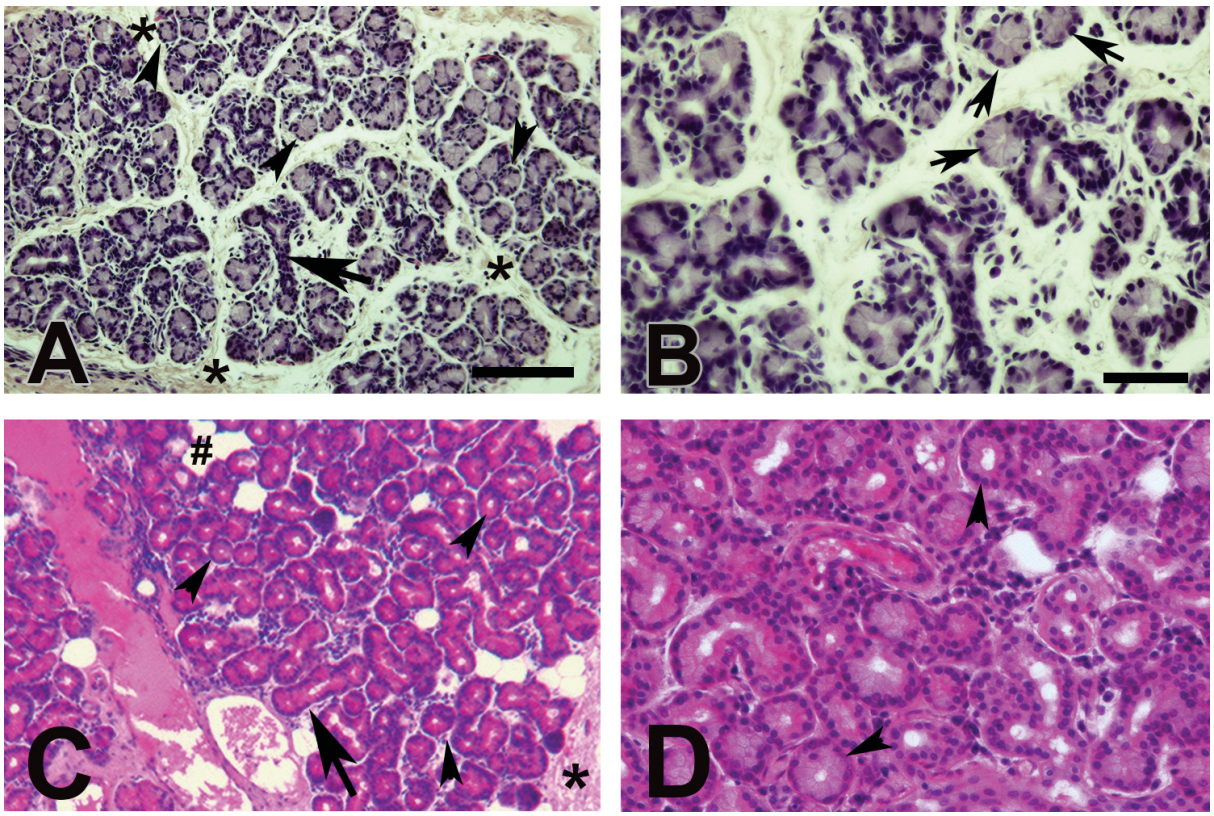

Figure 1: Hematoxylin and Eosin staining of the porcine and human lacrimal gland (LG).

A: The porcine LG contains several lobules and lobes, which are divided by connective tissue (asterisks). The lobes consist of several acini (arrowhead) and contain intralobular ducts (arrow). B: The higher magnification reveals the pyramid-shaped form of the acinar cells (arrow), which are circularly arranged around a central lumen to build the secretory acini. These cells predominantly show basally located nuclei (arrow). C / D: The human LG similarly contains roundish acini with basally located nuclei and a central lumen (arrowhead). Excretory ducts are visible (arrow) and in contrast to the porcine LG, some fat vacuoles are evident, which may speak for an age-related fatty degeneration. Connective tissue (asterisk) are less frequent and the lobular architecture is not as apparent as in the porcine LG, which was described elsewhere (Schechter et al., 2010). A / C: scale bar 100 µm, B / D: scale bar 25 µm. Images C and D were kindly supplied by Robert Kubitza. Differences in color are based on different staining and imaging modalities.

Taken together, porcine and human LG show a similar anatomical structure, while the porcine LG produces mucinoserous and the human LG mainly serous (around 90 %) secretions (Schechter et al., 2010) (Kühnel and Scheele, 1979).

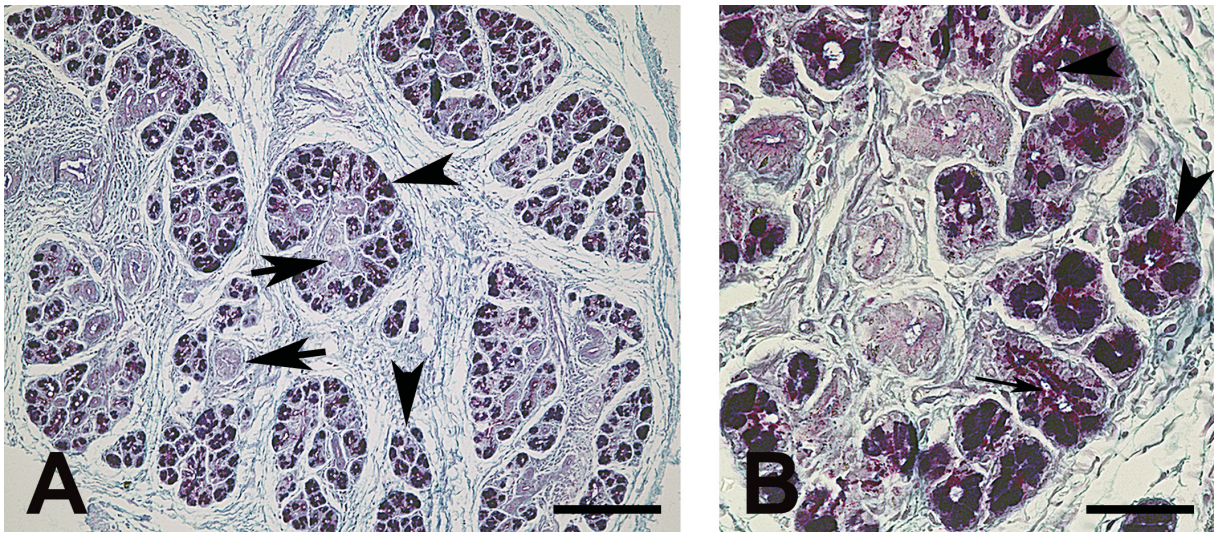

Figure 2: Periodic acid Schiff / alcian blue reaction of porcine lacrimal gland tissue. A: Several acinar cells show an intense pink staining as typical for mucinous secretions (arrowhead) while some do not show a positive reaction (arrow) indicating a more serous content rich in water and electrolytes. The higher magnification indicates the granular character of the secretions (arrowhead) and evidence of secretions in the lumen of a duct (narrow arrow). A: scale bar 200 µm; B: scale bar 50 µm.

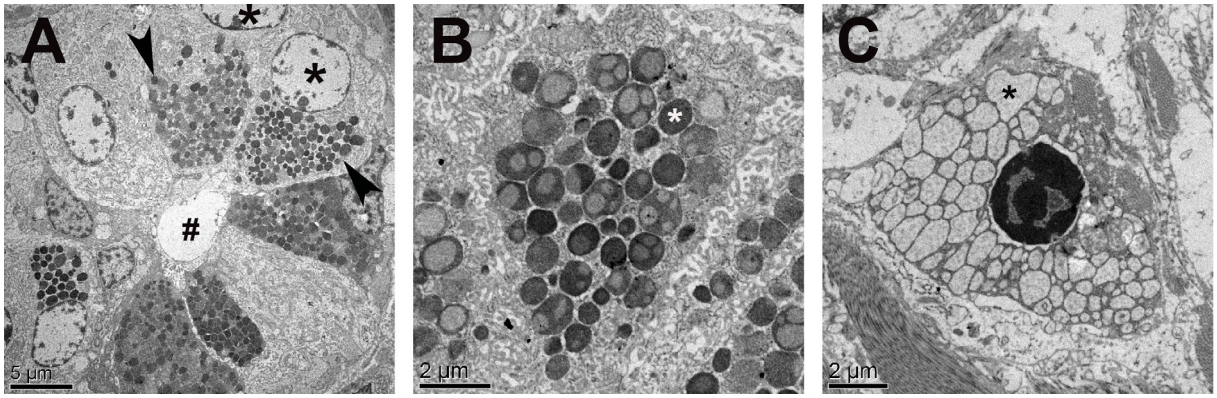

Figure 3: Transmission electron microscopy images of the porcine lacrimal gland. A: The acinar cells reveal a pyramid-shaped form with basally located nuclei (asterisk) and secretory granules in the cytoplasm (arrowhead) and are arranged around a central lumen (rhombus). B: The serous acinar cells contain roundish vesicles (asterisk) with electron dense content indicating water- and electrolyte-rich secretions. C: The mucinous acinar cells consist of densely packed, plump vesicles (asterisk) with much less electron dense content compared to the vesicles of the serous acinar cells. A: scale bar 5 µm; B, C: scale bar 2 µm. Images taken by Dr. med. Klaus Zanger and Elisabeth Wesbuer (Spaniol et al., 2015).

1.7 Culture of lacrimal gland cells

1.7.1 Secretory cells

The LG comprises three main cell types: acinar epithelial cells, myoepithelial cells, and mesenchymal cells (Schechter et al., 2010). The secretory active cells are the acinar epithelial cells, which produce about 80 % of the tear fluid and have been investigated most in the past (Schechter et al., 2010). Cultures of secretory competent cells have been performed for mouse, rat, rabbit, monkey, and human LG tissue, while in Europe – apart from one work by Hunt et al. who worked with human tissue – only rodent models have been investigated (McDonald et al., 2009) (Millar et al., 1996) (Schonthal et al., 2000) (Schrader et al., 2007) (Schrader et al., 2010) (Schechter et al., 2002) (Hann et al., 1989) (Kobayashi et al., 2012) (Ueda et al., 2009) (Fujii et al., 2013) (Nakajima et al., 2007) (Tiwari et al., 2012) (Yoshino et al., 1995) (Yoshino, 2000) (Hunt et al., 1996).

Hann et al. were the first who described the culture and maintenance of secretory competent rat LG acinar cells from four to ten weeks old rats in 1989 (Hann et al., 1989). The glands were mechanically minced and enzymatically digested with

ethylendiaminetetraacetic acid (EDTA), collagenase (200 units/ml), hyaluronidase (698 units/ml) and DNase (10 units/ml), filtered through a 500 µm and a 25 µm mesh, and purified by using a Ficoll gradient (three layers of 2 %, 3 %, 4 %, respectively), which produced a 90-95 % pure epithelial cell culture. Cells cultured on matrigel in serum free medium (supplemented among others with dexamethasone, epidermal growth factor (EGF), l-asorbic acid, insulin, transferrin, selenous acid, and reduced glutathione) showed more secretory cells but less proliferation than cells cultured in serum-containing medium (10-20 % fetal calf serum, FCS) and were secretory competent for about 25 days. Culture on plastic did not achieve sufficient cell attachment.

Ueda et al. isolated acinar cells of newborn mice-LG after digestion with 1 % collagenase, filtering through a 40 µm mesh and several washing steps receiving a 99.5 % pure epithelial cell culture (Ueda et al., 2009). Culture on matrigel in serum free medium (epidermal keratinozyte medium) induced the development of cell clusters with an acinar-like structure containing secretory granules. In addition, Kobayashi et al. established LG acinar cell cultures of newborn and adult mice after enzymatic LG digestion with collagenase (750 units/ml), hyaluronidase (500 units/ml), and 0.01 % DNase (Kobayashi et al., 2012). The cells were cultured in serum-free medium (epidermal keratinozyte medium, supplemented with 10 ng/ml EGF) on collagen I coated culture plates. The authors were able to induce sphere formation from single cells on plastic if the medium was supplemented with 100 ng/ml choleratoxin, which they attributed to the fibroblast-suppressing properties of choleratoxin (Ma et al., 2009).

Several groups worked with rabbit LGs (McDonald et al., 2009) (Millar et al., 1996) (Schonthal et al., 2000) (Schrader et al., 2007) (Schechter et al., 2002). Millar et al. used a similar isolation protocol as Hann et al. (Millar et al., 1996). After comparison of different support matrices they found cell attachment rates of 70-90 % on matrigel and plastic, respectively, while the attachment rate was reduced to 15 % on gelatin and 5 % on poly-L-lysine. Growth pattern was similar on all matrices. Immunohistochemically, the cells expressed cytokeratins but the purity of the epithelial cell culture was not quantified. The authors identified several PAS / alcian blue reaction-positive cells in the gland and reasoned that the rabbit LG is a seromucinous gland. A secretory response to parasympathetic stimulation after *in-vitro* culture was not measured.

Nakajima et al. were able to isolate monkey LG acinar cells; again, enzymatic digestion (200 units/ml collagenase, 698 units/ml hyaluronidase, 10 units/ml DNase) and several filtering procedures (100 µm and 40 µm nylon meshes, Percoll gradient) were applied (Nakajima et al., 2007). Three different species were used (macaques, savanna monkeys, crab-eating monkeys); the animal age was not given. The cells were cultured on collagen I coated plastic plates in serum-free medium (Dulbecco´s Modified Eagles Medium (DMEM), supplemented with dexamethasone, putrescine, EGF, l-asorbic acid, insulin-transferrin-sodium, selenite, and gentamycin) and showed a secretory response to parasympathetic stimulation with carbachol after 48 hours culture duration measured by immunoblotting for the tear-film protein lacritin in the cell culture supernatant. Another group applied similar isolation and culture conditions using LG from one to ten years old rhesus monkeys and proofed secretory capacity after 16 hours culture duration by measuring secretion of the tear proteins lipocalin and lactoferrin in the cell culture supernatant after parasympathetic stimulation with carbachol (Fujii et al., 2013).

Regarding human LG tissue, Hunt et al. established an *in-vitro* culture system with biopsy specimen of human accessory and main LG of organ donors or after autopsy (up to eight hours post-mortem) (Hunt et al., 1996). They produced tissue pieces with a maximum size of 1 mm^3 and cultured them on uncoated hydrophobic culture dishes in DMEM containing 10 % FBS and various supplements (dexamethasone, ascorbic acid, reduced glutathione, EGF, glucose, insulin-transferrin-sodium, selenite, gentamycin, penicillin, and streptomycin) with an oxygen concentration of 50 %. A secretory capacity measured by the amount of secretory IgA, lysozyme, and lactoferrin in the cell culture supernatant after stimulation with the second messenger cAMP or cGMP was evident up 72 hours of organ culture and secretory granules were detectable with electron microscopy until 22 days after culture initiation. Although this method seemed to mimic the *in-vivo* function of the LG quite closely, cell proliferation was not induced.

Yoshino et al. report the culture of main LG cells from donors younger than 40 years after LG-removal within 15 hours postmortem (Yoshino et al., 1995). As described for other species (see above), the cells were dissociated enzymatically and cultured with various growth factors. The medium contained 15 % FBS for three days, which was then reduced to 2.5 %. The growth pattern on plastic, collagen I coated plastic (with or without 3T3 feeder cells) and matrigel were compared. The authors reported a

nearly pure epithelial cell culture with best differentiation and secretory response - measured by lactoferrin quantification in the cell culture supernatant after seven to ten or ten to 14 days of culture - when the cells were cultured on matrigel. However, proliferation was best on plastic and low on matrigel while a 3T3 feeder layer supported an epithelial differentiation.

Similarly, Tiwari et al. isolated human LG acinar epithelial cells by enzymatic digest with collagenase and hyaluronidase (Tiwari et al., 2012). The tissue source were exenteration specimen, the patient age ranged from three to 65 years. The epithelial cells were identified by their initial adhesion to plastic; cell clumps that did not attach to plastic were plated on matrigel, collagen I coated plates or denuded human amniotic membrane and cultured with a serum-free medium (supplemented with dexamethasone, insulin-transferrin-sodium, selenite, EGF, L-glutamine, penicillin, and streptomycin). Ten percent FBS was added for the first three days and then omitted. The authors found secretory response until day 21 measured by elisa for the tear proteins secretory IgA, lactoferrin, and lysozyme. The cells were viable for up to 35 days of *in-vitro* culture. As described by Yoshino et al., secretory response was best on matrigel (Tiwari et al., 2012) (Yoshino et al., 1995).

Taken together, LG acinar epithel cells from rodent, non-human primate, and human LG´s have been isolated applying various enzymatic digestion and filtration steps and maintained *in-vitro* for up to one month. The best secretory response was found with an extracellular matrix support (e.g. matrigel), cells proliferated best on plastic, and a 3T3 feeder layer supported the epithelial differentiation.

1.7.2 Progenitor cells

Plenty of work has been published on progenitor/stem cells in salivary glands but there is little knowledge available about these cells in the LG (Zoukhri, 2010). For the adult murine LG, Zoukhri et al. showed that LG tissue is able to regenerate after an acute injury induced by interleukin 1 injection (Zoukhri et al., 2008). The authors used nestin as a progenitor marker and described an increase of nestin expressing cells through the regeneration period. Some of these cells also expressed α-smooth muscle actin as a marker for myoepithelial cells and the authors therefore assumed that the same progenitor cell might give rise to myoepithelial and acinar cells (Zoukhri et al., 2008). You et al. described the isolation of mesenchymal stem cells from the injured adult LG (You et al., 2011). The authors reported that most of the isolated cells expressed vimentin, nestin, ATP-binding cassette sub-family G member 2

(ABCG2), and stem cell antigen 1 (Sca-1), as markers for mesenchymal stem cells and could be differentiated into adipocytes using appropriate media (You et al., 2011). Roth et al. showed that the *in-vitro* expansion of LG mesenchymal stem cells at low oxygen (5 %) increases their proliferation rate and induces an up-regulation of the cell surface glycoprotein CD44, a potential marker for increased regenerative and anti-inflammatory capacity (Roth et al., 2015) (Herrera et al., 2007). Voronov et al. studied embryonic mice and underlined the potential progenitor capacity of central acinar and ductal epithelial cells (Voronov et al., 2013). These cells showed up-regulation of runt-related (Runx) factor 1 during tissue repair, a transcription factor, which is involved in proliferation and differentiation of secretory epithelial lineages (Fijneman et al., 2012). For the human LG (donor age three to 65 years), Tiwari et al. proofed evidence of aldehyde dehydrogenase 1 (ALDH-1) and ABCG2 expressing cells in the freshly isolated gland and – with decreasing amounts – until day 21 after culture on matrigel (Tiwari et al., 2012).

These data demonstrate that the LG possesses regenerative capacity but so far it remains unclear if the LG contains one common multipotent stem cell or if there are several lineage specific progenitor cells, which give rise to the acinar, myoepithelial, and mesenchymal LG cells (Voronov et al., 2013).

1.8 Tissue engineering of the lacrimal gland

Development of a three-dimensional, transplantable LG construct requires a suitable matrix, as well as secretory active, proliferative cells and finally, a vascular and neural supply (Atala, 2009). Attempting to culture three-dimensional LG tissue, Schrader et al. used rotary cell culture systems, which simulate microgravity and are known to induce cell-cell contact formation, provide low shear stress, and high transport of nutrients (Becker et al., 1993) (Schrader et al., 2009). The cultured LG acinar epithelial cells from adult rabbits developed secretory competent spheroids measuring around 400 µm diameter but revealed central necrotic areas, which increased with the size of the spheroids (Schrader et al., 2009).

Hirayama et al. report a so-called “organ-germ method” (Nakao et al., 2007) (Hirayama et al., 2013). The authors isolated single cells from the epithelial and mesenchymal tissue of embryonic day 16.5 murine LG and microscopically observed LG reconstitution after three days in organ culture (Hirayama et al., 2013). A monofilament was inserted to induce lacrimal duct formation and the bioengineered

glands were transplanted into seven weeks old LG deficient mice (Hirayama et al., 2013). Thirty days after engraftment the mean acinus diameter of the transplanted LG was similar to the natural murine LG (48.6±1.5 µm vs 46.0±1.2 µm) (Hirayama et al., 2013). The authors also showed connection of the graft to the recipient lacrimal duct and recovery of secretory capacity. Secretory function was proofed by significantly increased tear flow after parasympathetic stimulation (intraperitonial pilocarpin injection) and ocular surface cooling with menthol (Hirayama et al., 2013). The presence of lactoferrin as a main tear protein was verified and the amounts of tear lipids (alkyl triglycerides) was similar to the control group (Hirayama et al., 2013). However, the use of embryonic tissue prevents the application of this method in humans.

2 Aim of this work

In the past, rodents have been used for LG studies in Europe but these resemble the human anatomy and physiology insufficiently (Schechter et al., 2010). The domestic pig (*Sus scrofa*) is an easily available animal with similar anatomy and close genetic connections to humans and was explored here as a potential LG animal model (Groenen et al., 2012). So far, the isolation of secretory competent LG cells involves several enzymatic digestion and filtration steps (suspension culture, SC), which is time consuming and leads to cell damage and loss of cells (Yoshino, 2000). Aim of this work was to explore the feasibility of culturing secretory competent LG acinar epithelial cells using a straightforward, clinically applicable explant culture (EC) method and compare it to the established SC method (Spaniol et al., 2015). Finally, this work aimed to create a supportive, three-dimensional LG matrix as a scaffold for the culture of secretory competent LG acinar epithelial cells and potential matrix for LG engineering in humans in future (Figure 4) (Spaniol et al., 2015).

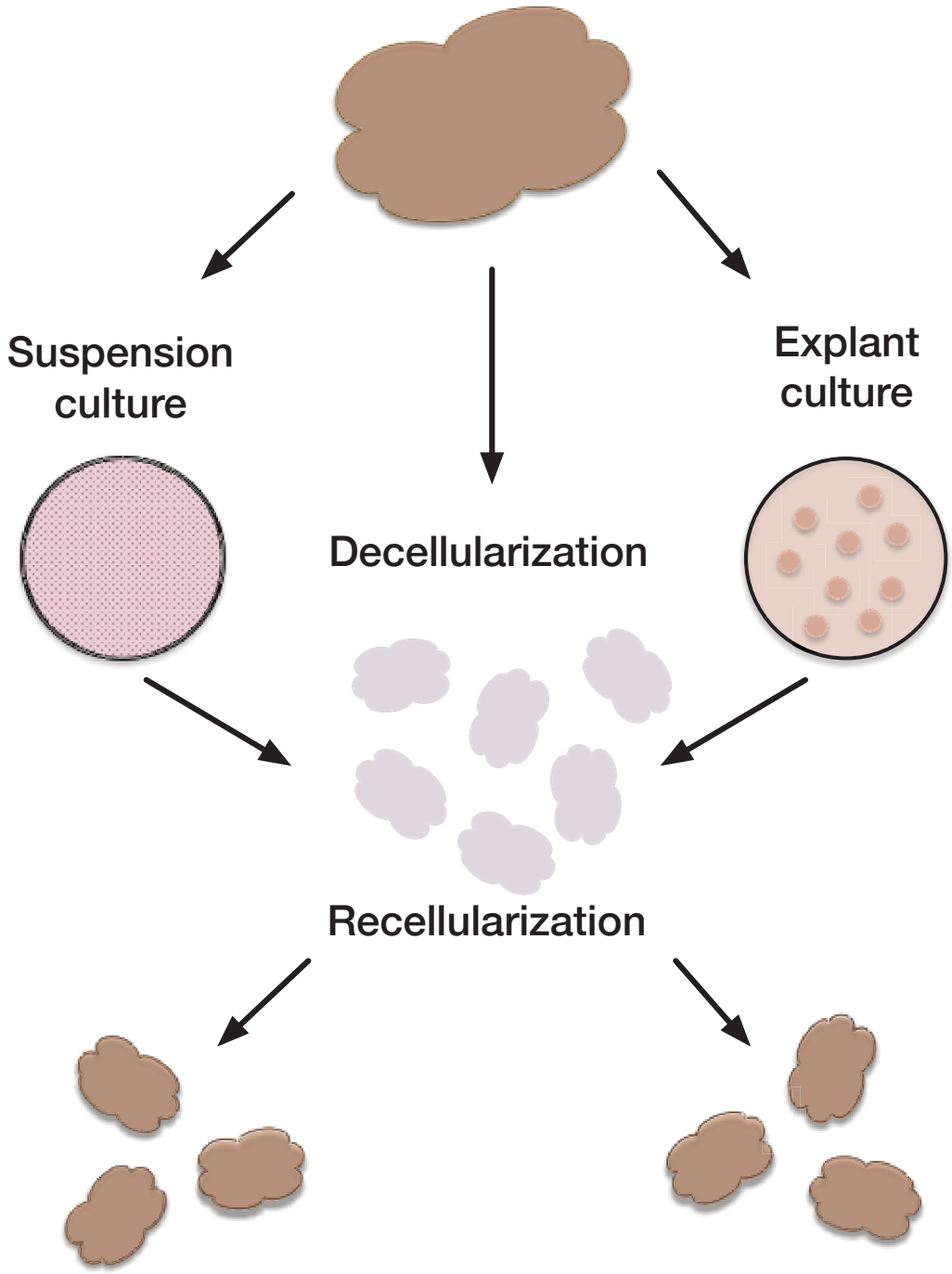

Figure 4: Schematic overview of the work plan.

Porcine lacrimal gland (LG) acinar epithelial cells were expanded either by an established suspension culture (SC) or by an explant culture (EC) method. Cells from SC and EC were compared regarding morphology, secretory, and proliferative capacity. LG tissue was cut into 3-4 mm diameter pieces and made cell free by decellularization. These pieces were recellularized with either SC or EC cells and again compared afterwards.

3 Material and Methods

3.1 Localization and removal of the porcine lacrimal gland

As described previously, the porcine LG is localized beneath the frontal bone in the temporal-superior, orbital fossa (Henker et al., 2013). The gland was extracted by performing a two to three cm long cut in the eyelid fold from the middle of the eyelid to the lateral orbital rim (Figure 5). The subcutaneous fat and orbicularis muscle were dissected down to the thin fascia overlying the LG. The fascia was cut carefully and the gland was hold with forceps at the anterior margin while care was taken not to change the position intending to harm as little tissue as possible by pressure with the forceps. The gland was taken out by cutting the surrounding tissue with a scalpel blade

3.2 Tissue harvesting and decellularization

All experiments were conducted in accordance with the Association for Research and Vision in Ophthalmology (ARVO) statement for the use of animals in ophthalmic research.

Fresh LG were obtained from a local slaughterhouse from eight-month old, female domestic pigs weighing about 80 kg (Stautenhof, Willich-Anrath, Germany). Rabbit LG were obtained from the animal testing facility of the Heinrich-Heine-University Düsseldorf from two-month old female New Zealand White rabbits

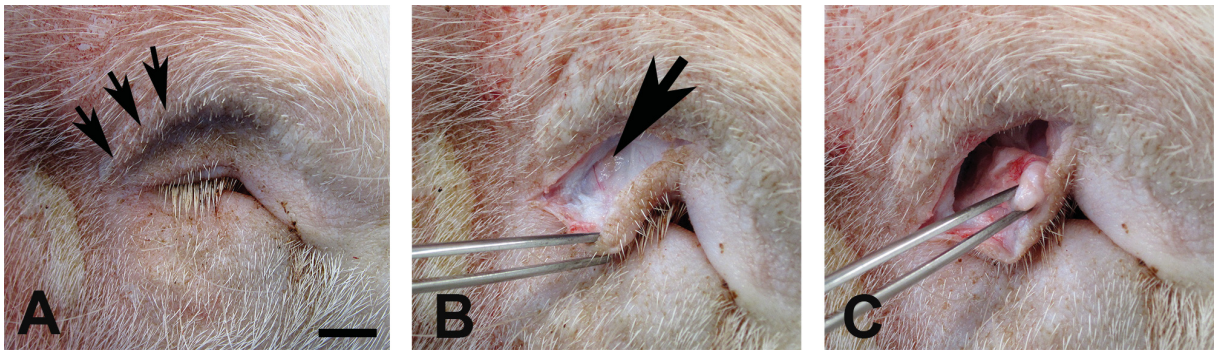

Figure 5: Removal of the porcine lacrimal gland (LG).
A: The porcine LG is localized beneath the lateral orbital rim (arrows). B: After performing an about three cm long cut in the lid fold, the subcutaneous fatty tissue, the orbicularis muscle, and the fascia were cut, so that the LG became visible (thick arrow). C: The LG was hold with forceps and dissected from the surrounding tissue. A, B, C: scale bar 1 cm.

(Charles River Laboratories, Wilmington, Massachusetts). The glands were stored in 4-8 °C cold culture medium prior to processing for cell culture or in ice-cold phosphate buffered saline (PBS) for histological analysis of the native tissue.

For decellularization, the LG was washed in PBS, residual fatty tissue was dissected with scalpel blades, and the LG was cut into pieces of about three mm diameter (Spaniol et al., 2015). The LG pieces were incubated in cold phosphate buffered saline solution (PBS, Sigma-Aldrich, Schnelldorf, Germany) containing 5 % (v/v) Penicillin/Streptomycin (Invitrogen, Carlsbad, CA, USA) overnight at 4 °C, then washed again with PBS and transferred into the decellularization solution containing 4 % sodium deoxychelate monohydrate solution (w/v) (Sigma-Aldrich, Hamburg, Germany), and incubated at 4 °C for 36 hours with three changes of decellularization solution after 12 hours, respectively. Next, the pieces were washed three times with PBS and transferred into DNase solution (200 U/ml) (Roche, Penzberg, Germany) and incubated for 24 hours with two changes of decellularization solution (each after 12 hours). For removal of chemical residues, the pieces were washed in PBS three times. All incubation steps were performed under continuous agitation. For tissue sterility, the decellularized scaffolds were γ-irridiated with 25 kGy overnight (BBF Sterilizationservice GmbH, Rommelshausen, Germany). The decellularized tissue was transferred into PBS containing 5 % (v/v) Penicillin/Streptomycin and stored at 4 °C.

3.3 Proof of decellularization

3.3.1 Collagen quantification

For collagen determination, native and decellularized LG pieces were transferred into 1.5 ml Eppendorf tubes (Eppendorf, Hamburg, Germany), dehydrated for two hours in a vacuum concentrator (Eppendorf concentrator plus) and mechanically dissolved at -70 °C in a tissue lyser (Qiagen, Hilden, Germany). The specimen were then incubated at a pepsin concentration of 0.1 mg/ml in 0.5 M acetic acid at 4 °C over night and processed according to the manufacturer´s protocol (Sircol collagen assay, Biocolor, Newtownabbey, UK). Collagen samples delivered by the manufacturer were dissolved in appropriate concentrations and used as standards; reagent solution without tissue probes was used as a negative control. Tissue samples, standards, and negative control were measured in duplicate in a 96 well plate at 550 nm, respectively (VICTOR™ X multilabel plate reader, PerkinElmer, Waltham, USA).

3.3.2 DNA quantification

Native and decellularized LG pieces were dehydrated for two hours in a vacuum concentrator (Eppendorf concentrator plus), weighed, chopped into smallest pieces with scalpel blades, and incubated at 56 °C overnight in lysis buffer containing 10 mM Tris pH 8, 100 mM sodium chloride, 10 mM EDTA pH 8, 0.5 % (w/v) SDS, and 0.4 mg/ml Proteinase K. Water-saturated phenol was added, incubated with chloroform/isoamyl alcohol (49:1), and centrifuged for 20 minutes at 10,000 rpm at 41 °C. The inter- and lower phase were used for DNA precipitation by adding 100 % (v/v) ethanol, incubating for five minutes at room temperature, and centrifuging again. The pellet was washed with 0.1 M sodium citrate and re-suspended in 75 % (v/v) ethanol. After centrifugation, the supernatant was decanted. The DNA pellet was dried and dissolved for 10 minutes at 68 °C in Tris-EDTA buffer (10 mM Tris-HCl, pH 8; 1 mM EDTA) and quantified at 280 nm using a Fluorescent DNA Quantitation Kit (Biorad, California, USA). Dilutions of calf thymus DNA were used to determine a standard curve. DNA was loaded on a gel for illustration (Gene Ruler 1kb DNA ladder, Thermo Scientific).

3.3.3 Cytotoxicity measurement

To evaluate a potential tissue toxicity, the decellularized tissue pieces were extracted using Dulbeccos Modified Eagle´s Medium (DMEM) containing 10 % (v/v) FBS for 48 hours at 37 °C. 3T3/J2 mouse fibroblast feeder cells (a donation from Julie Daniels, Moorfields Eye Hospital) were seeded in opaque-walled 96 well plates at a density of 50000 cells per well and cultured over night with DMEM containing 10 % (v/v) FBS. The next day, the medium was removed and 100 µl of the conditioned medium or DMEM with 10 % (v/v) FBS (control) was added to the tissue. After one hour and 24 hours, respectively, the amount of viable cells was measured by determining the number of viable cells based on the ATP amount as an indicator of metabolically active cells with a commercially available cell viability assay according to the manufacturer´s description (CellTiter-Glo® Luminescent Cell Viability Assay, Madison, USA). Briefly, 100 µl of the provided reagent containing recombinant luciferase was added to each well, the content was mixed for two minutes on an orbital shaker and incubated for ten minutes at room temperature. The luminescence was recorded with a VICTOR™ X multilabel plate reader (PerkinElmer, Waltham, MA, USA). More luminescence indicated higher ATP amounts based on the fact that the

mono-oxygenation of luciferin is catalyzed by luciferase when magnesium, ATP, and molecular oxygen are present. The medium-luminescence was taken as background signal and subtracted from each sample value.

3.3.4 Western blotting

Denaturated protein samples of native and decellularized LG were separated by 8 % (v/v) Bis-Tris gels and blotted to polyvinylidene fluoride (PVDF) membranes (Roche, Mannheim, Germany). The membranes were blocked with 5 % (w/v) skimmed milk powder in Tris-buffered saline with 0.05 % (v/v) Tween 20 (TBST) for one hour at room temperature and incubated over night at 4 °C with anti-collagen IV (rabbit polyclonal, dilution 1:250), anti-laminin (rabbit polyclonal, dilution 1:500), or anti-fibronectin (mouse monoclonal, dilution 1:200) (all Abcam, Cambridge, England). As secondary antibodies, the peroxidase-conjugated goat-anti-rabbit (Sigma-Aldrich, dilution 1:10,000), horse-anti-mouse (Cell Signaling, dilution 1:4,000), and goat-anti-mouse (Sigma-Aldrich, dilution 1:10,000) antibodies were used for one hour at room temperature. Mouse-anti-β-actin (Sigma-Aldrich, dilution 1:10,000) served as housekeeping protein.

3.4 Cell culture

3.4.1 Cell culture medium

The 3T3/J2 mouse fibroblasts were maintained in DMEM (Dulbecco´s modified Eagle´s medium, Life Technologies, Carlsbad, California, USA) supplemented with 10 % FBS (v/v) (Life Technologies). Epithelial cells were cultured in an epithelial cell culture medium (ECM) (DMEM with glutamax (DMEM/F12)) supplemented with 10 % (v/v) fetal bovine serum (FBS) (Life Technologies), 0.4 µg/ml hydrocortisone, 0.1 nM cholera toxin, 0.18 mM adenine, 5 µg/ml transferrin, 5 µg/ml insulin (all Sigma-Aldrich), 10 ng/ml EGF, and antibiotic/antimycotic solution (Life Technologies). Cells were cultured at 37°C at 5% CO_2.

3.4.2 3T3/J2 feeder cells

The 3T3/J2 mouse fibroblast feeder cells (a donation from Julie Daniels, Moorfields Eye Hospital, London, UK) were routinely maintained by seeding a 1:5,000 or 1:10,000 split of subconfluent cells in 75 cm^2 flasks. The medium was changed every two to three days. For co-culture application, the 3T3/J2 cells were inactivated with *10^{-5} M mitomycin C* for two hours, washed with PBS, incubated with 1 % (w/v) in for

about five minutes to detach the cells from the bottom of the culture flask, centrifuged at 1000 rpm for five minutes, resuspended with culture medium, and seeded at a density of $2.4x10^4$ cells per cm^2 in DMEM containing 10 % (v/v) FBS. After allowing the 3T3/J2 cells to attach, the medium was removed and the LG acinar cells were cultured on the feeder layer in ECM.

3.4.3 Epithelial cell suspension culture

For SC the gland was washed with warm PBS, the surrounding fatty and connective tissue was removed from the gland and a 100 mm^3 LG piece (10 mm length x 5 mm width x 2 mm height) was chopped into smallest pieces using forceps while keeping it lightly moistened with ECM. The pieces were transferred into 50 ml Falcon tubes (Falcon™ 50 ml Conical Centrifuge Tubes, Fisher Scientific, Pittsburgh, Pennsylvania, USA) containing Hank´s Balanced Salt Solution (Thermo Scientific, Waltham, Massachusetts, USA) and the solution was allowed to stand until the tissue pieces had settled. The supernatant was removed and the previous step was repeated using serum free cell culture medium (Ham´s F12 Nutrient Mixture, Thermo Scientific, Waltham, Massachusetts, USA). After removal of the supernatant, the pieces were incubated with an enzyme cocktail containing collagenase (350 U/ml), hyaluronidase (300 U/ml), and DNase (40 U/ml) (Sigma-Aldrich, Schnelldorf, Germany) for 20 minutes at 37 °C under intermittent shaking. Thereafter, the solution was mixed, the tissue pieces further comminuted manually with a pipette, and again incubated in the same enzyme cocktail for 30-40 minutes at 37 °C under intermittent shaking until the solution became opaque. The suspension was filtered through a 70 µm mesh (Roth, Karlsruhe, Germany), centrifuged at 100 G for five minutes (Heraeus Megafuge 16, Thermo Scientific, Schwerte, Germany), and filtered through a Ficoll gradient (from bottom to the top: 4 %, 3 %, 2 %, each 5 ml) (Sigma-Aldrich). The cell pellet was re-suspended with ECM, centrifuged again 100 G for 5 minutes, resuspended with ECM and the cells seeded at a density of $4x10^4$ cells per cm^2 onto the 3T3/J2 feeder cells.

3.4.4 Epithelial cell explant culture

For EC the gland was washed with warm PBS, the surrounding fatty and connective tissue was removed from the gland and an approximately 1.5 mm x 1.5 mm x 1.5 mm LG piece was torn into smallest possible pieces using forceps while keeping it lightly moistened with ECM. Fifteen to 20 pieces were spread onto a 3T3/J2 feeder layer

and allowed to dry for five to ten minutes, which induced attachment to the culture flask before ECM was carefully added. The time required for SC and EC from starting the tissue preparation until putting the flasks into the incubator was stopped with a stopwatch (n=3).

3.5 Recellularization of the decellularized matrices

For recellularization, decellularized LG pieces of about three mm diameter were stored in cell culture medium for a minimum of 12 hours and dap-dried on sterile, non-woven swabs (BeeSana, Beese, Barsbüttel, Germany). Pieces were put into 96 well plates (one piece per cavity), one million cells in 150 µl ECM carefully added to each piece and allowed to adhere for three hours. Thereafter, 100 µl fresh ECM were added carefully aside the reseeded pieces. The medium was changed daily.

3.5.1 Testing for secretory capacity (ß-hexosaminidase assay)

After passage zero at 80 % confluence, the cells were washed with warm PBS and incubated with 1 % (w/v) trypsin for about five minutes to detach the 3T3/J2 feeder cells from the bottom of the culture flask. The trypsin reaction was stopped with DMEM containing 10 % FBS (v/v) and the cells were washed three times with warm PBS carefully to remove the feeder cells. To detach the epithelial cells, they were incubated with 10 % (v/v) trypsin. The reaction was stopped with DMEM containing 10 % (v/v) FBS and the suspension was centrifuged at 3000 rpm for five minutes. The cells were resuspended with ECM and seeded at a density of $5x10^5$ cells per well in 24 well plastic plates (Corning® Costar® cell culture plates, Sigma Aldrich, St. Louis, Missouri, USA). Three wells were set for each biological replicate. The cells were allowed to adhere over night, then washed three times with 500 µl serum free DMEM and incubated with 500 µl serum free DMEM for two hours to determine the baseline value. After removal of a baseline sample carbachol was added at a final concentration of 100 µM, the cells were incubated for 15 minutes and a stimulated sample was removed. All samples were centrifuged for five minutes. For measurement of ß-hexosaminidase activity, 4-methylumbelliferyl N-acetyl-β-D-glucosaminide (Sigma) was dissolved in 133 mM citric acid with 133 mM NaCl at pH 4.3 and used as substrate at a concentration of 7.5 mM. Fluorescence intensity was determined at 360 nm excitation and 450 nm emission (FLUOstar Omega, BMG LABTECH, Ortenberg, Germany).

3.6 Protein detection

3.6.1 Hematoxylin and Eosin staining

For H&E staining, paraffin embedded sections were cut with a microtome (RM2255, Leica, Wetzlar, Germany) (6 µm) were deparaffinized using Xylol for five minutes twice. The sections were then rehydrated using decreasing alcohol concentrations starting with 100 % isopropanol for one minute twice, then 96 % (v/v), 70 % (v/v), and 50 % (v/v) ethanol for one minute, respectively (all Carl Roth GmbH&Co.KG, Karlsruhe, Germany)). Finally the sections were washed in bi-distilled water for one minute, incubated in hematoxylin solution for five minutes, and washed with bi-distilled water. The sections were rinsed in running tab water for five minutes and incubated in eosin solution for seven minutes, dipped into 70 % (v/v) ethanol, incubated in 96 % (v/v) ethanol for two minutes twice, and 100 % ethanol for five minutes twice, finally incubated in Xylol for five minutes twice and embedded (Roti-Histokit 2, Carl Roth GmbH&Co.KG).

3.6.2 Periodic acid Schiff reaction

For PAS / alcian blue reaction (Merck, Darmstadt, Germany), sections were deparaffinized and rehydrated as described above, incubated in alcian blue solution for five minutes, washed with running tab water for three minutes, rinsed with distilled water, and incubated with Schiff´s reagent for 15 minutes. Nuclear staining was performed with hematoxylin solution for five minutes and the sections were embedded (Roti-Histokit 2, Carl Roth GmbH&Co.KG).

3.6.3 Immunohistochemistry and Immunocytochemistry

For immunostaining, pan-anti cytokeratin (mouse monoclonal, ab6401, dilution 1:400, Abcam), anti-smooth muscle actin (SMA) (mouse monoclonal, M0851, dilution 1:400, Dako), anti-vimentin (rabbit monoclonal, D21H3, dilution 1:500, Cell Signaling), anti-Rab3D-C-terminal (rabbit polyclonal, ab170057, dilution 1:200, Abcam), anti-collagen IV (rabbit polyclonal, dilution 1:250), anti-laminin (rabbit polyclonal, dilution 1:500), and anti-fibronectin (mouse monoclonal, dilution 1:200) were used (all Abcam, Cambridge, England). To induce antigen retrieval in paraffin sections, the slices were deparaffinized as described above, washed with PBS, and boiled for five minutes in 0.01 M citric acid buffer at pH 6 containing 0.05 % (v/v) Tween 20, and cooled at room temperature. Cryosections were washed with PBS for ten minutes, fixed with

methanol for ten minutes, and permeabilized with 0.1 % (v/v) Triton X100 in PBS. The cells were fixed with ice-cold methanol or 10 % (v/v) PFA at room temperature for five miuntes. The slices or cells were blocked for one hour at room temperature with 5 % (v/v) normal goat serum (VWR), incubated over night at 4 °C with the primary antibody, washed, and incubated with the appropriate fluorochrome-conjugated secondary antibody (Alexa flour®) for one hour at room temperature. As a control, the samples were incubated with the secondary antibody, only. Microscopic analysis and visualization was performed with an optical microscope (Leica DM4000 B and camera system Leica DFC450 C, or with BIOREVO BZ9000, Keyence, Montabaur, Germany). Human LG are shown for comparison purposes (kindly provided by the Institute for Anatomy I, Heinrich-Heine-University Düsseldorf). LG were obtained from whole body donors and prepared by Robert Kubitza, technical assistant.

3.6.4 Flow cytometry

For cytokeratin staining, the cells were fixed with Cytofix/Cytoperm™ buffer supplemented with 0.2 % (v/v) Triton X-100 for 30 minutes at 4 °C (BD Bioscience, Heidelberg, Germany) and washed with appropriate washing buffers. One million cells were incubated with 2 µl of Alexa Fluor® 488 conjugated isotype control antibody (mouse IgG1 kappa) or with Alexa Fluor® 488 conjugated anti-pan-cytokeratin (AE1/AE3) antibody (both eBioscience, Affymetrix, Santa Clara, California, U.S.) for 30 minutes at room temperature.

An ALDEFLOUR™ kit was used for the detection of aldehyde-dehydrogenase-1 (ALDH-1) activity (StemCell Technologies, Köln, Germany). One million cells were incubated with 1 µmol/L ALDH substrate-containing buffer or with 50 mmol/L of the ALDH-1 specific inhibitor diethylaminobenzaldehyde (negative control) for one hour at 37 °C in the dark. Excitation was performed using a 20 mW 488 nm Argon-laser and emission was detected at 520 nm in FL1.

Hoechst 33342 dye exclusion technique was used for side population analysis. One million cells were incubated for 90 minutes at 37 °C in DMEM containing 2 % (v/v) FCS either with 5 µg/ml Hoechst 33342 or 50 µM verapamil (Sigma-Aldrich). For nuclear staining 2 µg/ml propidium-iodide were added. The analysis was performed with a flow cytometer (Cyflow Space Partec, Münster, Germany) equipped with a 16 mW 375 nm UV-laser diode for excitation and emission was detected at 455 nm in

FL4 and 660 nm in FL5. Data presentation and processing were performed using the FLoMax-software (Quantum Analysis, Münster, Germany).

3.7 Cell population doublings and colony forming assay

For calculation of the cell population doubling time (PDT) the formula PDT [d]=H*ln2 / ln(c2/c1) was used with H=duration of passage (days), c2=cell count at the end of the passage, c1=cell count at start of the passage. To determine the colony-forming units, 3T3/J2 feeder cells were seeded at a density of $2.4x10^4$ cells per cm^2 into six well plates and 1,000 epithelial cells per well were plated on the feeder layer. The cells were fixed after 8-12 days and stained with 1 % (w/v) Rhodamine red (Sigma-Aldrich). Cell aggregates with more than 50 cells were considered as a colony-forming unit.

3.8 Electron microscopy

For electron microscopy, two to three mm diameter pieces of native and porcine LG were washed carefully with PBS three times. At 80 % confluence after passage zero, SC or EC cells were harvested by two trypsinization steps (step 1: 1 % (w/v) with trypsin EDTA for about five minutes at room temperature for detachment of the 3T3/J2 feeder cells, step 2: 10 % (v/v) trypsin EDTA for five to ten minutes at room temperature for detachment of the epithelial cells). The EC cells were filtered through a 40 µm mesh (Roth, Karlsruhe, Germany) to remove residual tissue pieces.

The tissue pieces of the native or decellularized LG and the SC- or EC-cell pellets were fixed in 2.5 % (v/v) glutaraldehyd with 4 % (v/v) PFA in 0.1 M cacodylate buffer and embedded in Spurr media (Modified SPURR Embedding Kit, Serva, Heidelberg, Germany). The tissue block was cut into 60-80 nm thin sections and analyzed with a Hitachi H600 transmission electron microscope (Krefeld, Germany). Images were taken with a Gatan BioScan camera (München, Germany). Tissue sectioning and capturing were performed by Dr. med. Klaus Zanger and Elisabeth Wesbuer (technical assistant) of the Core Facility Electron Microscopy, Institute of Anatomy I, Heinrich-Heine-University Düsseldorf.

3.9 Statistical analysis

All experiments were performed with a minimum of three biological replicates. For statistical analysis SPSS 21.1 was used (IBM, Ehningen, Germany). To analyze the significance of difference between related or unrelated samples a paired or

independent Student´s t-test were applied with $p \leq 0.05$ as level of significance. To describe the amount of data variation mean ± standard deviation were calculated. For multiple testing Bonferroni post hoc testing was applied.

4 Results

4.1 Main cell types of the porcine lacrimal gland

The different cell types of the porcine lacrimal gland were not analyzed previously, so that immunostaining for detection of the main expected cell types, which are epithelial, myoepithelial, and mesenchymal cells, was performed. As the human LG, the porcine LG predominantly contained acinar and ductal epithelial cells. Herein, the acinar cells are the secretory active endpieces, which drain into the ducts carrying the fluid to the ocular surface (Schechter et al., 2010). Another abundant cell type in the human LG are the myoepithelial cells, which express alpha SMA (Obata, 2006). These cells surround the acinar and ductal epithelial cells in an octopus like manner and have been found to cover 80 % of the initial ductal segments in human LGs (Schechter et al., 2010). A similar configuration was found in the porcine LG in this work. Vimentin expressing mesenchymal cells are the third dominant cell type normally found in the human LG and are predominantly located interstitially. This configuration was also true for the porcine LG (Figure 6).

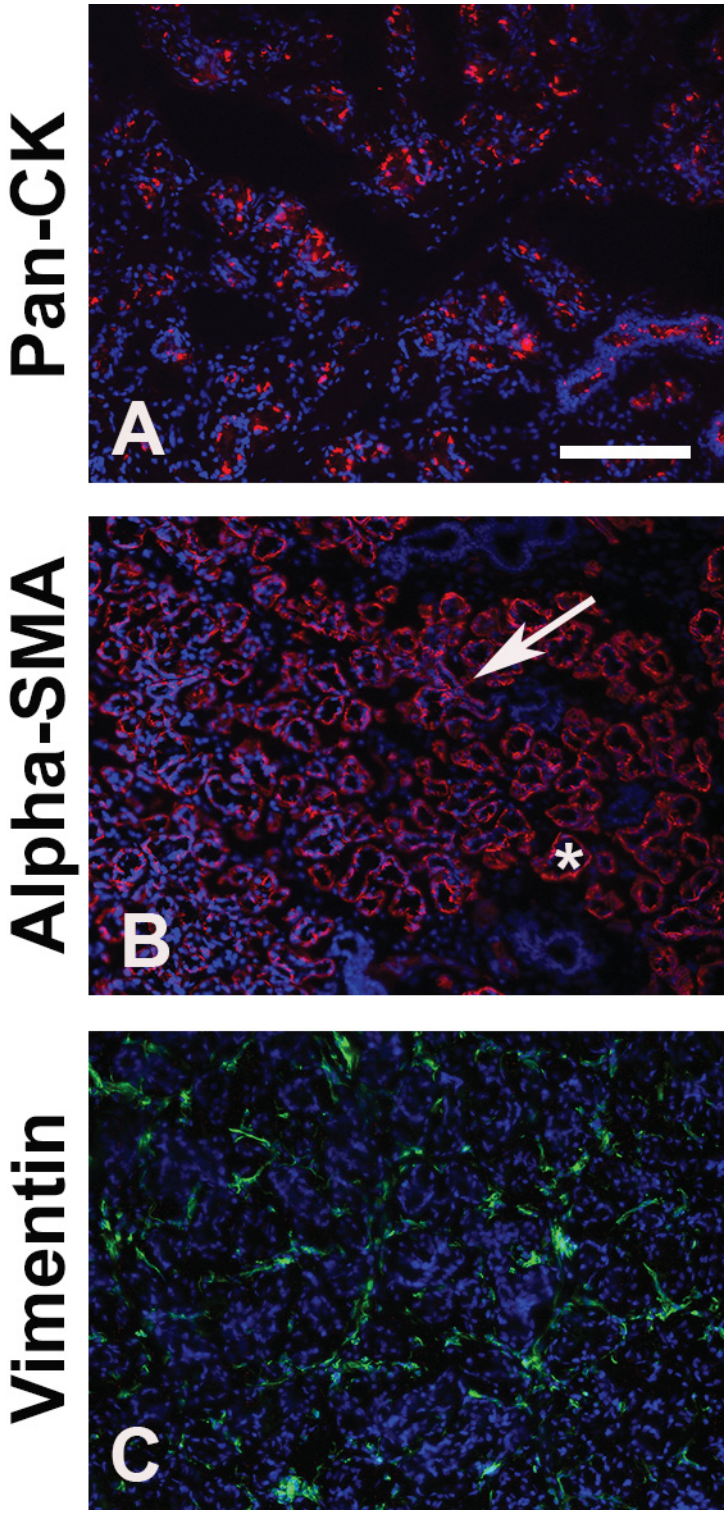

Figure 6: Main cell types of the porcine lacrimal gland. A: Most cells were pan-cytokeratin (Pan-CK) expressing acinar and ductal epithelial cells (red). B: The acini (asterisk) and some ducts (arrow) were surrounded by alpha-smooth muscle actin (Alpha-SMA) expressing myoepithelial cells (red). C: Vimentin expressing cells (green) were found predominantly in the connective tissue between the acini and ducts. Nuclei were counterstained with DAPI (blue). A-C: scale bar 100 µm.

4.2 Decellularized porcine lacrimal gland

Compared to the tissue wet weight, dehydration reduced the tissue weight by 62.8±10 % to around 37.1±10 % (66.5±30 mg to 22.8±9 mg, $p<0.001$). The decellularization process reduced the weight by 78.6±3 % to 21.4±3 % of the original tissue weight (102.5±15 mg to 22.3±6 mg, $p=0.03$), which was a further decrease of around 16 % and indicates the loss of cells through the decellularization process. This process resulted in a whitish, stable tissue, which appeared to have a sponge like structure (Figure 7).

The H&E staining showed a nearly complete removal of the cellular components after decellularization while the basket-like extracellular matrix structure of the acini was mainly preserved apart from some connective tissue-interruptions (Spaniol et al., 2015). As a main extracellular matrix component is collagen, the electron microscopic analysis showed a collagen network with intact collagen fibers while no cellular debris was visible (Figure 8) (Spaniol et al., 2015).

To verify the collagen-preservation quantitatively, the mean collagen I-V content was measured. The collagen content decreased non-significantly from 20.7±4.1 % in the native LG to 13.7±2.6 % in the decellularized LG ($p=0.08$) (Figure 9) (Spaniol et al., 2015).

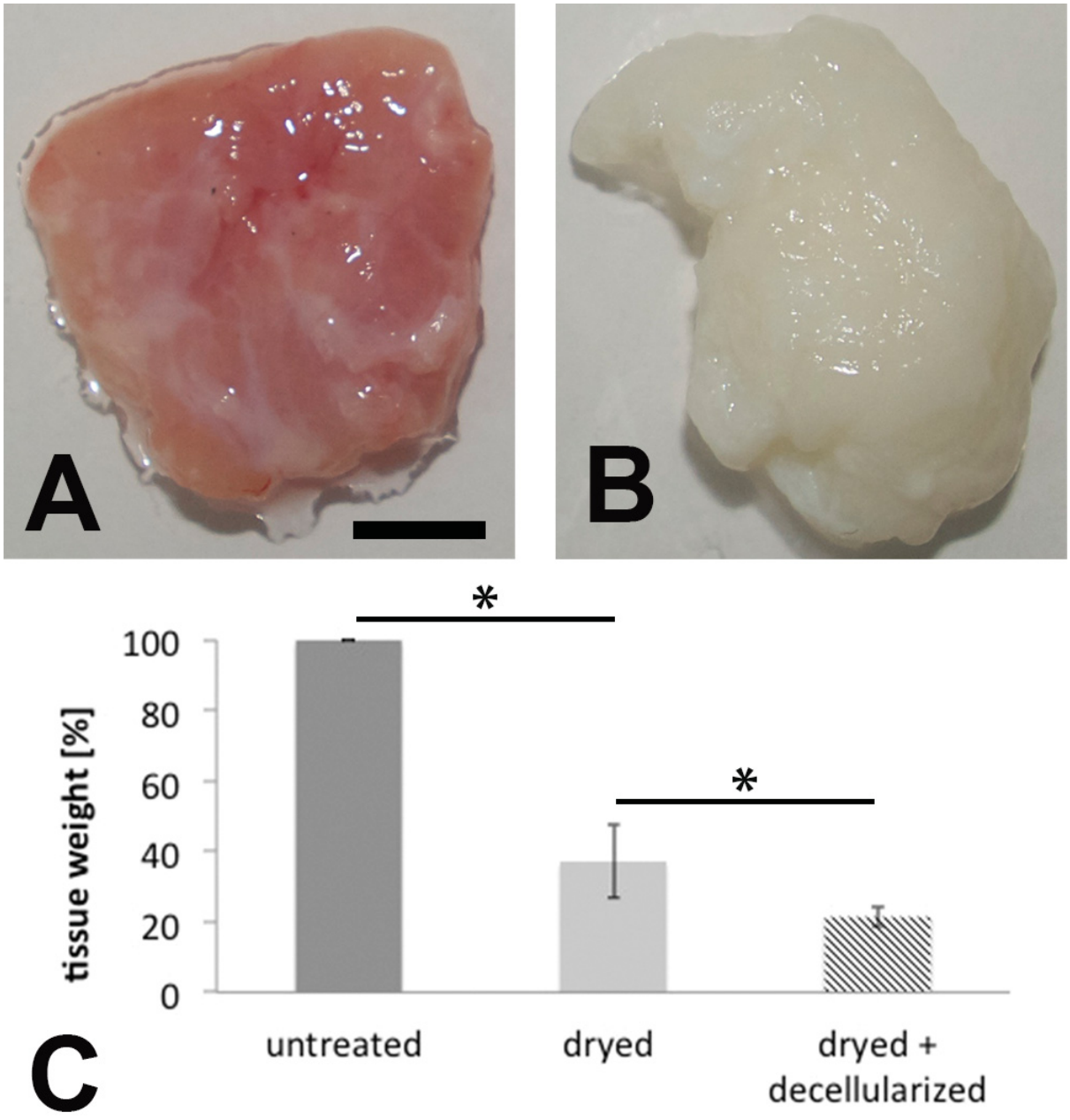

Figure 7: Comparison of native and decellularized lacrimal gland (LG) tissue.
A: The untreated LG revealed a reddish color and a stable, three-dimensional shape. B: Compared to the untreated gland, the decellularized LG exhibited a whitish color indicating loss of residual blood and cells. It still comprised a stable, three-dimensional structure and seemed to have a sponge like texture (Spaniol et al., 2015). C: Comparing the percentage tissue weight, dehydration caused a significant weight-reduction of around 63 % percent ($p<0.0001$), while the decellularization process induced a further tissue weight decrease of around 16 % ($p=0.03$). A, B: scale bar 1 mm.

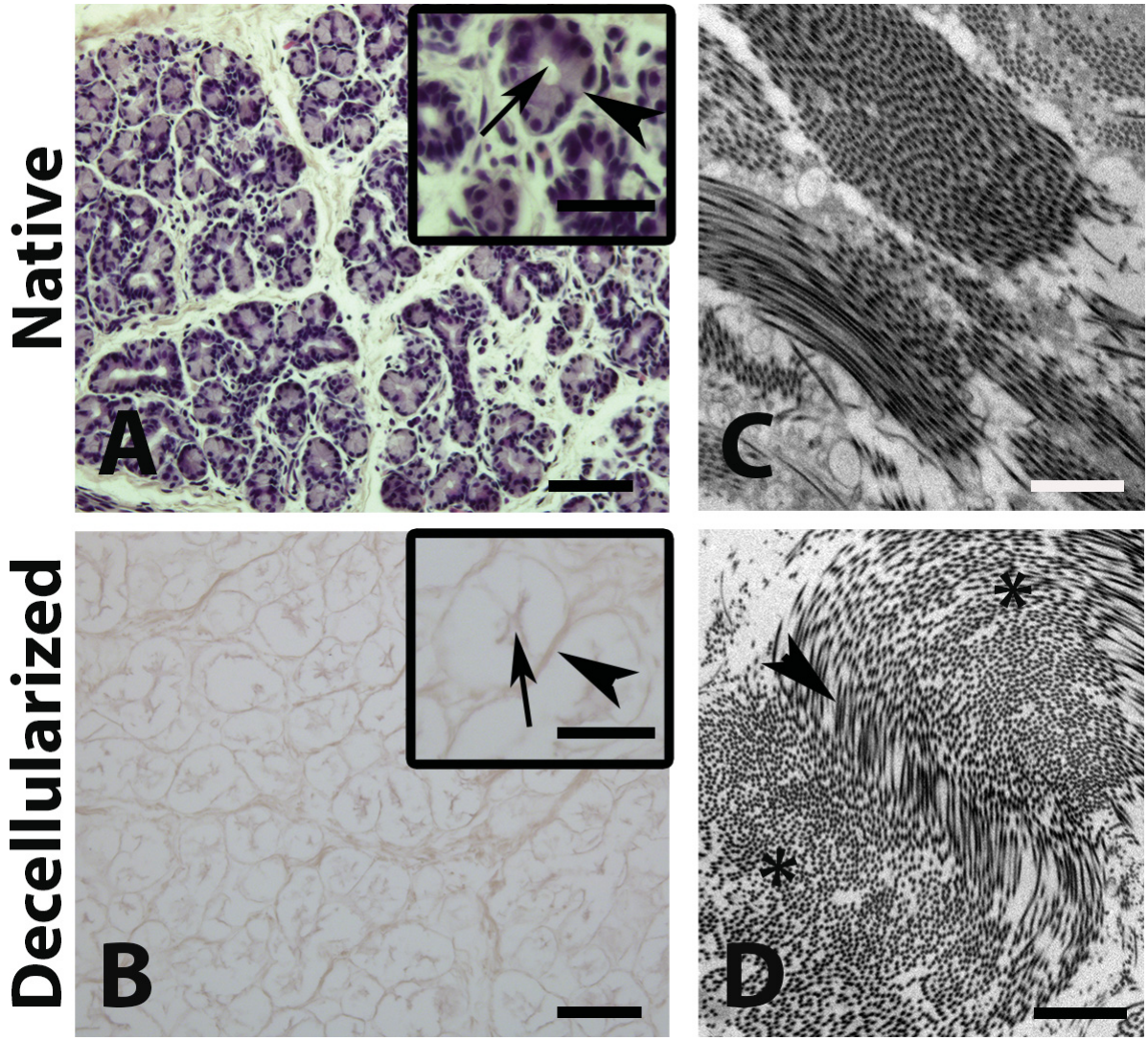

Figure 8: Histological analysis of the untreated and decellularized lacrimal gland (LG).

(Native LG upper row, decellularized LG below) A, B: The hematoxylin and eosin staining of the untreated (A) and decellularized LG (B) revealed that the extracellular matrix structure forming the basket-like acini (arrowhead) and a central lumen (arrow) was at large preserved after decellularization. C, D: The ultra-structural analysis by transmission electron microscopy showed that the collagen network of the native gland (C) was mainly preserved after decellularization (D) showing longitudinal (arrowhead) and transverse (asterisk) sections through the collagen fibers. A, B: scale bar 100 µm, box: scale bar 25 µm; C, D: scale bar 2 µm (Spaniol et al., 2015).

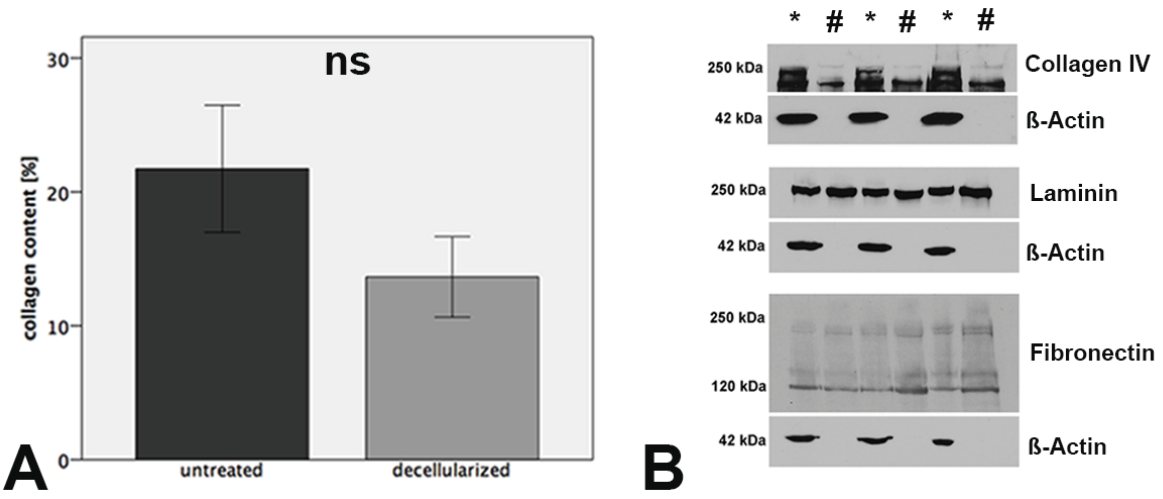

Figure 9: Collagen quantification and immunoblotting of extracellular matrix proteins.

A: The quantitative measurement of the percentage collagen I-V content revealed a non-significant collagen decrease in the decellularized lacimal gland compared to the untreated tissue. B: Comparing the untreated (asterisk) with the decellularized tissue (rhomb), immunoblotting for the basement membrane proteins laminin, fibronectin, and collagen IV showed a decrease in the collagen IV content while laminin and fibronectin were mainly preserved. The absence of ß-actin in the decellularized tissue underlined the removal of cytoplasm and nuclei due to the decellularization process (Spaniol et al., 2015).

4.2.1 Basement membrane components

In the untreated LG, collagen IV and laminin were expressed at the basement membrane of the acini and ducts, remodeling the basket-like structure of the acini (Figure 10). After decellularization, these proteins were still expressed at the basement membranes and the net-like structure was mainly preserved (Spaniol et al., 2015). However, some interruptions of the otherwise linear staining indicated interruptions of the extracellular matrix or loss of the basement membrane proteins to some extent. The third main basement membrane protein analyzed in this work was fibronectin. Before and after the decellularization process it revealed a more diffuse staining of the extracellular matrix, which was not limited to the basement membrane (Spaniol et al., 2015). To verify the preservation of collagen IV, laminin, and fibronectin, immunoblotting was performed (Figure 9). The collagen IV amount was found to be reduced but still clearly evident after decellularization. Laminin and fibronectin were similarly expressed before and after decellularization (Spaniol et al., 2015).

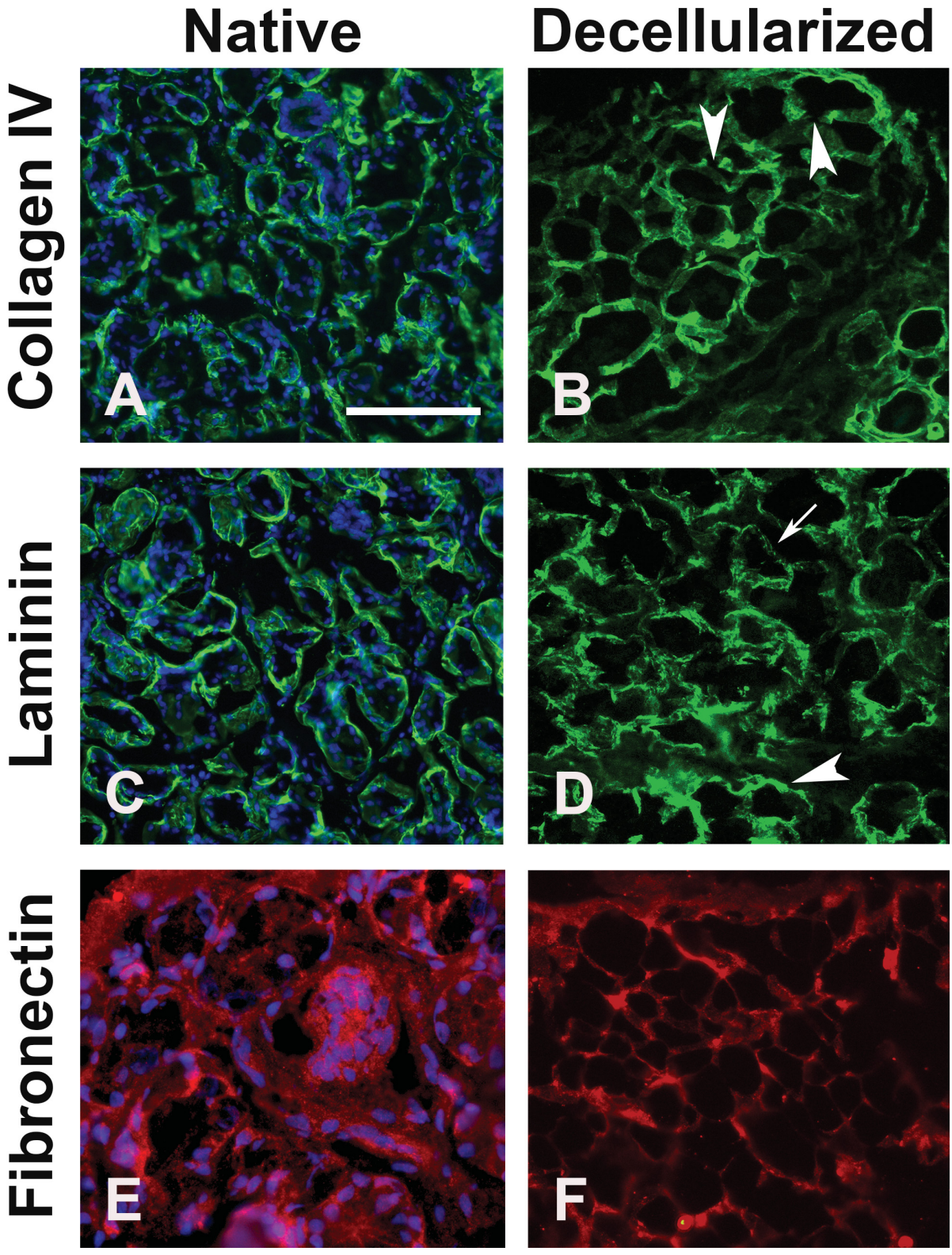
Native
Decellularized
Collagen IV
Laminin
Fibronectin
A
B
C
D
E
F

Figure 10: Basement membrane components in the untreated and decellularized lacrimal gland (LG).

(Native LG left, decellularized LG right) A / B: In the native tissue, collagen IV was expressed along the basement membrane of the acini forming basket-like structures. After decellularization collagen IV was still expressed resembling the acinar basement membrane. Some interruptions of the staining were visible due to tissue breaks or diminished collagen IV content. C / D: Similarly to collagen IV, laminin was expressed along the acinar basement membrane before and after decellularization. After decellularization some areas depicted a more intense staining (arrowhead) while some exhibited a patchy staining pattern (thin arrow) compatible with a partial loss of laminin. E / F: The fibronectin expression was more diffuse, not limited to the basement membrane, and seemed to be also located intracellularly. After decellularization, the expression along the acinar basement membrane remained. A-F: scale bar 100 µm (Spaniol et al., 2015).

4.2.2 Removal of the cellular components

A first qualitative assessment of the cell removal was done by Feulgen staining, which indicates DNA and chromosomal material by a pink staining. The Feulgen reaction induced an intense pink staining of cellular components in the native gland, while there was no or minimal residual staining in the decellularized LG (Figure 11) (Spaniol et al., 2015).

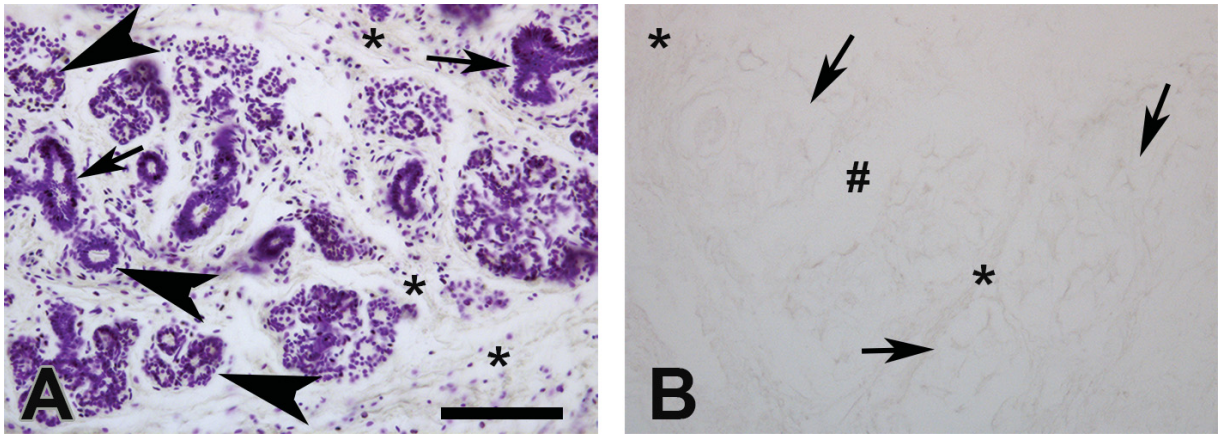

Figure 11: Feulgen reaction of the untreated and decellularized lacrimal gland (LG). A: The Feulgen reaction illustrated the pink staining of the cellular DNA in the untreated LG. The cells formed several acini (arrowhead) and ducts (arrow). Some cells were found in the connective tissue surrounding the acini and ducts (asterisk) likely to be interstitial fibroblasts. B: After decellularization the pink staining was missing, indicating the DNA removal through the decellularization process. Apart from some tissue interruptions (hash) the acinar and duct like structure (arrow) and the surrounding connective tissue (asterisk) were still visible while a clear distinction between acini and ducts was not possible due to the missing cells. A, B: scale bar 100 µm (Spaniol et al., 2015).

To further quantify this finding, a DNA quantification was performed, which revealed a significant DNA reduction from 2565.1±893.5 ng/mg before to 15.2±26.4 ng/mg after decellularization ($p<0,01$) (Figure 12 B) (Spaniol et al., 2015). Further, a DNA gel electrophoresis did not show evidence of DNA residues (Figure 12 A).

Residual cellular material or toxic residues of the decellularization process can harm cells, which are cultured on the matrix. Therefore, a cytotoxicity assay was performed in which 3T3/J2 feeder cells were cultured with conditioned media from the decellularized matrices. This assay showed no toxic effects of the decellularized LG on cultured cells, which confirmed the previous histological results and quantitative DNA measurements indicating absence of potentially toxic cellular material (Figure 12 C) (Spaniol et al., 2015).

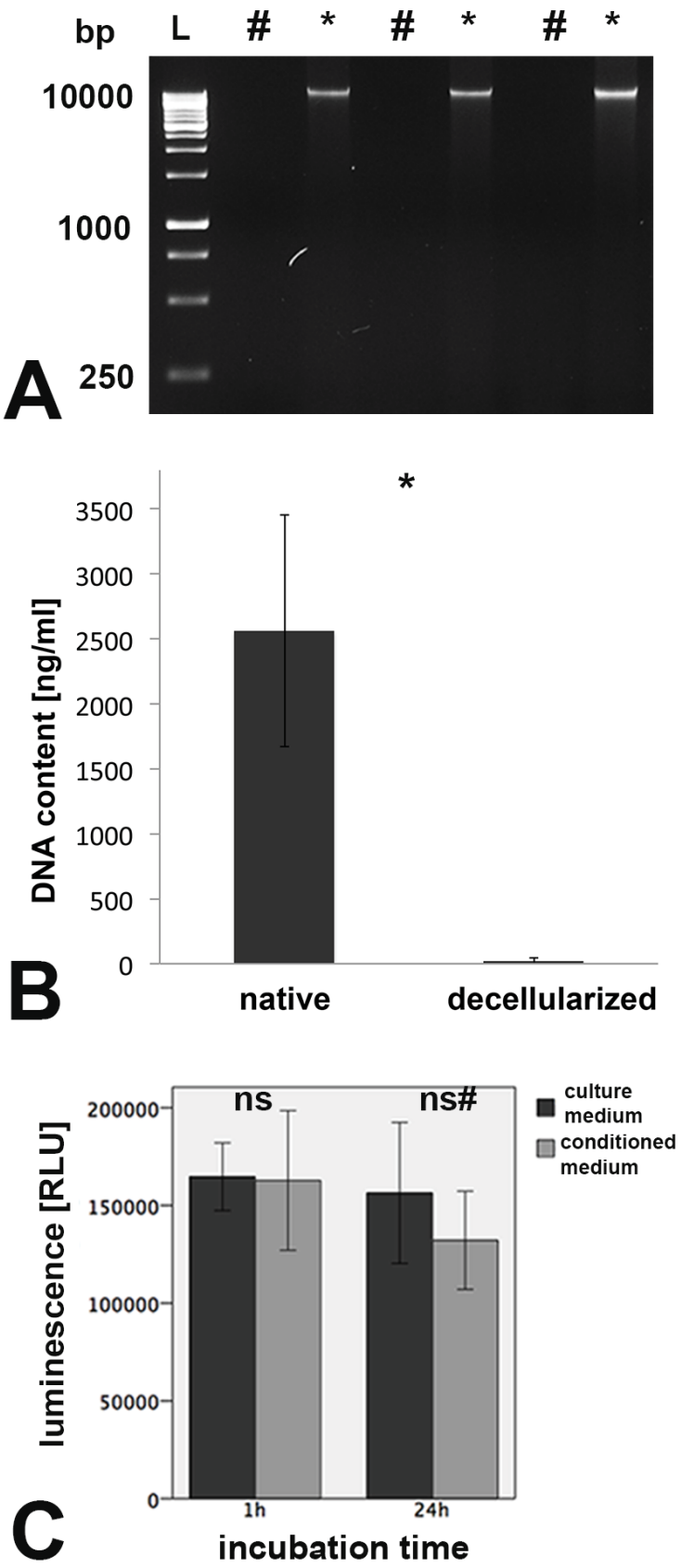

Figure 12: Illustration of the DNA removal and cytotoxicity testing of the decellularized lacrimal gland (DC-LG).

A: The DNA gel electrophoresis of three untreated LG (asterisk) and three DC-LG samples (hash) visualized the absence of DNA in the DC-LG tissue (bp, base pairs) (Spaniol et al., 2015). B: Accordingly, quantification of the DNA content revealed a significant reduction from 2565.1±893.5 ng/mg before to 15.2±26.4 ng/mg after decellularization (*p<0,01).

C: To determine a potential cytotoxicity of the DC-LG, a cytotoxicity assay was performed, which measures the luminescence (RLU, relative light units) as a linear measure of viable cells (X-axis) after incubating 3T3/J2 feeder cells either with standard culture medium or with the conditioned medium of the DC-LG. After one and 24 hours the number of viable cells did not differ significantly (Y-axis; ns, not significant) (ns, p=0.9; ns#, p=0.3) (Spaniol et al., 2015).

4.3 Cell isolation and characterization - comparison of explant and suspension culture cells

4.3.1 Cell gain and phenotype

For both isolation methods, the surrounding connective tissue and fat were removed from the gland. To obtain enough viable cells for cell culture, a 100 mm^3 LG piece was used for the SC method while a 3.4 mm^3 LG piece was sufficient for the EC method. Including all steps the isolation by SC vs. EC took 173±8 min vs. 20±3 min ($p<0.001$). After the above described washing and enzymatic digestion steps, the SC method obtained about 2.8±1.1 million viable cells. Applying the EC method, 2.7±0.6 million viable cells grew out from the explant pieces, which was an about 30 times greater cell gain compared to the SC method in relation to the tissue volume (Spaniol et al., 2015). The SC cells build colonies after three to five days, which became 90 % sub-confluent after 9±1 days while from the explant pieces cells grew out after about seven days and became 90 % sub-confluent after 16±2 days (Spaniol et al., 2015).

Microscopically, cells from SC and EC method both revealed a cobblestone-like, epithelial phenotype (Figure 13). This finding was verified by the expression of pan-cytokeratin demonstrated by immunostaining and verified by flow cytometry (14.7 and 12.6 fold increase in fluorescence intensity compared to the isotype control for the SC and EC cells, respectively) (Figure 13) (Spaniol et al., 2015).

For both isolation methods, few cells exhibited immunoreactivity for the myoepithelial marker alpha-SMA or the mesenchymal marker vimentin (Figure 14) (Spaniol et al., 2015).

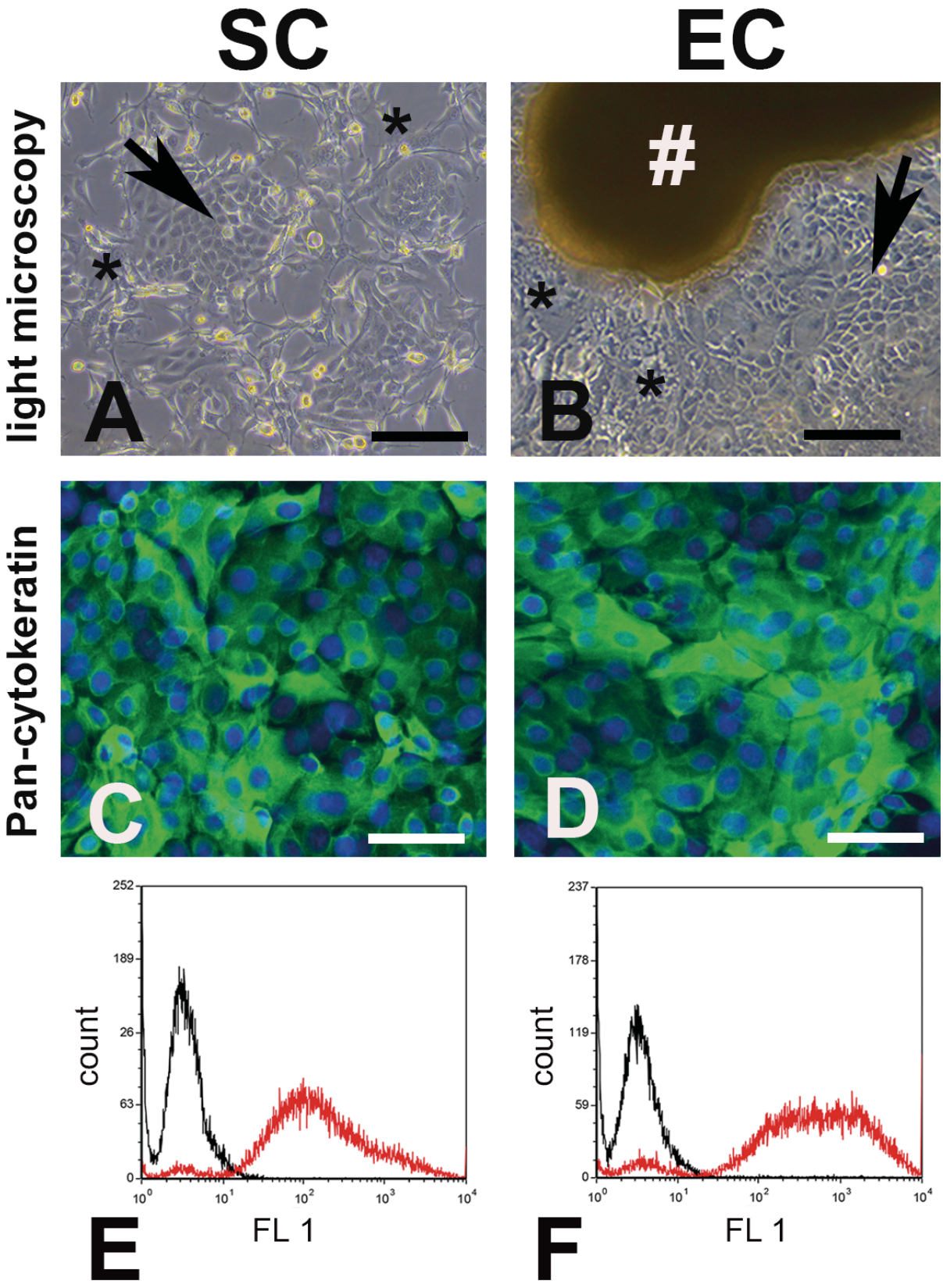
SC
EC
light microscopy
A
B
Pan-cytokeratin
C
D
count
252
189
26
63
0
FL 1
E
count
237
178
119
59
0
FL 1
F

Figure 13: Epithelial phenotype of the suspension culture (SC) and explant culture (EC) cells.

SC cells are illustrated on the right, EC cell on the left. A, B: Regarding cells expanded by SC (A), the epithelial cells (arrow) formed colonies after three to five days while the EC cells (B) grew out from the explants (rhomb) after about seven days. The epithelial cells (arrow) revealed a cobblestone-like morphology and grew between the 3T3/J2 feeder cells (asterisk). C, D: The immunostaining demonstrated the pan-cytokeratin expression of the SC (C) and EC cells (D). E, F: Flow cytometric measurement of the pan-cytokeratin expression. SC (E) and EC cells (F) showed a strong pan-cytokeratin expression (red graph) while the isotype control (black graph) did not exhibit a specific signal. A, B: scale bar 100 µm; C, D: scale bar 50 µm (Spaniol et al., 2015).

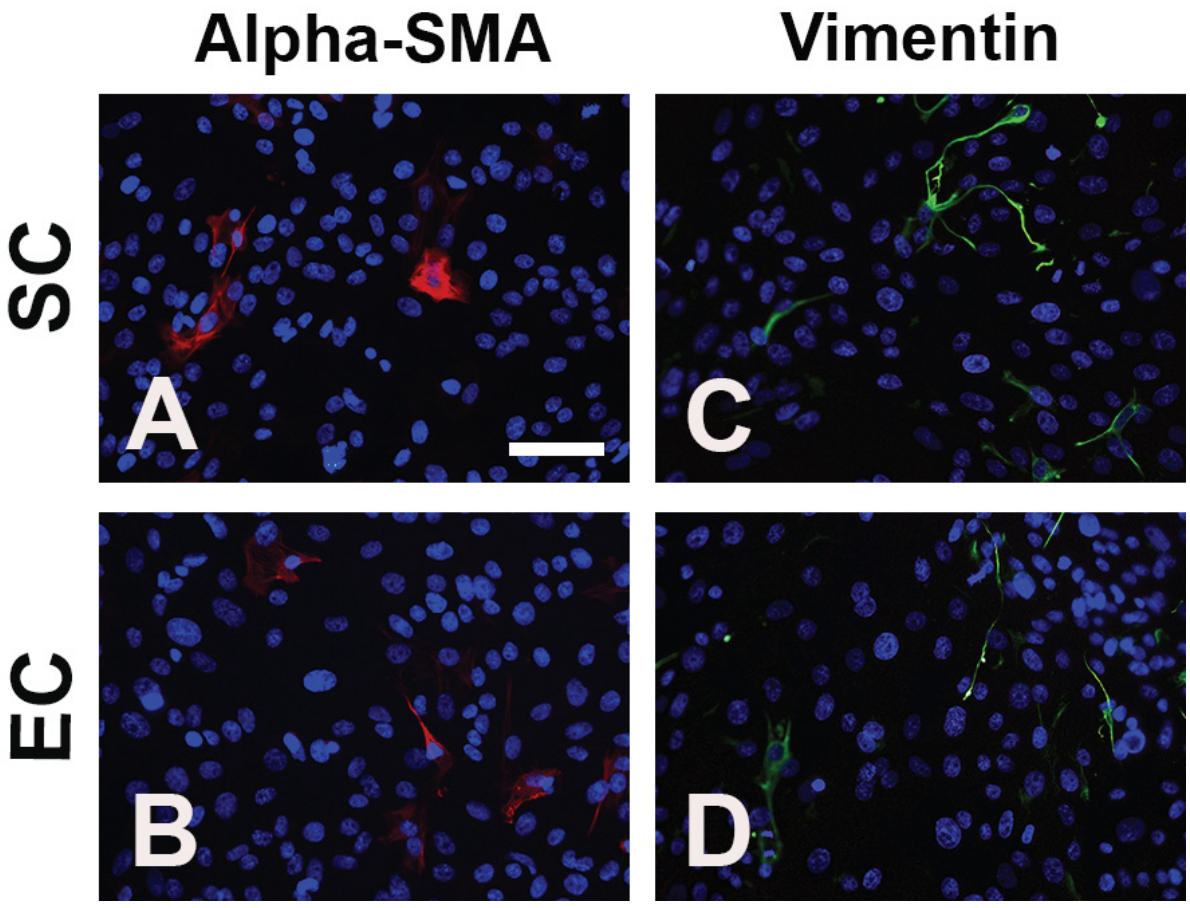

Figure 14: Immunohistochemical characterization of the cultured cells.
(SC cells upper row, EC cells below) A, B: Only few SC and EC cells expressed the myoepithelial marker alpha smooth muscle actin (Alpha-SMA). C, D: Similarly, the mesenchymal marker vimentin was expressed by few SC and EC cells. A-D: scale bar 100 µm.

4.4 Functional capacity

To determine the functional capacity of the cultured cells, the secretory function was tested by the ß-hexosaminidase assay after stimulation with the parasympathetic agent carbachol. The ß-hexosaminidase is a lysosomal hydrolase, which consists of an α- and ß-subunit forming the catalytically active enzyme (Andersson et al., 2006). Both subunits were evident in the SC and EC cells (Figure 15). After parasympathetic stimulation, cells from both isolation methods exhibited a significant secretory response for up to about 35 days of *in-vitro* culture (10-15 days: SC: p=0.004 / EC: p=0.01; 20-25 days: SC: p=0.03 / EC: p=0.04; 30-35 days: SC: p=0.03 / EC: p=0.005). The secretory response was not significantly different between the SC and EC cells (10-15 days: p=0.19; 20-25 days: p=0.88, 30-35 days: p= 0.21) and declined over time for both isolation methods (Figure 16).

The functional capacity was further verified histologically. As demonstrated in the native gland, the cultured cells exhibited secretory granula in the PAS / alcian blue reaction for up to around 30 days of *in-vitro* culture. They further expressed Rab 3D, which has been found to be a marker for mature secretory vesicles (Figure 17 A, B) (Spaniol et al., 2015). Electron microscopy further proofed evidence of the secretory phenotype by showing densely packed secretory vesicles (Spaniol et al., 2015). Cells from both isolation methods comprised vesicle-forming Golgi apparatus indicating metabolic activity (Figure 17 C-F). In line with the decreased secretory response after longer culture duration, the secretory granula were not detectable by PAS / alcian blue reaction after 40-50 days of *in-vitro* culture (Figure 16).

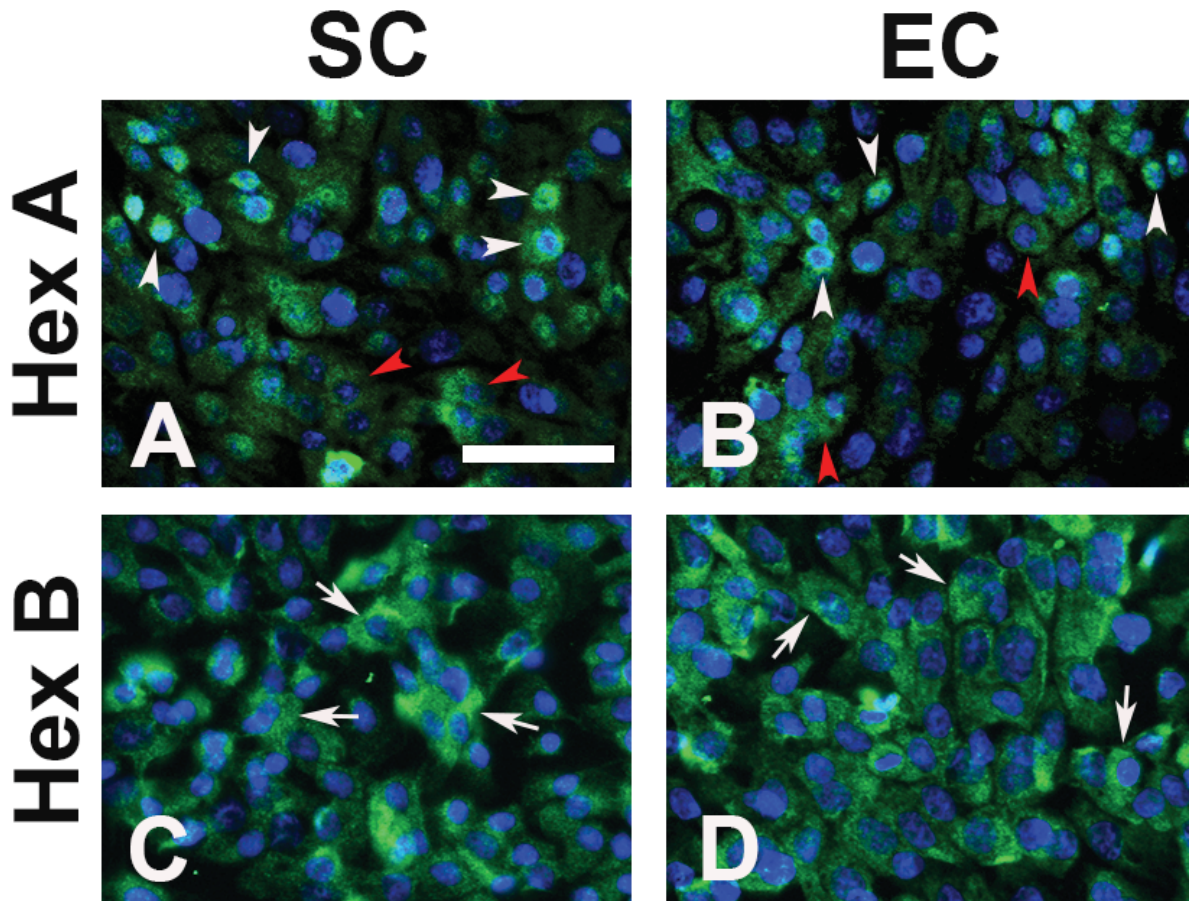

Figure 15: Hexosaminidase-expression in the suspension culture (SC) and explant culture (EC) cells.

(SC cells left, EC cells right) A, B: Cells from both culture conditions expressed hexosaminidase A (Hex A, green), which was predominantly located in the nucleus (white arrowhead) and partly in the cytoplasm (red arrowhead). C, D: The cells also expressed hexosaminidase B (Hex B, green), which was found in the cytoplasm (arrows). Scale bar A-D: 50 µm.

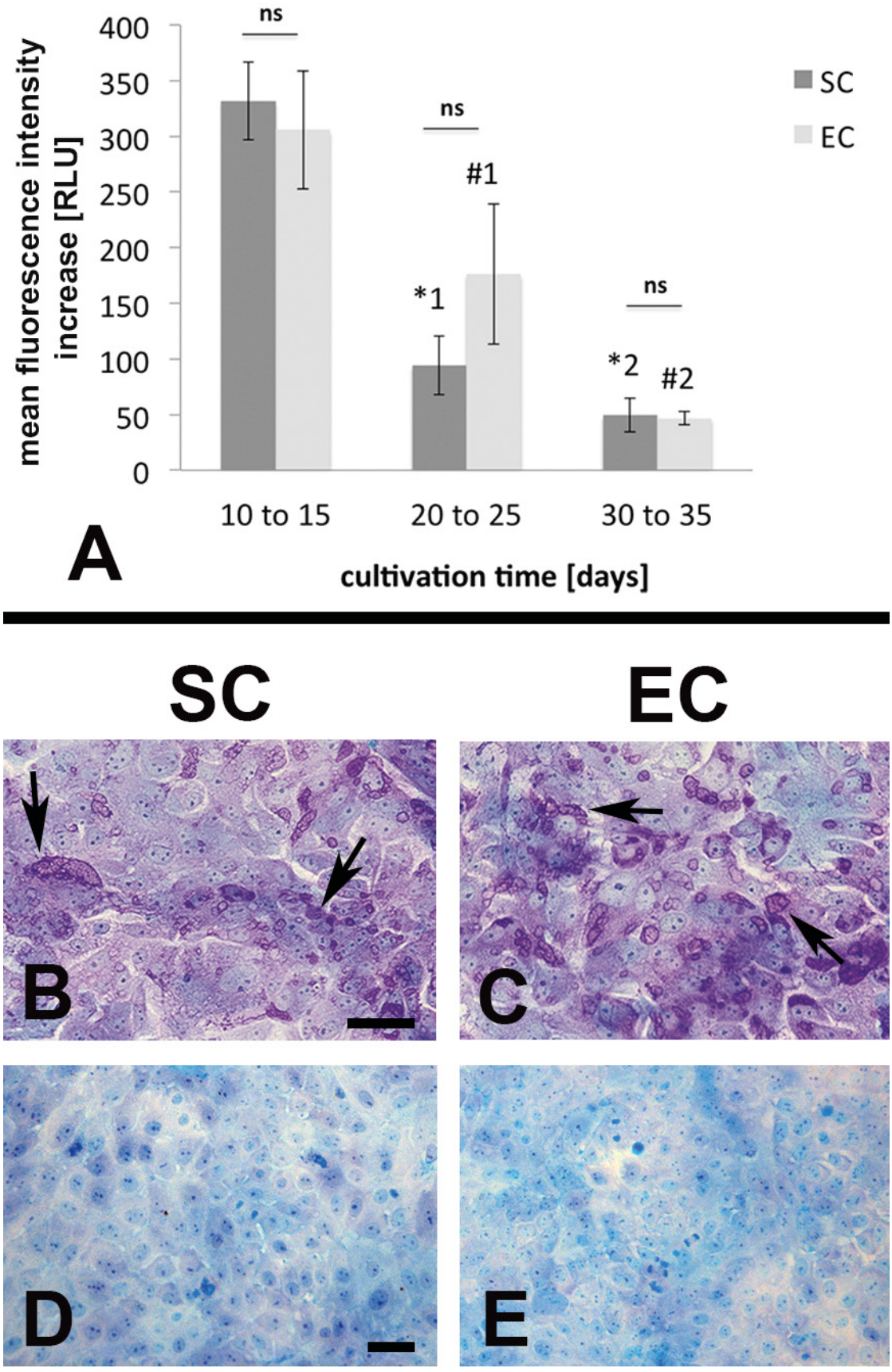
mean fluorescence intensity increase [RLU]
400
350
300
250
200
150
100
50
0
ns
ns
ns
*1
#1
*2
#2
SC
EC
10 to 15
20 to 25
30 to 35
cultivation time [days]
A
SC
EC
B
C
D
E

Figure 16: Secretory capacity of suspension culture (SC) and explant culture (EC) cells.

A: SC and EC cells revealed a secretory response to parasympathetic stimulation with carbachol for a cultivation time of up to 35 days (X-axis) indicated by a significant increase in the mean fluorescence intensity (Y-axis). There was no significant difference comparing the secretory response of SC and EC cells at the different time points (ns). The secretory response declined over time for both culture conditions (SC: *1: p=0.0007, *2: p=0.06. EC: #1: p=0.05, #2: p=0.02). * SC cells; # EC cells. 1: 10-15 days versus 20-25 days; 2: 20-25 days versus 30-35 days. RLU, relative light units. B-E (SC cells left, EC cells right): Perdiodic acid Schiff / alcian blue reaction of the cultured cells A, B: After 10-15 days of *in-vitro* culture SC (B) and EC cells (C) exhibited multiple secretory vesicles as indicated by the pink granular staining (arrows). D, E: After 40-50 days of *in-vitro* culture cells from both culture conditions lost the secretory granula. B, C: scale bar 25 µm. D, E: scale bar 25 µm.

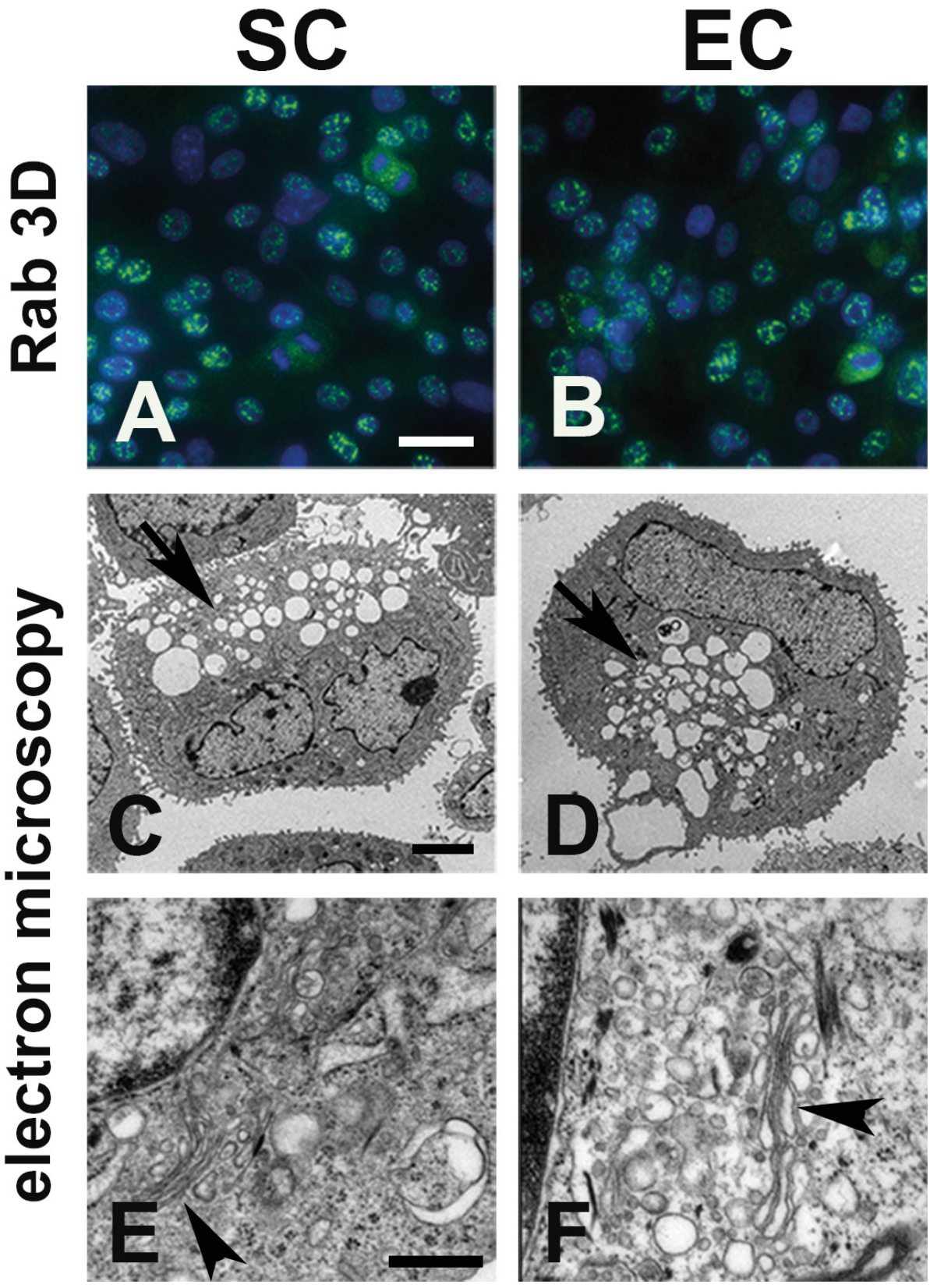
SC
EC
Rab 3D
A
B
electron microscopy
C
D
E
F

Figure 17: Secretory phenotype of the suspension culture (SC) and explant culture (EC) cells.
(SC cells left, EC cells right) A, B: Cells from both culture conditions contained multiple cells expressing Rab 3D (green), a marker for mature secretory vesicles (Spaniol et al., 2015). C-F: Electron microscopy showed multiple secretory vesicles (arrow) in SC and EC cells, while the higher magnification revealed Golgi apparatus (arrowhead) forming vesicular organelles. A, B: scale bar 20 µm. C, D: scale bar 2.5 µm. E, F: scale bar 0.5 µm. Image C-F taken by Dr. med. K. Zanger and E. Wesbuer.

4.4.1 Proliferative capacity and stem cell character

To determine the proliferative capacity of SC and EC cells, population doublings and colony forming units were analyzed until passage three. The population doubling times of cells from both expansion methods did not show significant differences (passage one: p=0.41; passage two: p=0.88; passage three: p=0.20) (Figure 18 A). Counts of colony forming units were performed for cells from passage zero and were not significantly different as SC cells contained 43.3±19.2 and EC cells 51.8±14.0 colony forming units on one thousand cells (p=0.19) (Figure 18 B, C) (Spaniol et al., 2015).

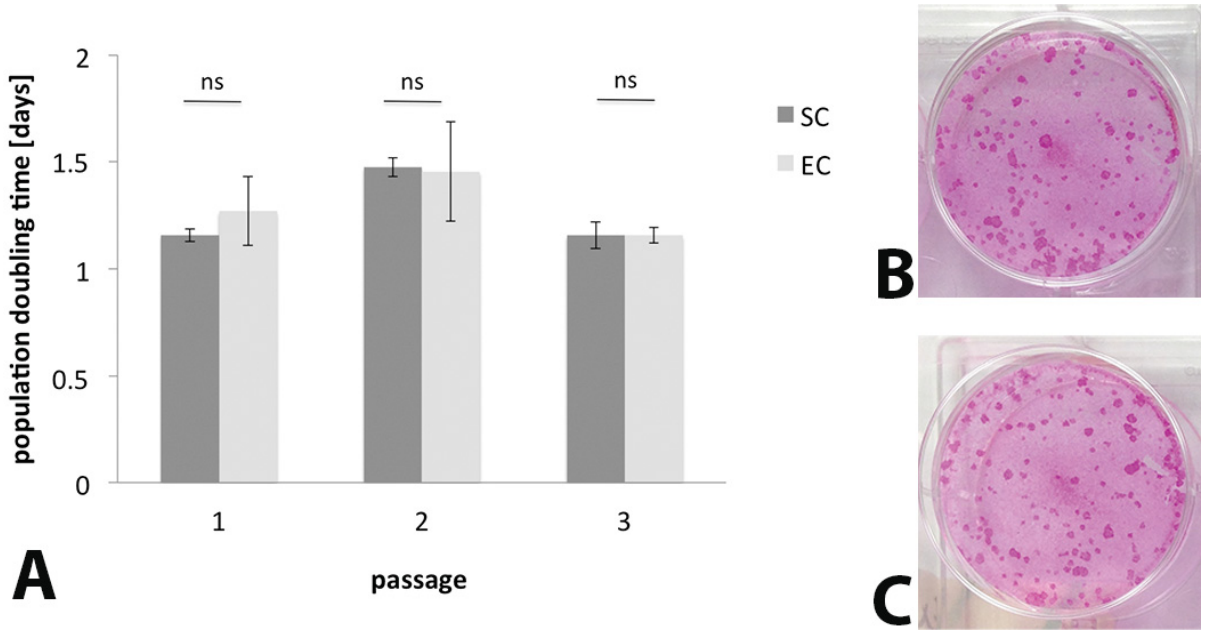

Figure 18: Population doublings and colony forming units of suspension culture (SC) and explant culture (EC) cells.

A: The population doubling times of SC and EC cells (X-axis) were not significantly different from passage one to passage three (Y-axis) (passage one: SC: 1.2±0.3 days, EC: 1.3±0.2 days; passage two: SC: 1.5±0.04 days, EC: 1.5±0.2 days; passage three: SC: 1.2±0.1 days, EC: 1.3±0.03 days). B / C: The number of colony forming units on one thousand cells was 43.3±19.2 for the SC (B) and 51.8±14.0 for the EC cells (C), which was not significantly different (p=0.19).

To investigate a potential stem cell capacity, ALDH1-high cells and side population cells were measured at three time points (time point one: 10 to 15 days, time point two: 20-25 days, time point three: 30-35 days). Both, SC and EC cells contained ALDH1-high and side population cells and the percentage of these cells did not differ significantly between both isolation methods at the different time points.

For the SC cells, the amount of ALDH1-high cells decreased significantly from 13.35±1.2 % at time point one to 4.60±1.2 % at time point two (p=0.0001) and showed only a slight, non-significant decrease at time point three to 2.45±1.1 %, (p=0.18) (Figure 19). Also for the EC cells, the number of ALDH1-high cells decreased significantly from 11.79±1.2 % at time point one to 4.80±2.3 % at time point two (p=0.011) but remained more or less stable at time point three (3.38±0.3 %, p=0.18).

The number of side population expressing cells decreased significantly at time point two (from 5.43±0.5 % to 1.08±1.0 %, p=0.014) and showed a further non-significant decrease at time point three (0.36±0.4, p=0.03, level of significance p=0.02 due to multiple testing) regarding the SC cells (Figure 20). For the EC cells, the amount of side population expressing cells showed a strong tendency to decrease over time (from 4.7±2.9 % at time point one to 0.58±0.2 % at time point three, p=0.03), which was not statistically significant due to higher standard deviations and after correction for multiple testing.

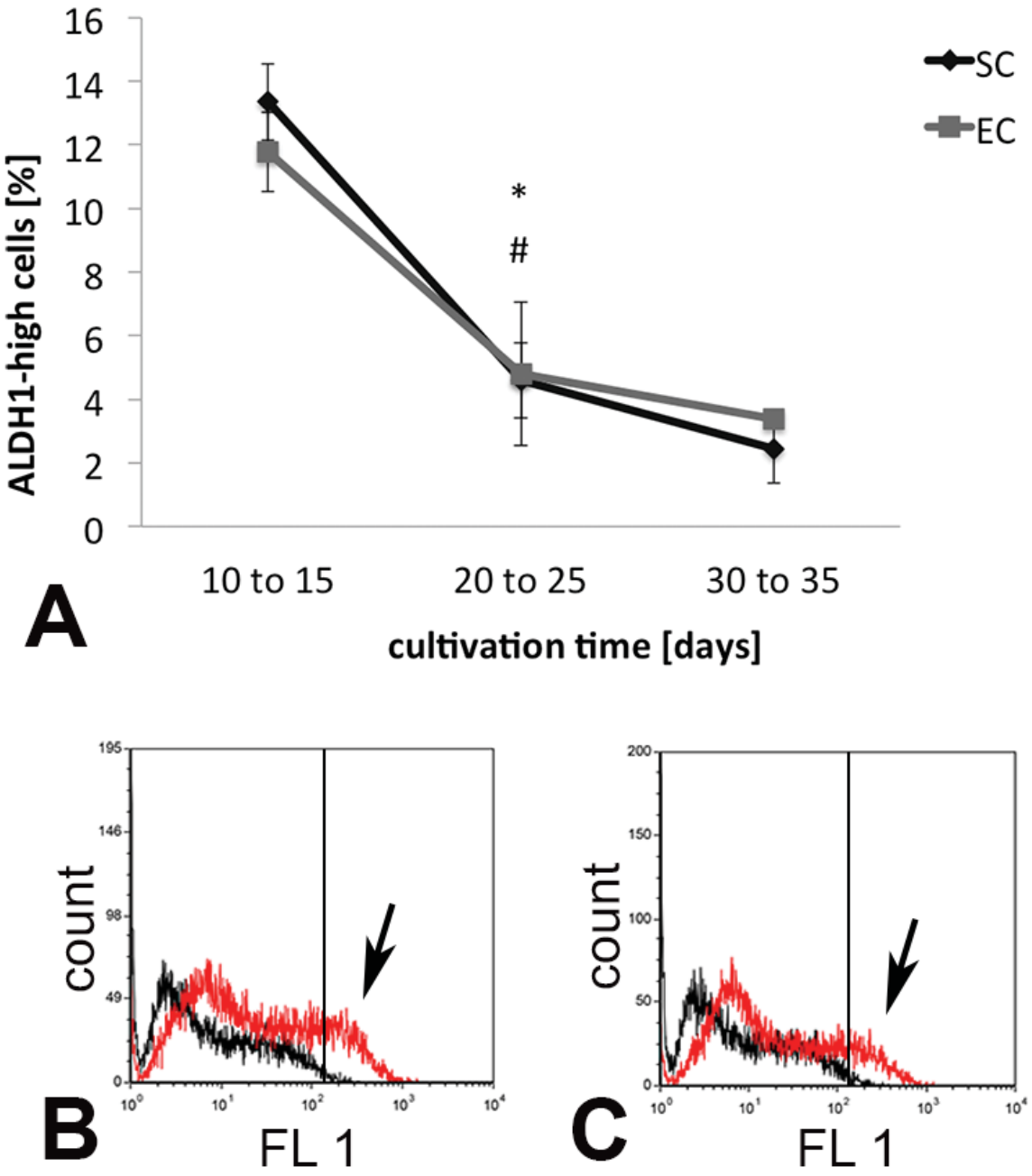

Figure 19: Determination of aldehyde dehydrogenase 1 (ALDH1)-high cells.
A: Suspension culture (SC) and explant culture (EC) cells contained a similar amount of ALDH1-high cells (Y-axis) at all time points (X-axis) (10-15 days: p=0.19; 20-25 days: p=0.88; 30-35 days: p=0.21). There was a significant decrease after 20-25 days of culture (* SC cells: p=0.0001; # EC cells: p=0.011). B, C (SC left, EC right): Example measurement of the SC (B) and EC cells (C) (Spaniol et al., 2015). The area below the red graph illustrates the ALDH1-high cells (arrow) and the area under the black graph the respective control measurement (ALDH1 activity blocked by diethylaminobenzaldehyde (DEAB)).

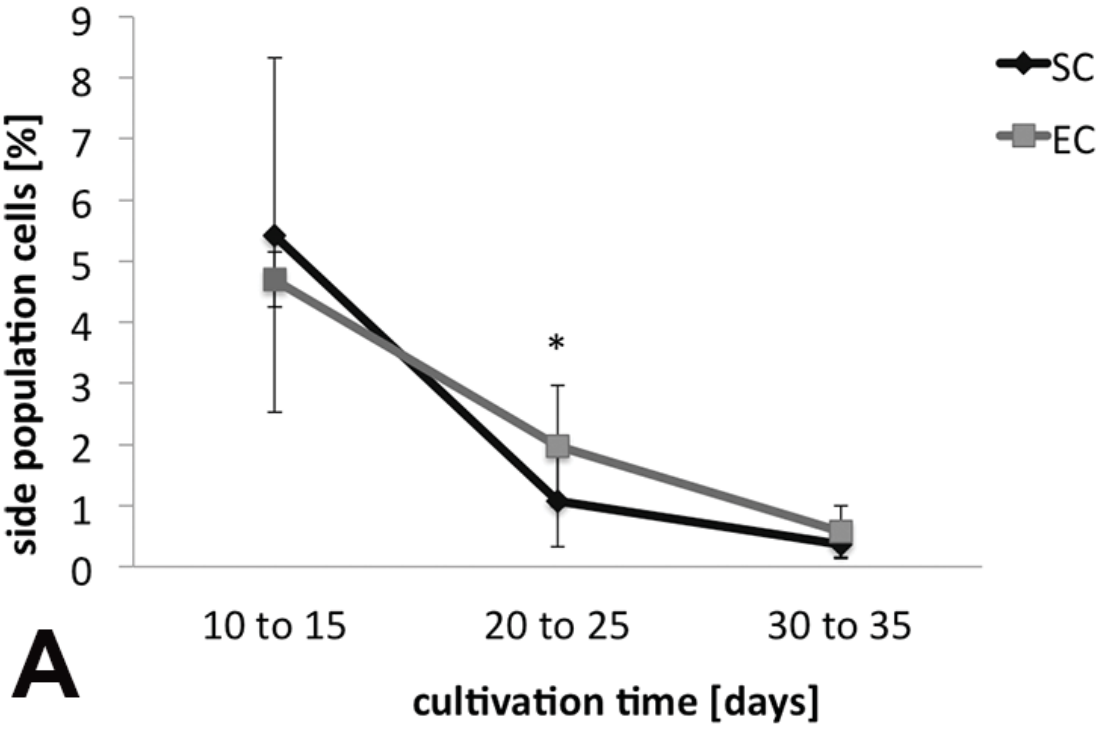
side population cells [%]
9
8
7
6
5
4
3
2
1
0
SC
EC
*
10 to 15
20 to 25
30 to 35
cultivation time [days]
A

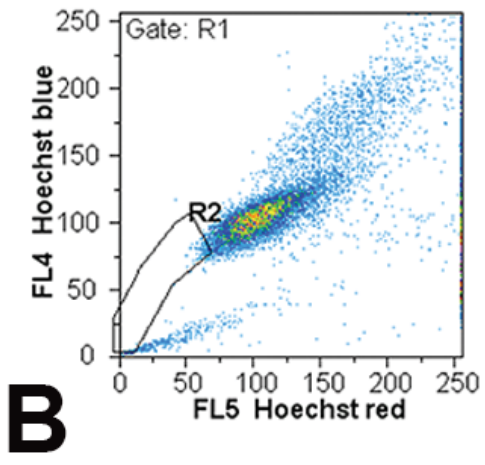
Gate: R1
R2
FL4 Hoechst blue
FL5 Hoechst red
0
50
100
150
200
250
B

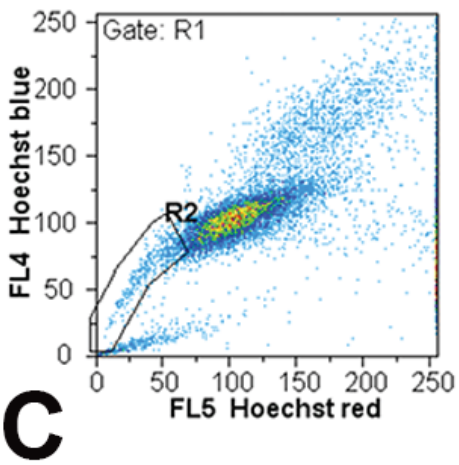
Gate: R1
R2
FL4 Hoechst blue
FL5 Hoechst red
0
50
100
150
200
250
C

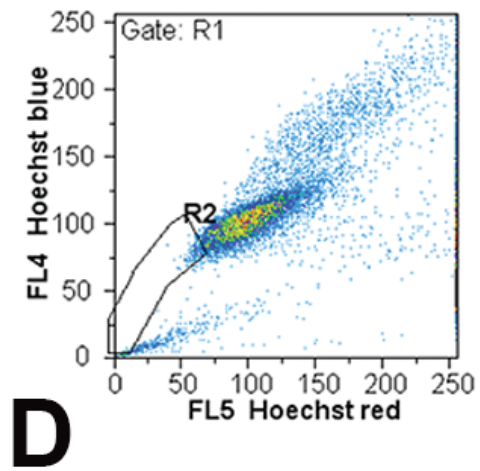
Gate: R1
R2
FL4 Hoechst blue
FL5 Hoechst red
0
50
100
150
200
250
D

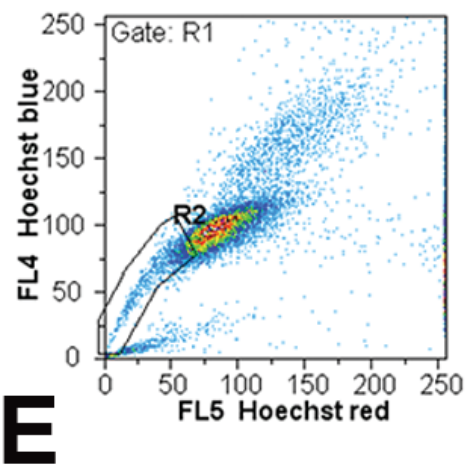
Gate: R1
R2
FL4 Hoechst blue
FL5 Hoechst red
0
50
100
150
200
250
E

Figure 20: Determination of side population cells.

A: Suspension culture (SC) and explant culture (EC) cells contained a similar amount of side population cells (Y-axis) at all time points (X-axis) (10-15 days: p=0.75; 20-25 days: p=0.10; 30-35 days: p=0.43). For the SC and EC cells, the amount of side population cells decreased over the culture period (* p=0.014). B-E: Example measurement of the SC and EC cells (SC above, EC below). In the control measurements (B, D), verapamil sufficiently blocked the ABC transporter activity, while the side population cells appeared in the R2 gate without transporter blockage (C, E) (Spaniol et al., 2015).

4.4.2 Recellularization of the decellularized porcine lacrimal gland

SC and EC cells from passage zero were cultured on the DC-LG for one week. Histologically, the cells grew into the matrix forming an epithelial multilayer. The epithelial phenotype of SC and EC cells was verified by immunostaining for pancytokeratin (Figure 21) (Spaniol et al., 2015).

The cells kept their secretory capacity as cells from both isolation methods responded with a significant increase in β-hexosaminidase activity to parasympathetic stimulation with carbachol (SC: $p=0.007$, EC: $p=0.001$) (Spaniol et al., 2015). The secretory response was not significantly different between cells from both isolation methods ($p=0.88$). This finding was confirmed histologically: the PAS / alcian blue reaction identified mucinous secretions in the cells seeded on the decellularized matrix and the Rab3D staining proofed evidence of mature secretory vesicles (Figure 22) (Spaniol et al., 2015).

Accordingly, as for the 2D culture, the TEM analysis revealed secretory vesicles in cytoplasm of SC and EC cells after culture in the DC-LG (Figure 23) (Spaniol et al., 2015). Underlining the epithelial phenotype, the cells showed apical microvilli on the cell surface and basal nuclei, which indicated polarization of the cells. Some cells grew deeper into the matrix and seemed to form structures similar to ducts or spheres. These cells partly exhibited a different phenotype compared to the cells located more superficially as they were smaller, showed an increased nucleus to cytoplasm ratio, and had less secretory vesicles (Figure 24) (Spaniol et al., 2015).

To examine the possibility of a long-term culture in the DC-LG, EC cells were cultured for 28 days in the DC-LG (Figure 25) (Spaniol et al., 2015). The cells grew deeper into the matrix and continued to organize themselves in roundish, acinus-like structures.

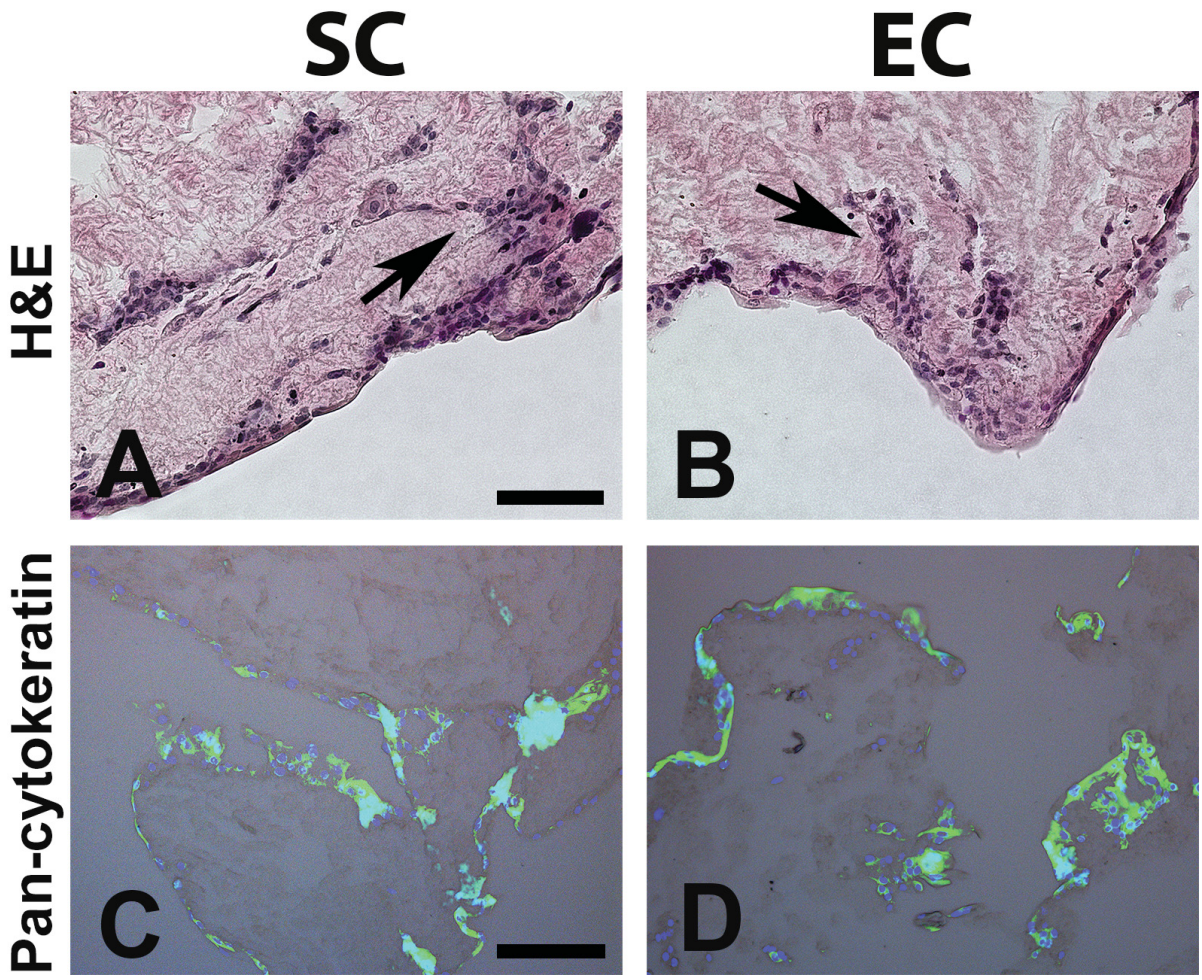

Figure 21: Cell culture on the decellularized lacrimal gland (DC-LG).
(Suspension culture (SC) cells left, explant culture (EC) cells right). A, B: After a seven-day culture period on the DC-LG, SC and EC cells formed a multilayer on the decellularized matrix and partly grew into the tissue in duct like structures (black arrows), hematoxylin and eosin staining (H&E). C, D: SC and EC cells mostly retained their epithelial phenotype as shown by pan-cytokeratin expression (green). A, B: scale bar 50 µm. C, D: scale bar 50 µm (Spaniol et al., 2015).

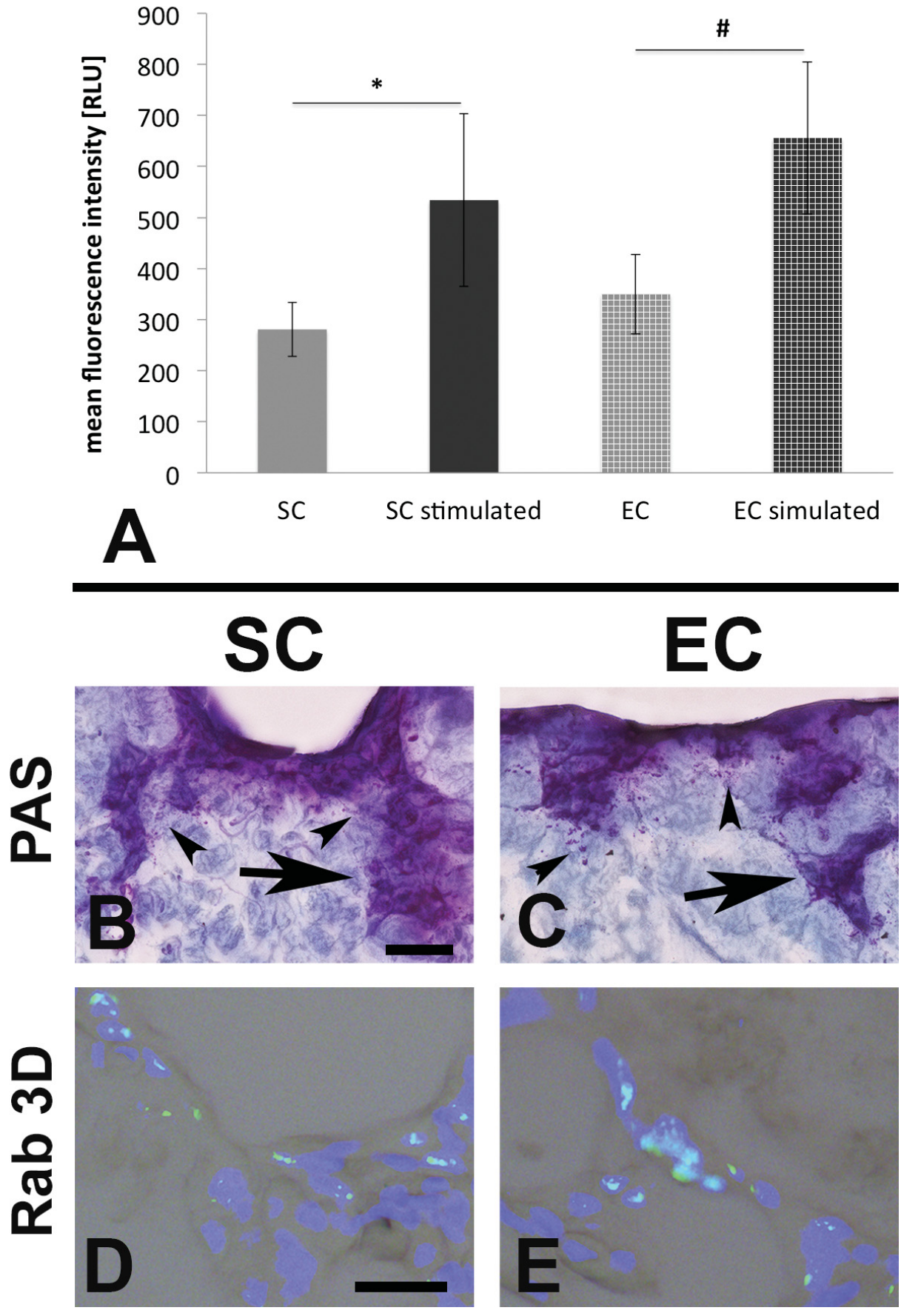
mean fluorescence intensity [RLU]
900
800
700
600
500
400
300
200
100
0
*
#
SC
SC stimulated
EC
EC simulated
A
SC
EC
PAS
B
C
Rab 3D
D
E

Figure 22: Secretory capacity after culture on the decellularized lacrimal gland (DC-LG).

A: After a seven-day culture period on the DC-LG, suspension culture (SC) and explant culture (EC) cells responded with a significant increase in ß-hexosaminidase activity to parasympathetic stimulation with carbachol (*p=0.007, #p=0.001). B, C: The periodic acid Schiff / alcian blue reaction (PAS) illustrated secretory granula (arrowheads) in the SC (B) and EC cells (C) by a pink staining and revealed the growth of the secretory cells into the DC-LG (arrows). D, E: The cells expressed Rab 3D (green) as a marker for mature secretory vesicles, which underlines the secretory phenotype (Spaniol et al., 2015). B, C: scale bar 50 µm. D, E: scale bar 25 µm. RLU, relative light units.

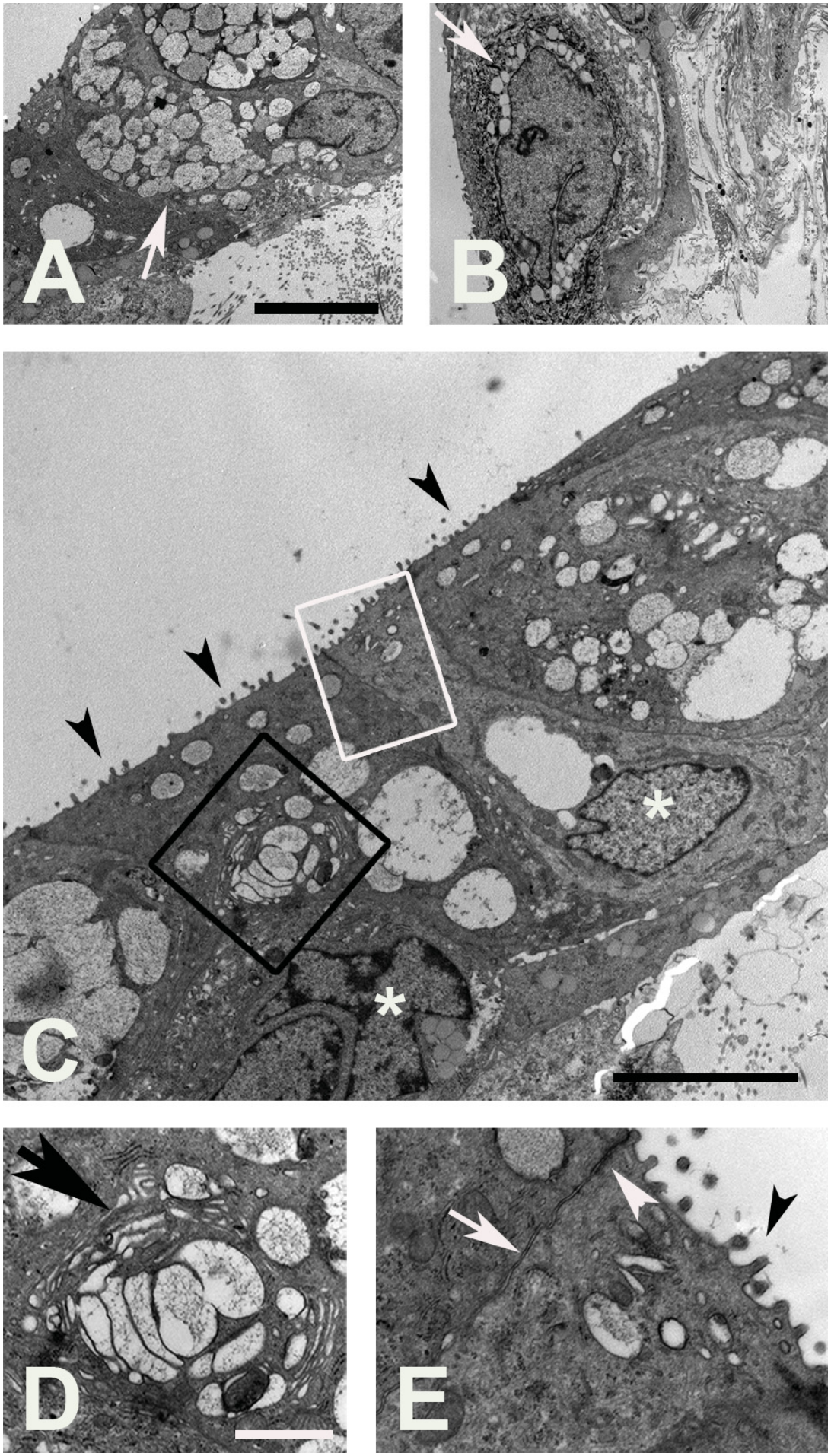
A
B
C
D
E

Figure 23: Ultrastructural analysis of the suspension (SC) and explant culture (EC) cells after culture on the decellularized lacrimal gland (DC-LG).
A, B: SC (A) and EC cells (B) contained secretory vesicles (white arrows) after seven days of culture in the DC-LG. C: The cells organized themselves in a polarized manner with apical microvilli (black arrowhead) and basal nuclei (asterisk). D, E: The higher magnification (D, black box in C) showed Golgi apparatus with secretory vesicles and development of cell-cell connections (E, white box in C) as desmosomes (white arrow) and tight junctions (white arrowhead). A, B: scale bar 5 µm. C: scale bar 10 µm. D, E: scale bar 1 µm (Spaniol et al., 2015). Images taken by Dr. med. K. Zanger.

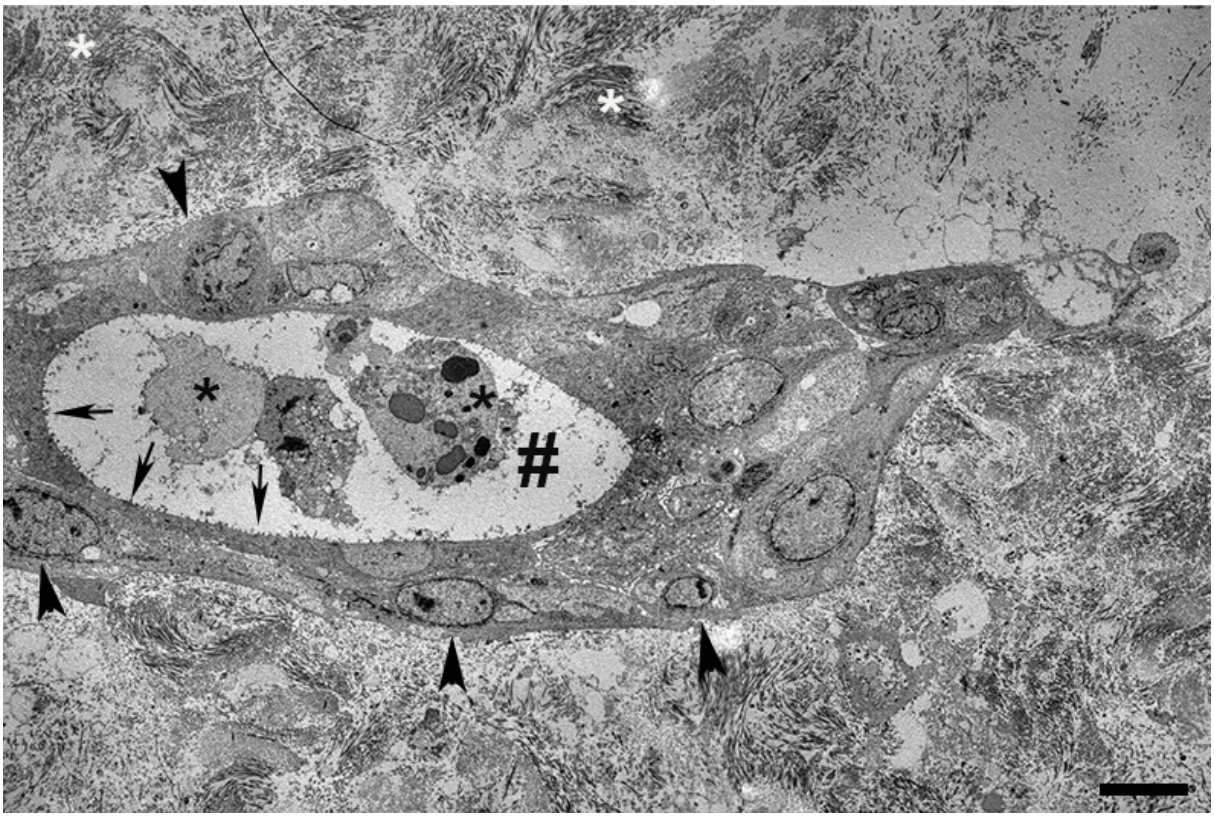

Figure 24: Central sections of the reseeded decellularized lacrimal gland (DC-LG).
In the middle of the DC-LG (measuring about 3 mm in diameter), the cells arranged themselves between the collagen fibers (white asterisks) in a duct like manner around a central “lumen” (rhomb). They were polarized with basally located nuclei (arrowheads) and apical microvilli (arrows) facing the lumen. However, these cells revealed an increased nucleus to cytoplasm ratio and did not exhibit secretory vesicles, indicating immaturity. Further, the lumen contained cell debris possibly due to an apoptosis inducing lack of nutrients and oxygen. Scale bar 10 µm. Image taken by Dr. med. K. Zanger.

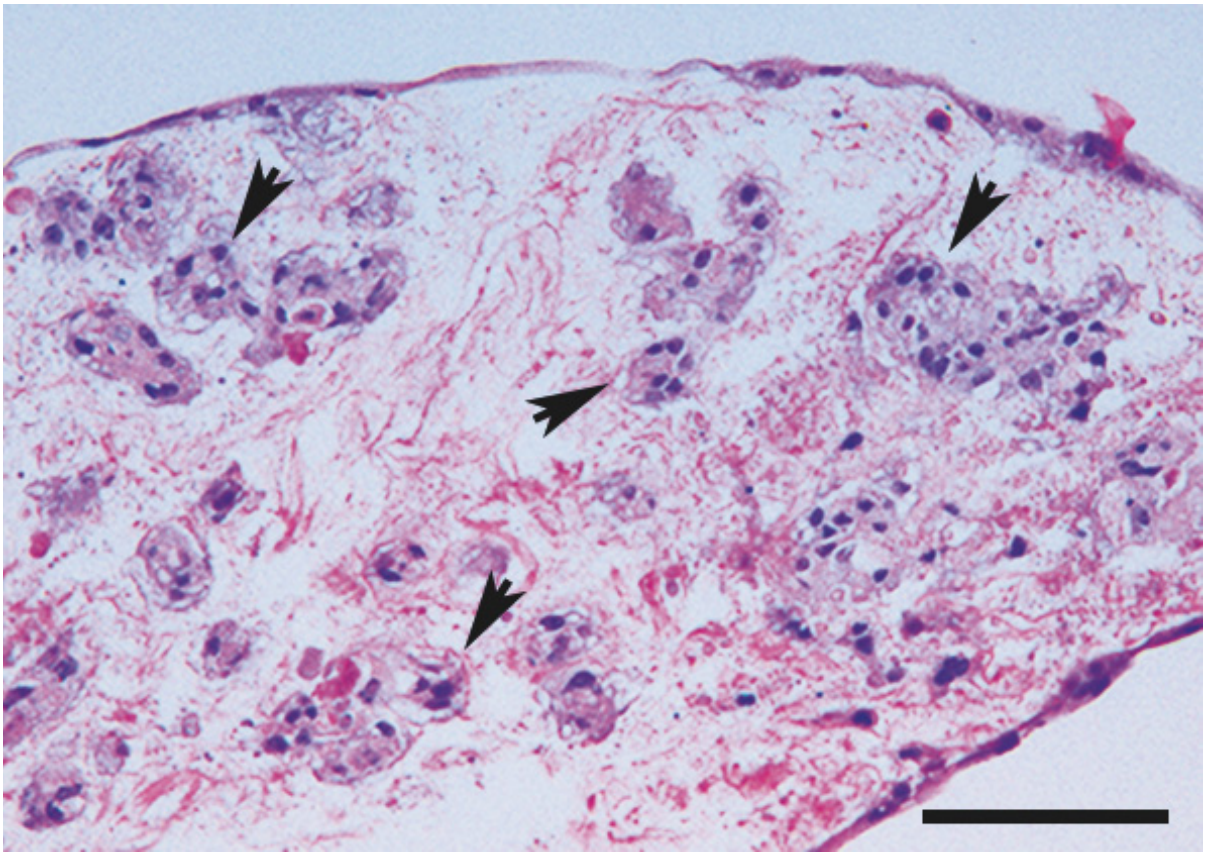

Figure 25: Long-term culture in the decellularized porcine lacrimal gland (DC-LG). After 28 days of culture in the DC-LG, the cells recellularized deeper parts of the DC-LG and kept organizing themselves in roundish, acinus-like structures (arrow). Scale bar 100 µm (Spaniol et al., 2015).

4.5 Culture of rabbit lacrimal gland acinar cells

To investigate the possibility of an allogeneic cell culture in the porcine DC-LG, rabbit LG acinar cells were expanded by EC and cultured on the porcine DC-LG. After expansion in the two dimensional culture, which took around two weeks, the cells revealed a cobblestone like, epithelial morphology (Figure 26) and the ß-hexosaminidase assay revealed a significant response to parasympathetic stimulation with carbachol indicating secretory capacity ($p<0.001$).

When the cells were cultured in the DC-LG, they formed a multilayer on the matrix and started to remodel the extracellular matrix. They arranged themselves in roundish, acinus-like structures with duct-like connections (Figure 27).

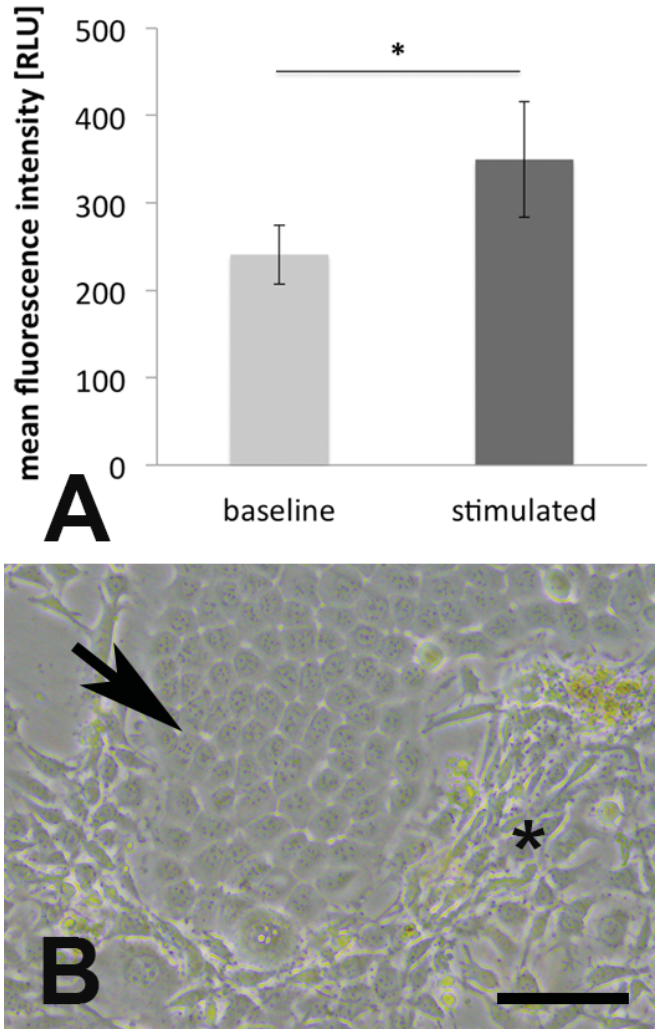

Figure 26: Secretory response and histology of the rabbit lacrimal gland (LG) epithelial cells after expansion on plastic. A: The ß-hexosaminidase assay showed a significant increase in fluorescence intensity after stimulation with carbachol (241±33.9 to 349.8±66.2, $p<0.001$) indicating secretory capacity. RLU: relative light units. B: In the two dimensional culture, the cells revealed a cobblestone like epithelial morphology (arrow), as shown previously for rabbit LG acinar epithelial cells (Schonthal et al., 2000). Surrounding cells are 3T3/J2 feeder cells (asterisk). B: scale bar 100 µm.

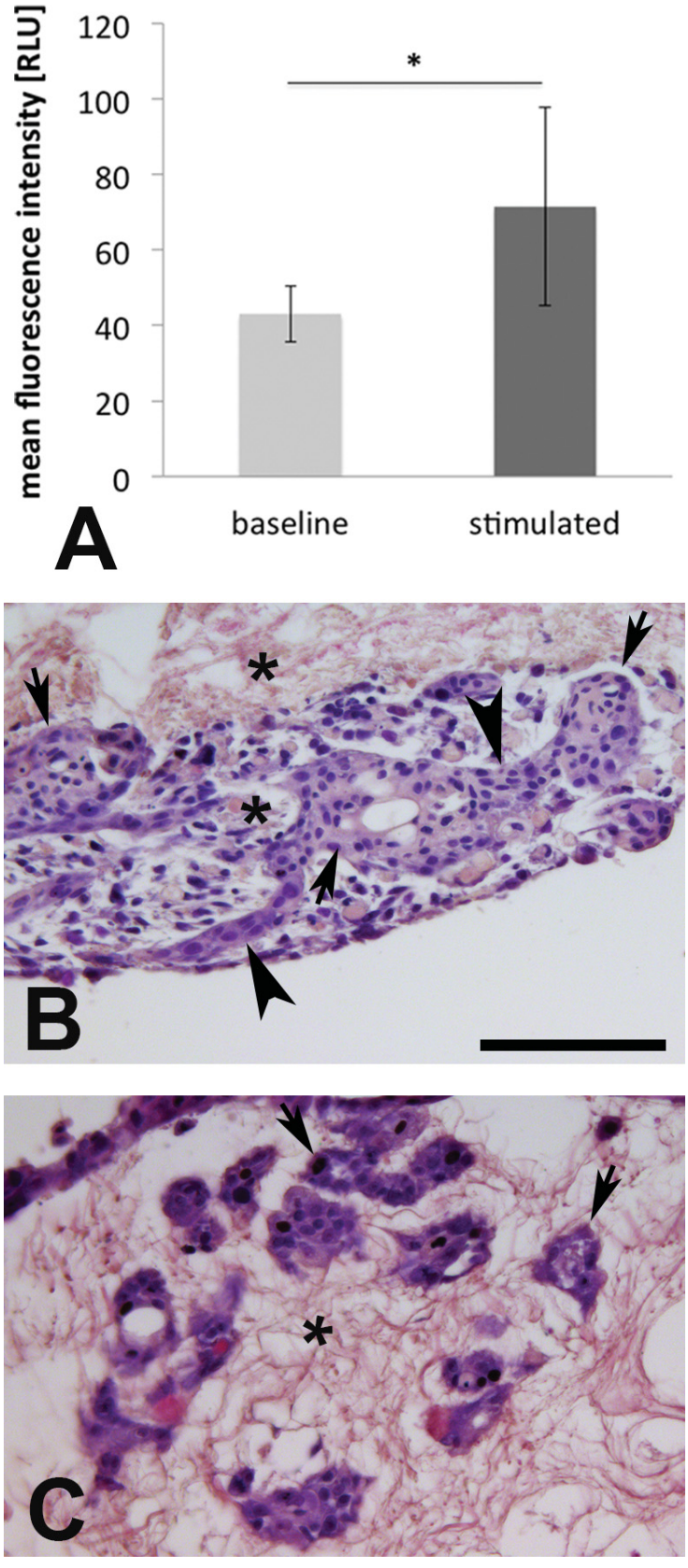

Figure 27: Secretory capacity of the decellularized porcine lacrimal gland (DC-LG) recellularized with rabbit lacrimal gland epithelial cells.

A: The ß-hexosaminidase assay revealed a significant increase in fluorescence intensity after stimulation with carbachol (43±7.4 to 71.5±26.2, p=0.01) indicating secretory capacity. B, C: Histology (hematoxylin and eosin staining) showed that the cells formed a multilayer on the DC-LG. They seemed to migrate into the connective tissue of the DC-LG (asterisk) and to rebuild the extracellular matrix. They formed round, acinus-like structures, which partly exhibited a central lumen (arrows) and arranged themselves in a tube-like manner reminding of ducts (arrowhead). B, C: scale bar 100 µm.

5 Discussion

A cause of severe aqueous deficient dry eye syndrome is LG insufficiency, which leads to a failure of lacrimal tear secretion (Perry, 2008) (Schechter et al., 2010). If after chronic, mostly T-cell mediated inflammation fibrosis of the LG occurs, tear secretion decreases dramatically or stops and the patients suffer from ocular surface disturbances, pain, risk of infection, and eventually loss of sight (Borrelli et al., 2010). Even applying eye drops every quarter of an hour may fail to alleviate the patients´ symptoms or restore the ocular surface to a satisfactory level. Today, no curative treatment strategy exists and therefore engineering of functional competent LG tissue is a clinically highly relevant goal. This work aimed to expand secretory competent LG cells and create a biocompatible, three-dimensional, transplantable scaffold for these cells (Spaniol et al., 2015).

To study human diseases requires an animal model as tissue source for *in-vitro* testing and to later analyze (patho)-physiological processes *in-vivo*. In Europe, mostly rodents are used for LG studies as human tissue is scarce and the use of non-human primates implies ethical concerns. However, rodents do not resemble humans with regard to anatomy and size of the LG (Schechter et al., 2010). The pig (*Sus scrofa*) is genetically similar to humans as both belong to the same descent community and it is easily available as it breads perennially (Kumar and Hedges, 1998). Further, anatomy and size of the porcine LG are similar to the human, which enables future surgical studies (Henker et al., 2013) (Walters et al., 2012). As the pig has not been used to study LG diseases and secretory cells of the porcine LG have not been isolated and cultured before, these cells were explored in the present work (Spaniol et al., 2015).

5.1 Comparison of suspension and explant culture

The secretory competent cells of the LG are the acinar epithelial cells and most attempts have been made to isolate and culture these cells under maintenance of their secretory capacity. Hann et al. were the first who successfully isolated this lineage from rat LG in 1989 by several enzymatic digestion steps using e.g. collagenase, hyaluronidase, and DNase followed by different filtration steps with meshes of decreasing sizes and purifying gradients (Hann et al., 1989). Reviewing the literature reveals that other groups more or less adopted the same isolation

protocol with some changes in the enzyme concentration and composition, the incubation time or the filter pore size (McDonald et al., 2009) (Millar et al., 1996) (Schonthal et al., 2000) (Schrader et al., 2007) (Schrader et al., 2010) (Schechter et al., 2002) (Hann et al., 1989) (Kobayashi et al., 2012) (Ueda et al., 2009) (Fujii et al., 2013) (Nakajima et al., 2007) (Tiwari et al., 2012) (Yoshino et al., 1995) (Yoshino, 2000). This “suspension” method is able to isolate secretory competent acinar epithelial cells with a purity of around 90 % but it comprises important, clinically relevant disadvantages. First, it is time consuming. This work showed that preparing the tissue for EC took around 20 minutes, which was 9 times faster than using SC (Spaniol et al., 2015). Saving preparation time can increase cell viability and reduce the risk of metabolic cell changes. In a clinical setting personnel costs can be reduced, which is of importance with regard to a clinical translation as health care expenditures increase continuously (Breyer and Felder, 2006). Second, SC required an about 30 times larger tissue piece than EC (100 mm^3 vs. 3.4 mm^3) to reach the similar number of cells (Spaniol et al., 2015). As LG tissue is scarce, this is one of the most relevant arguments for EC (Hunt et al., 1996). In the clinical context only a small biopsy would be available, which rules out the use of SC. Third, the enzymatic digest required for SC may harm the cells or alter their phenotype (Chang, 1997). Proteolytic enzymes lead to loss of cell surface receptors, loss of adhesive glycoproteins as fibronectin, and loss of the negatively charged extracellular matrix proteins (Yamada and Olden, 1978) (Turley, 1980). Enzymatic digest by collagenase and hyaluronidase can deteriorate the secretory function of cells (Raven et al., 1983). For LG tissue the literature shows, that longer incubation periods and higher enzyme concentrations were required for non-human primate and human tissue compared to rodent LGs; an ideal protocol for each species and age is not available (Hann et al., 1989) (Nakajima et al., 2007) (Yoshino et al., 1995). This would be required for a clinical application of SC. As the extracellular matrix alters with age and is variable between different individuals it would be difficult to determine adequate enzyme compositions and incubation periods for each individual patient´s biopsy, which also speaks against application of SC in a clinical setting (Singh et al., 2009). EC circumvents these problems.

Hunt et al. showed, that human LG tissue can be kept vital in explant organ culture when cultured in a special, serum and second messenger (cAMP, cGMP) containing medium at 37°C in an atmosphere of 50% O_2, 45% N_2, and 5% CO_2 (Hunt et al.,

1996). Tissue pieces with a maximum size of one mm^3 were secretory active for up to 22 days and maintained their histological ultrastructure (Hunt et al., 1996). However, this work only intended to create an *in-vitro* model for LG studies but did not explore outgrowth of cells from the explants or cell proliferation. It is known that EC leads to the outgrowth of viable, defined cells under specific culture conditions as shown for e.g. adult human renal tubular epithelia or embryonic rat neurons and glia cells (Wilson et al., 1985) (Silverman et al., 1999). EC also is an established method for the culture of ocular tissue. Human conjunctival epithelial cells were successfully expanded by EC (Schrader et al., 2009) (Schrader et al., 2010) (Drechsler et al., 2015). Corneal limbal epithelial cells can be outgrown from a small limbal biopsy under maintenance of their epithelial phenotype and proliferative capacity and the ocular surface of patients with limbal stem cell deficiency was successfully reconstructed after transplantation of these cells (Tsai et al., 2000) (Selver et al., 2011) (Haagdorens et al., 2016).

This work showed for the first time that EC is applicable to expand LG acinar epithelial cells with a similar purity as SC and under maintenance of their secretory capacity (Spaniol et al., 2015). A difference between SC and EC was found for the expansion time in passage zero. It took around 9 days for SC cells and 16 days for EC cells to form a sub-confluent layer in the tissue culture flask (Spaniol et al., 2015). This may be due to the fact that the SC cells were already dissociated from the surrounding connective tissue while the EC cells needed to leave this network. However, at the end of passage zero SC and EC cells revealed a uniform, epithelial phenotype and flow cytometry confirmed that both cultures contained nearly exclusively epithelial cells (Spaniol et al., 2015). However, for both SC and EC, epithelial cell purity was not 100% as verified by flow cytometry. Small numbers of mesenchymal and myoepithelial cells were identified by immunocytochemistry. Other cell types apart from epithelial cells were not further investigated in this study and need to be addressed in greater detail in the future. In addition, vascular endothelial cells were not regarded here and could have been present after SC and EC. Vascular endothelial cells were recently found to influence the epithelial development of salivary glands independently from perfusion as immuno-depletion of CD 31 positive endothelial cells induced an increase of ductal and a decrease of progenitor cells in a mouse model (Kwon et al., 2017). Presence and / or different amounts of

vascular endothelial cells could have affected the growth pattern and proliferative as well as secretory capacity of the cultured epithelial cells.

The most important goal in the culture of acinar epithelial LG cells is maintenance of the secretory capacity. An ultrastructural analysis by TEM identified secretory vesicles in cells from both culture conditions, which are accepted visible signs for secretory capacity (Spaniol et al., 2015) (Kühnel, 1968). Cells from both isolation methods equally exhibited a positive PAS / alcian blue reaction, which identifies mucinous secretions in the LG, and expressed Rab 3D, a marker for mature secretory vesicles (Spaniol et al., 2015) (Obata, 2006) (Wu et al., 2006). Further, both responded with an increased secretory capacity to parasympathetic stimulation, as measured by ß-hexosaminidase assay, which is typical for secretory competent LG cells (Spaniol et al., 2015). According to these findings, the author´s laboratory now changed from SC to EC for the culture of LG acinar epithelial cells. However, this work only focused on epithelial differentiation as the goal was to culture secretory competent cells. For LG bioengineering also mesenchymal and myoepithelial cells need to be isolated and expanded *in-vitro* to mimic the native environment more closely. Further, a vascular supply is required to enable long-term survival of a bioengineered organ, which implies isolation and propagation of vascular endothelial cells. These cell types need to be addressed in further studies.

5.2 Proliferative capacity

Although LG regeneration after acute injury is possible in-vivo (after Interleukin 1 injection in the murine model), which proofs regenerative capacity, the distinct origin of the LG stem or progenitor cells still remains unclear (Zoukhri et al., 2008). Shatos et al. investigated adult rat LG myoepithelial cells, which are known to modify the LG tear secret (Shatos et al., 2012). These cells differentiated into multiple lineages *in-vitro* (myoepithelial, neuronal, and epithelial cells) and the authors assumed them to be possible LG progenitor cells (Shatos et al., 2012). Hann et al. stated that rat LG acinar epithelial cells – in contrast to salivary or pancreatic secretory cells – do not proliferate (Hann et al., 1989). However, Voronov et al. found proliferative capacity of mouse LG epithelial cells but concluded it was unclear whether the LG comprises one multipotent or multiple lineage specific progenitors (Voronov et al., 2013).

This study revealed that epithelial cells from the porcine LG – isolated either by SC or EC – comprise colony forming capacity and show stable population doubling times

until passage three, which indicates a proliferative potential of this lineage. To further investigate this potential, the amount of ALDH-1 high and side population containing cells was measured by flow cytometry (Spaniol et al., 2015).

ALDH-1 was found to be an important functional enzyme in stem cells from various tissues such as liver, breast, muscle, bone marrow, neural tissue, and salivary glands, and constitutes a useful marker for stem cell identification and isolation (Banh et al., 2011) (Ma and Allan, 2011). For the adult human LG, Tiwari et al. described the presence of around 3.8 % ALDH1-high cells in a freshly isolated heterogeneous population of epithelial, myoepithelial, and mesenchymal cells (Tiwari et al., 2012). The amount of these cells decreased to around 2.7 % after 14 days of culture on matrigel. Compared to the cells isolated from human LG, the porcine LG epithelial cells contained about 4 fold more ALDH-1 high cells (around 12 %) after expansion in passage 0 after 10-15 days (Spaniol et al., 2015). Certain reasons may account for these differences. Tiwari et al. used tissue from three to 65 years old patients. In this heterogenic cohort, tissue from older patients may have contained less proliferative cells. The tissue used in the study presented here was harvested from around six month old pigs, which is a homogeneous, young group comprising probably higher amounts of proliferative cells. Further, Tiwari et al. omitted serum from the cell culture at day three while the author of this study used 10 % serum through the whole culture period, which might have influenced the amount of ALDH-1 high cells, too. Also, the 3T3 feeder layer used in the presented work could have supported a proliferative phenotype, while the matrigel used by Tiwari et al. is known to promote differentiation and reduce proliferation (Tiwari et al., 2012) (Balasubramanian et al., 2008) (Hann et al., 1989). Interestingly, this study found a strong decrease of the ALDH-1 high cells during the culture period. The amount of ALDH-1 high cells decreased significantly to about 4 % at day 20-25 and again non-significantly at day 30-35 to around 3 % without differences between SC and EC cells. It has been reported, that ALDH expression underlies a phenotypic plasticity and that it can be “switched off” in cell culture if many ALDH high cells are present (Doherty et al., 2011). This fact could explain the decrease of the ALDH-1 expression and might speak against extended culture periods.

The side population method was found to identify stem and progenitor cells in several tissues as muscle, kidney, liver, lung, and glandular tissue like the mammary glands (reviewed in (Golebiewska et al., 2011)). Side population cells can be identified by

flow cytometry due to the ability to exclude Hoechst dye through ATP-binding cassette (ABC) transporter proteins, mainly ABCG 2, in the cell membrane (Golebiewska et al., 2011) (Greve et al., 2012). Mishida et al. isolated side population cells from mouse salivary glands and LGs and these cells induced functional recovery of irradiated glands after transplantation (Mishima et al., 2012). Side population cells expressed CD 31, ABCG 1, Sca-1, and CD 105 and were suspected to be predominantly endothelial cells and belong to the mesenchymal lineage (Mishima et al., 2012). The present study found that epithelial LG cells comprise side population cells, which is an additional indicator for the regenerative potential of this lineage (Spaniol et al., 2015).

Compared to the data available on human LG cells, the amount of side population cells in the porcine cells was around 16 times higher after around two weeks of *in-vitro* culture, which might be due to the different culture conditions and the tissue source, as mentioned above (Tiwari et al., 2012). However, as it was true for the ALDH-1 high cells, the amount of side population cells decreased over time from about 5 % after 10-15 days to around 1 % after 30-35 days without significant differences between the SC and EC cells, confirming that supportive short *in-vitro* culture periods are advisable for this cell type.

Further work is required to elucidate the potential stem cell character of the LG epithelial cells. This may include to sort and isolate side population or ALDH-1 high cells by flow cytometry to analyze the proliferative capacity of these subgroups in greater detail, e.g. by colony forming efficacy compared to unsorted LG epithelial cells. In addition, evaluation of LG tissue from older pigs would be interesting to evaluate age induced changes of the side population or ALDH-1 high cells in this animal model and possibly compare these data to human tissue, which normally originates from older donors. Moreover, although immunocytochemically only few mesenchymal and myoepithelial cells were evident in SC and EC, the exact number of these cells was not quantified and they might have been part of the ALDH-1 high or side population cells. Co-staining of the ALDH-1 high and side population cells for epithelial, mesenchymal, and myoepithelial markers could further explore this question. Endothelial cells were not addressed here and might have been present in small numbers in SC and EC cells, which could have influenced the proliferative potential of the epithelial cells and needs to be investigated further (Kwon et al., 2017).

The author´s group further isolated MSC´s from adult murine LG, which expressed typical stem cell markers as CD 29, CD 49, CD 90, CD 105, CD 106, CD 166, and Sca-1, and could be differentiated into osteocytes and adipocytes (Roth et al., 2015). If the porcine acinar epithelial cells are cultured with conditioned media from the LG MSCs, they show increased proliferation and migration indicated by the gap closure time in a migration assay (Roth et al., 2015). MSCs are known to secret trophic factors like fibroblast growth factor, hepatozyte growth factor, insulin like growth factor, platelet derived growth factor, or interleukin 6, which can enhance proliferation, migration, and epithelial differentiation even if of xenogeneic origin (Maxson et al., 2012). Therefore, the author´s group currently isolates and characterizes also the porcine mesenchymal LG cells, which has not been done so far (Massie et al., 2016). The group could show, that these cells express typical stem cell markers and can be differentiated into adipocytes and osteocytes (Massie et al., 2016). Further, co-culture of porcine epithelial and mesenchymal cells with human endothelial cells in matrigel lead to the formation of three-dimensional, secretory active spheroids, which comprised tube like structures lined with endothelial cells (Massie et al., 2016). Nevertheless, matrigel has certain disadvantages precluding its application in a clinical context, as describes below. It consists of a tissue unspecific mixture of extracellular matrix proteins, it is derived from a sarcoma cell line, which prohibits its clinical application in humans, and it is surgically not manageable due to its soft texture (Kleinman and Martin, 2005). Also cells from different species were combined in this model and potential interactions between the allogeneic cells are yet unclear so that these first attempts towards rebuilding a vascularized LG matrix need further validation.

5.3 Decellularized porcine lacrimal gland for lacrimal gland bioengineering

To mimic a three-dimensional environment, induce sphere formation, and maintain the secretory capacity, LG epithelial cells were mostly cultured on matrigel, a soluble extract from the Engelbreth-Holm-Swarm (EHS) mouse sarcoma (Yoshino et al., 1995) (Hann et al., 1989) (Kleinman and Martin, 2005). Matrigel contains a mixture of several basement membrane components (laminin, collagen IV, perlecan etc.) and growth factors (transforming growth factor, fibroblast growth factor, epithelial growth factor etc.) (Kleinman and Martin, 2005). Nevertheless, each organ has an individual

extracellular matrix composition, which cannot be resembled by matrigel (Badylak et al., 2011). Moreover, there are concerns about a potential clinical application. Matrigel is derived from a tumor cell line, which bears the risk of uncontrolled carcinogenic proliferation after transplantation (Kleinman and Martin, 2005). Due to its soft texture, it is surgically hardly manageable.

Decellularized organ matrices provide a specific protein composition and distribution, which serves as a “landscape” for the cells and induces an organ specific differentiation (Arenas-Herrera et al., 2013). Within the extracellular matrix, glycosaminoglycans can bind free growth factors such as fibroblast growth factor or vascular endothelial growth factor, transforming growth factor ß, and platelet derived growth factor via heparan sulphate and thus protect them from degradation through the decellularization process (Arenas-Herrera et al., 2013). These factors additionally stimulate cellular proliferation and differentiation. Xenogeneic decellularized tissues can be transplanted into humans, while the risks of bacterial, viral or prion transmission from allo- and xenografts, as well as immunologic reactions are minimal depending on the method for tissue processing (Kretlow et al., 2009). In ophthalmology, decellularized xenogeneic matrices have already been used clinically, for example to repair corneal ulcers (bovine pericardium, case report), for tendon elongation in strabismus surgery (xenogeneic fascia lata, 38 patients), and to reconstruct the lacrimal drainage system (bovine dermis, five patients) (Kroll et al., 2014) (van Rijn et al., 2016) (Chen et al., 2014). In all cases the decellularized matrices showed good biocompatibility without signs of graft rejection, were well integrated into the host tissue, and functionally competent. The corneal ulcer healed with acceptable restoration of visual acuity (Kroll et al., 2014). Regarding strabismus surgery, the squint angle was reduced but due to a certain duction limitation after surgery the authors recommend to reserve the decellularized transplant for cases, which cannot be cured by conventional strabismus surgery (van Rijn et al., 2016). The reconstructed lacrimal drainage systems were patent with alleviation of epiphora in all patients (Chen et al., 2014).

In the present work, LG decellularization resulted in a cell free, whitish, and sponge-like tissue (Spaniol et al., 2015). Apart from some tissue interruptions the extracellular matrix structure remained histologically intact. The collagen I-V content was not significantly reduced, which indicates stability. While extracellular matrix molecules are highly preserved through development and tolerated even after

xenogeneic transplantation, retarded cellular material induces a M1 type macrophage, pre-inflammatory immune response, which can induce scarring (Yurchenco, 2011). Therefore, acceptable amounts of residual DNA after decellularization have been defined to be <50 ng dsDNA per mg dry weight, and <200 bp DNA fragment length, which was not exceeded in this study based on Feulgen staining and DNA quantification (Spaniol et al., 2015) (Crapo et al., 2011) (Nagata et al., 2010). Further, potential tissue toxicity was excluded by a cell viability assay. Therefore, the DC-LG seems to be applicable as a xenogeneic matrix but *in-vivo* studies are clearly needed to validate this assumption.

Collagen IV, laminin, and fibronectin are main extracellular matrix proteins. They carry important functions in terms of cell adhesion, proliferation, and differentiation: Collagen IV is one of the most abundant BM molecules; it forms networks to other macromolecules via cross-linked polymers and thus stabilizes the BM, it regulates chemotaxis and enhances cell adhesion and migration (Yurchenco, 2011) (Zhu and Clark, 2014). Laminin is a binding partner of integrins and its receptor activation can influence self-renewal and proliferation of stem cells. It is especially tissue specific as different laminin isoforms have been found depending on the laminin-secreting cell type (Gattazzo et al., 2014) (Paulsson, 1992). Fibronectin has several binding sites for different growth factors, such as hepatocyte growth factor, vascular endothelial growth factor, fibroblast growth factor and others and can induce epithelial cell proliferation (Zhu and Clark, 2014) (Kuwada and Li, 2000) (Rahman et al., 2005). Apart from a slight collagen IV reduction, the extracellular matrix proteins were mainly preserved, as proven by immunostaining and immunoblotting (Spaniol et al., 2015). This finding is a prerequisite to provide a cell-friendly, LG specific environment for recellularization. Future work will be required to also study the growth factors and the glycosaminoglycan content remaining after decellularization to further evaluate the regenerative potential of the DC-LG compared to native LG tissue. Also vascular structures were not investigated in detail in this work. Vessels were evident after decellularization but the integrity of the vascular extracellular matrix and thus the vascular network need to be elucidated more closely when aiming for recellularizing vessels.

5.4 Recellularization of the decellularized lacrimal gland

After a seven-day culture period, the LG acinar cells – both, isolated by SC or EC –

built a multilayer on the DC-LG, grew into the matrix, and formed roundish, acinus-like structures (Spaniol et al., 2015). This “sphere” formation has only been found on extracellular matrix components such as collagen gels or matrigel before (Yoshino et al., 1995). For the salivary gland, Lombaert et al. showed that salivary gland epithelial cells develop “salispheres” after cultivation in three-dimensional collagen gels but only cell clumps with intact cell-cell contacts were able to do so (Lombaert et al., 2008). Also in case of human LG acinar cells, sphere-like structures were formed from cell clumps (Tiwari et al., 2012). Therefore it was supposed that cell-cell contacts are necessary for sphere-formation (Lombaert et al., 2008). In this work, cells from single cell suspensions of either SC or EC formed spheroidal structures in the DC-LG and the TEM analysis revealed the development of inter-cellular contacts as desmosomes and tight junctions (Spaniol et al., 2015). This finding confirms the supportive character of the DC-LG and may be explained by the organ specific extracellular matrix composition, wherein laminin can induce an acinus-like differentiation and collagen IV supports the migration into matrices (Kibbey et al., 1992) (Yurchenco, 2011). Other authors argued that sphere formation from single cells applies as a stem cell sign (Kobayashi et al., 2012). However, SC and EC cells did not build spheres on plastic but only in the DC-LG. The epithelial cells cultured in a monolayer contained cells with proliferative capacity but the extracellular matrix of the DC-LG was needed to induce the organ specific alignment of the cells. As another sign for LG-like differentiation, the cells retained their secretory capacity, as proven by ß-hexosaminidase assay and electron microscopy. The cells in the outer part of the DC-LG adopted a polarized structure with basal nuclei and apical microvilli, which is typical for acinar LG cells (Spaniol et al., 2015) (Hann et al., 1989). These cells also expressed Rab 3D, a marker that labels large, subapical, mature secretory vesicles (Wu et al., 2006). However, cells deeper in the matrix showed a more undifferentiated phenotype with large nuclei and only small secretory vesicles. The extracellular matrix is known to act as an organ-specific stem cell niche and the DC-LG seemed to support an immature cellular phenotype after ingrowth into the matrix (Gattazzo et al., 2014). Nevertheless, also apoptotic cells were found in the center of these areas indicating a lack of nutrients and oxygen (Spaniol et al., 2015). A competent vascular system seems therefore indispensable and this aspect needs to be worked up with regard to potential *in-vivo* testing.

It was possible to culture the cells for a culture period of up to four weeks in the DC-

LG and the cells grew deeper into the tissue and seemed to rebuild it under formation of acinus-like structures, which proofs the possibility of long-term culture in the DC-LG (Spaniol et al., 2015). However, secretory competence and a more detailed analysis of the cellular phenotype after long-term culture have to be explored in future studies.

The DC-LG was nearly free from retarded cellular material and it can thus be supposed that it is not immunogenic although this assumption has not been validated *in-vivo* here (Arenas-Herrera et al., 2013). To also explore the feasibility of xenogeneic culture on the DC-LG *in-vitro*, rabbit LG acinar cells were isolated by EC and cultured in the DC-LG. After a seven-day culture period, the cells grew into the DC-LG similar to the porcine epithelial cells. The cells were secretory active and formed acinus-like structures with a partly lumen-like shape and tube-like connections. Therefore, xenogeneic culture in the DC-LG can – at least *in-vitro* – be considered possible.

5.5 Limitations of this work

This work only aimed to isolate cells from the epithelial lineage and to culture these cells in the DC-LG, which does not resemble the native LG environment very closely. The isolation, propagation, and characterization of other main LG cell types as mesenchymal, myoepithelial, and endothelial cells is of interest to later co-culture these cells with the epithelial lineage and analyze their influence on e.g. proliferation, differentiation, long-term survival, and secretory competence. In addition, SC and EC did not provide epithelial cell cultures of 100% purity as small numbers of mesenchymal and myoepithelial cells were still evident and need to be quantified and analyzed in more detail in future. Also vascular cells were not addressed in this work, which is required when aiming to reconstruct a vascularized organ as a prerequisite for long-term survival in potential transplantation studies. The vascular network of the DC-LG needs to be investigated more closely in the future as an intact vascular extracellular matrix may be required for the recellularization of vessels. The native LG also comprises a sympathetic and parasympathetic nerve supply, which has not been addressed in this work. With regard to pharmacological studies or clinical translation a nerve supply should be investigated in future studies. Although lack of toxicity and the possibility of xenogeneic cell culture were shown *in-vitro*, a point of criticism is that the feasibility of the DC-LG has not yet been explored *in-vivo*. Such

studies are required to examine the physiological compatibility and further approach a possible application in humans in the future.

5.6 Conclusion

This work introduces the pig (*Sus scrofa*) as a new model for LG studies. It is easily available, similar to the human being with regard to anatomy and genetics, and does not imply ethical concerns as primate tissue. In the past, LG acinar epithelial cells were isolated by a rather complicated and time-consuming SC method, which required nearly the whole gland as tissue source and is thus not applicable in a clinical setting. This work proofs the possibility of an EC isolation method, which is easy, fast, and requires only a small tissue biopsy. LG acinar epithelial cells need specific substrates (e.g. matrigel) to differentiate into secretory active, acinus-like, three-dimensional structures. Here, the DC-LG is introduced as a supportive, stable, and three-dimensional matrix, which enables the culture of secretory competent LG acinar cells and can be used xenogeneic. In conclusion, this work illustrates the possibility to bioengineer secretory active, three-dimensional LG tissue with primary LG cells from a small biopsy, which is a step towards enabling LG regeneration.

In future studies, these results have to be validated *in-vivo*, further cell types such as mesenchymal, myoepithelial, vascular, and nerval cells need to be isolated and characterized, and the DC-LG needs to be investigated in greater detail regarding e.g. the growth factor content and the integrity of the vascular extracellular matrix.

6 Appendix

6.1 List of abbreviations

ALDH	Aldehyde dehydrogenase
ATP	Adenosine triphosphate
ß	Beta
BM	Basement membrane
°C	Degree celcius
c1	Cell count at start of passage
c2	Cell count at the end of passage
cAMP	Cyclic adenosine monophosphate
CD	Cluster of differentiation
cGMP	Cyclic guanosine monophosphate
cm	Centimeter
d	Days
DC-LG	Decellularized lacrimal gland
DAPI	4′,6-Diamidin-2-phenylindol
DMEM	Dulbecco´s Modified Eagles Medium
DNA	Desoxyribonucleid acid
DNase	Desoxyribonuclease
Dr. med.	Doctor medicinae
EC	Explant culture
ECM	Epithelial cell culture medium
EDTA	Ethylendiaminetetraacetic acid
e.g.	Exempli gratia (for example)
EGF	Epithelial growth factor
FL	Fluorescence
FBS	Fetal bovine serum
g	Gramm
H	Duration of passage (days)
Hex A/B	Hexosaminidase A/B
H&E	Hematoxylin and eosin

L	Liter
LG	Lacrimal gland
ln	Natural logarithm
M	Molar (mol/l)
M1 macrophages	Classically activated macrophages
m	Milli (10^{-3})
µ	Mikro (10^{-6})
n	Nano
ns	not significant
PAS	Periodic acid Schiff
PBS	Phosphate buffered saline
PDT	Population doubling time
PFA	Paraformaldehyde
R	Region
Rab 3D	Ras-reated protein 3D
RLU	Relative light units
SC	Suspension culture
SMA	Smooth muscle actin
TEM	Transmission electron microscopy
TM	Trademark
vs	Versus
w/v	Weight per volume
v/v	Volume per volume
γ	Gamma

6.2 References

Andersson SV, Edman MC, Bekmezian A, Holmberg J, Mircheff AK, Gierow JP. **Exp Eye Res** Characterization of beta-hexosaminidase secretion in rabbit lacrimal gland. 2006 Nov; (83) : 1081-1088

Arenas-Herrera JE, Ko IK, Atala A, Yoo JJ. **Biomed Mater** Decellularization for whole organ bioengineering. 2013 Feb; (8) : 014106

Atala A. **Curr Opin Biotechnol** Engineering organs. 2009 Oct; (20) : 575-592

Atala A, Bauer SB, Soker S, Yoo JJ, Retik AB. **Lancet** Tissue-engineered autologous bladders for patients needing cystoplasty. 2006 Apr 15; (367) : 1241-1246

Badylak SF. **Semin Cell Dev Biol** The extracellular matrix as a scaffold for tissue reconstruction. 2002 Oct; (13) : 377-383

Badylak SF, Taylor D, Uygun K. **Annu Rev Biomed Eng** Whole-organ tissue engineering: decellularization and recellularization of three-dimensional matrix scaffolds. 2011 Aug 15; (13) : 27-53

Balasubramanian S, Jasty S, Sitalakshmi G, Madhavan HN, Krishnakumar S. **Indian J Med Res** Influence of feeder layer on the expression of stem cell markers in cultured limbal corneal epithelial cells. 2008 Nov; (128) : 616-622

Banh A, Xiao N, Cao H, Chen CH, Kuo P, Krakow T, Bavan B, Khong B, Yao M, Ha C, Kaplan MJ, Sirjani D, Jensen K, Kong CS, Mochly-Rosen D, Koong AC, Le QT. **Clin Cancer Res** A novel aldehyde dehydrogenase-3 activator leads to adult salivary stem cell enrichment in vivo. 2011 Dec 1; (17) : 7265-7272

Becker JL, Prewett TL, Spaulding GF, Goodwin TJ. **J Cell Biochem** Three-dimensional growth and differentiation of ovarian tumor cell line in high aspect rotating-wall vessel: morphologic and embryologic considerations. 1993 Mar; (51) : 283-289

Bitar KN, Raghavan S. **Neurogastroenterol Motil** Intestinal tissue engineering: current concepts and future vision of regenerative medicine in the gut. 2012 Jan; (24) : 7-19

Black AF, Berthod F, L'heureux N, Germain L, Auger FA. **FASEB J** In vitro reconstruction of a human capillary-like network in a tissue-engineered skin equivalent. 1998 Oct; (12) : 1331-1340

Borrelli M, Schroder C, Dart JK, Collin JR, Sieg P, Cree IA, Matheson MA, Tiffany JM, Proctor G, van Best J, Hyde N, Geerling G. **Am J Ophthalmol** Long-term

follow-up after submandibular gland transplantation in severe dry eyes secondary to cicatrizing conjunctivitis. 2010 Dec; (150) : 894-904

Bourget JM, Gauvin R, Larouche D, Lavoie A, Labbe R, Auger FA, Germain L. **Biomaterials** Human fibroblast-derived ECM as a scaffold for vascular tissue engineering. 2012 Dec; (33) : 9205-9213

Breyer F, Felder S. **Health Policy** Life expectancy and health care expenditures: a new calculation for Germany using the costs of dying. 2006 Jan; (75) : 178-186

Chang NS. **Am J Physiol** Hyaluronidase enhancement of TNF-mediated cell death is reversed by TGF-beta 1. 1997 Dec; (273) : C1987-94

Chen F, Yoo JJ, Atala A. **World J Urol** Experimental and clinical experience using tissue regeneration for urethral reconstruction. 2000 Feb; (18) : 67-70

Chen L, Gong B, Wu Z, Jetton J, Chen R, Qu C. **Br J Ophthalmol** A new method using xenogeneicacellular dermal matrix in the reconstruction of lacrimal drainage. 2014 Nov; (98) : 1583-1587

Crapo PM, Gilbert TW, Badylak SF. **Biomaterials** An overview of tissue and whole organ decellularization processes. 2011 Apr; (32) : 3233-3243

Dehoux JP, Gianello P. **Front Biosci** The importance of large animal models in transplantation. 2007; (12) : 4864-4880

Doherty RE, Haywood-Small SL, Sisley K, Cross NA. **Biochem Biophys Res Commun** Aldehyde dehydrogenase activity selects for the holoclone phenotype in prostate cancer cells. 2011 Nov 4; (414) : 801-807

Drechsler CC, Kunze A, Kureshi A, Grobe G, Reichl S, Geerling G, Daniels JT, Schrader S. **J Tissue Eng Regen Med** Development of a conjunctival tissue substitute on the basis of plastic compressed collagen. 2015 Feb 10; :

El-Kassaby A, AbouShwareb T, Atala A. **J Urol** Randomized comparative study between buccal mucosal and acellular bladder matrix grafts in complex anterior urethral strictures. 2008 Apr; (179) : 1432-1436

El-Kassaby AW, Retik AB, Yoo JJ, Atala A. **J Urol** Urethral stricture repair with an off-the-shelf collagen matrix. 2003 Jan; (169) : 170-3; discussion 173

Erdogmus S, Govsa F. **J Craniofac Surg** Importance of the anatomic features of the lacrimal artery for orbital approaches. 2005 Nov; (16) : 957-964

Fijneman RJ, Anderson RA, Richards E, Liu J, Tijssen M, Meijer GA, Anderson J, Rod A, O'Sullivan MG, Scott PM, Cormier RT. **Cancer Sci** Runx1 is a tumor suppressor gene in the mouse gastrointestinal tract. 2012 Mar; (103) : 593-599

Fujii A, Morimoto-Tochigi A, Walkup RD, Shearer TR, Azuma M. **Invest Ophthalmol Vis Sci** Lacritin-induced secretion of tear proteins from cultured monkey lacrimal acinar cells. 2013 Apr; (54) : 2533-2540

Gattazzo F, Urciuolo A, Bonaldo P. **Biochim Biophys Acta** Extracellular matrix: A dynamic microenvironment for stem cell niche. 2014 Jan 10; :

Gayton JL. **Clin Ophthalmol** Etiology, prevalence, and treatment of dry eye disease. 2009; (3) : 405-412

Geerling G, Maclennan S, Hartwig D. **Br J Ophthalmol** Autologous serum eye drops for ocular surface disorders. 2004 Nov; (88) : 1467-1474

Golebiewska A, Brons NH, Bjerkvig R, Niclou SP. **Cell Stem Cell** Critical appraisal of the side population assay in stem cell and cancer stem cell research. 2011 Feb 4; (8) : 136-147

Greve B, Kelsch R, Spaniol K, Eich HT, Gotte M. **Cytometry A** Flow cytometry in cancer stem cell analysis and separation. 2012 Apr; (81) : 284-293

Groenen MA, Archibald AL, Uenishi H, Tuggle CK, Takeuchi Y, Rothschild MF, Rogel-Gaillard C, Park C, Milan D, Megens HJ, Li S, Larkin DM, Kim H, Frantz LA, Caccamo M, Ahn H, Aken BL, Anselmo A, Anthon C, Auvil L, Badaoui B, Beattie CW, Bendixen C, Berman D, Blecha F, Blomberg J, Bolund L, Bosse M, Botti S, Bujie Z, Bystrom M, Capitanu B, Carvalho-Silva D, Chardon P, Chen C, Cheng R, Choi SH, Chow W, Clark RC, Clee C, Crooijmans RP, Dawson HD, Dehais P, De Sapio F, Dibbits B, Drou N, Du ZQ, Eversole K, Fadista J, Fairley S, Faraut T, Faulkner GJ, Fowler KE, Fredholm M, Fritz E, Gilbert JG, Giuffra E, Gorodkin J, Griffin DK, Harrow JL, Hayward A, Howe K, Hu ZL, Humphray SJ, Hunt T, Hornshoj H, Jeon JT, Jern P, Jones M, Jurka J, Kanamori H, Kapetanovic R, Kim J, Kim JH, Kim KW, Kim TH, Larson G, Lee K, Lee KT, Leggett R, Lewin HA, Li Y, Liu W, Loveland JE, Lu Y, Lunney JK, Ma J, Madsen O, Mann K, Matthews L, McLaren S, Morozumi T, Murtaugh MP, Narayan J, Nguyen DT, Ni P, Oh SJ, Onteru S, Panitz F, Park EW, Park HS, Pascal G, Paudel Y, Perez-Enciso M, Ramirez-Gonzalez R, Reecy JM, Rodriguez-Zas S, Rohrer GA, Rund L, Sang Y, Schachtschneider K, Schraiber JG, Schwartz J, Scobie L, Scott C, Searle S, Servin B, Southey BR, Sperber G, Stadler P, Sweedler JV, Tafer H, Thomsen B, Wali R, Wang J, Wang J, White S, Xu X, Yerle M, Zhang G, Zhang J, Zhang J, Zhao S, Rogers J, Churcher C, Schook LB. **Nature** Analyses of pig genomes provide insight into porcine demography

and evolution. 2012 Nov 15; (491) : 393-398

Haagdorens M, Van Acker SI, Van Gerwen V, Ní Dhubhghaill S, Koppen C, Tassignon MJ, Zakaria N. **Stem Cells Int** Limbal Stem Cell Deficiency: Current Treatment Options and Emerging Therapies. 2016; (2016) : 9798374

Hann LE, Tatro JB, Sullivan DA. **Invest Ophthalmol Vis Sci** Morphology and function of lacrimal gland acinar cells in primary culture. 1989 Jan; (30) : 145-158

Henker R, Scholz M, Gaffling S, Asano N, Hampel U, Garreis F, Hornegger J, Paulsen F. **PLoS One** Morphological features of the porcine lacrimal gland and its compatibility for human lacrimal gland xenografting. 2013; (8) : e74046

Herrera MB, Bussolati B, Bruno S, Morando L, Mauriello-Romanazzi G, Sanavio F, Stamenkovic I, Biancone L, Camussi G. **Kidney Int** Exogenous mesenchymal stem cells localize to the kidney by means of CD44 following acute tubular injury. 2007 Aug; (72) : 430-441

Hirayama M, Ogawa M, Oshima M, Sekine Y, Ishida K, Yamashita K, Ikeda K, Shimmura S, Kawakita T, Tsubota K, Tsuji T. **Nat Commun** Functional lacrimal gland regeneration by transplantation of a bioengineered organ germ. 2013; (4) : 2497

Hunt S, Spitznas M, Seifert P, Rauwolf M. **Exp Eye Res** Organ culture of human main and accessory lacrimal glands and their secretory behaviour. 1996 May; (62) : 541-554

Jacobsen HC, Hakim SG, Lauer I, Dendorfer A, Wedel T, Sieg P. **J Craniomaxillofac Surg** Long-term results of autologous submandibular gland transfer for the surgical treatment of severe keratoconjunctivitis sicca. 2008 Jun; (36) : 227-233

Jayo MJ, Jain D, Ludlow JW, Payne R, Wagner BJ, McLorie G, Bertram TA. **Regen Med** Long-term durability, tissue regeneration and neo-organ growth during skeletal maturation with a neo-bladder augmentation construct. 2008 Sep; (3) : 671-682

Kibbey MC, Royce LS, Dym M, Baum BJ, Kleinman HK. **Exp Cell Res** Glandular-like morphogenesis of the human submandibular tumor cell line A253 on basement membrane components. 1992 Feb; (198) : 343-351

Kivela T. **J Histochem Cytochem** Antigenic profile of the human lacrimal gland. 1992 May; (40) : 629-642

Kleinman HK, Martin GR. **Semin Cancer Biol** Matrigel: basement membrane matrix with biological activity. 2005 Oct; (15) : 378-386

Kobayashi S, Kawakita T, Kawashima M, Okada N, Mishima K, Saito I, Ito M, Shimmura S, Tsubota K. **Mol Vis** Characterization of cultivated murine lacrimal gland epithelial cells. 2012; (18) : 1271-1277

Kretlow JD, Young S, Klouda L, Wong M, Mikos AG. **Adv Mater** Injectable biomaterials for regenerating complex craniofacial tissues. 2009 Sep 4; (21) : 3368-3393

Kroll J, Merte RL, Eter N. **Ophthalmologe** [Defect covering of a perforated corneal ulcer with bovine pericardium transplant]. 2014 Jan; (111) : 58-60

Kühnel W. **Zeitschrift für Zellforschung und Mikroskopische Anatomie** Comparative histological, histochemical and electron mecroscopic studies of lacrimal glands. VI. Human lacrimal gland 1968 (4) : 550-572

Kühnel W, Scheele G. **Anat Anz** Zur Feinstruktur der Glandula lacrimalis des Schweines (Sus scropha L.) 1979; (145) : 87-106

Kumar S, Hedges SB. **Nature** A molecular timescale for vertebrate evolution. 1998 Apr 30; (392) : 917-920

Kuwada SK, Li X. **Mol Biol Cell** Integrin alpha5/beta1 mediates fibronectin-dependent epithelial cell proliferation through epidermal growth factor receptor activation. 2000 Jul; (11) : 2485-2496

Kwon HR, Nelson DA, De Santis KA, Morrissey JM, Larsen M. **Development** Endothelial cell regulation of salivary gland epithelial patterning. 2017 Jan; (144) : 211-220

Linke K, Schanz J, Hansmann J, Walles T, Brunner H, Mertsching H. **Tissue Eng** Engineered liver-like tissue on a capillarized matrix for applied research. 2007 Nov; (13) : 2699-2707

Lombaert IM, Brunsting JF, Wierenga PK, Faber H, Stokman MA, Kok T, Visser WH, Kampinga HH, de Haan G, Coppes RP. **PLoS One** Rescue of salivary gland function after stem cell transplantation in irradiated glands. 2008; (3) : e2063

Ma I, Allan AL. **Stem Cell Rev** The role of human aldehyde dehydrogenase in normal and cancer stem cells. 2011 Jun; (7) : 292-306

Ma X, Shimmura S, Miyashita H, Yoshida S, Kubota M, Kawakita T, Tsubota K. **Invest Ophthalmol Vis Sci** Long-term culture and growth kinetics of murine corneal epithelial cells expanded from single corneas. 2009 Jun; (50) : 2716-

2721

Massie I, Spaniol K, Geerling G, Metzger M, Schrader S. **Association for Vision and Research (ARVO)** Formation of functionally competent 3D lacrimal gland cell spheroids - towards regeneration of lacrimal gland tissue. Conference abstract 2016 May

Maxson S, Lopez EA, Yoo D, Danilkovitch-Miagkova A, Leroux MA. **Stem Cells Transl Med** Concise review: role of mesenchymal stem cells in wound repair. 2012 Feb; (1) : 142-149

McDonald ML, Wang Y, Selvam S, Nakamura T, Chow RH, Schechter JE, Yiu SC, Mircheff AK. **Invest Ophthalmol Vis Sci** Cytopathology and exocrine dysfunction induced in ex vivo rabbit lacrimal gland acinar cell models by chronic exposure to histamine or serotonin. 2009 Jul; (50) : 3164-3175

Millar TJ, Herok G, Koutavas H, Martin DK, Anderton PJ. **Tissue Cell** Immunohistochemical and histochemical characterisation of epithelial cells of rabbit lacrimal glands in tissue sections and cell cultures. 1996 Jun; (28) : 301-312

Mishima K, Inoue H, Nishiyama T, Mabuchi Y, Amano Y, Ide F, Matsui M, Yamada H, Yamamoto G, Tanaka J, Yasuhara R, Sakurai T, Lee MC, Chiba K, Sumimoto H, Kawakami Y, Matsuzaki Y, Tsubota K, Saito I. **Stem Cells** Transplantation of side population cells restores the function of damaged exocrine glands through clusterin. 2012 Sep; (30) : 1925-1937

Moss SE, Klein R, Klein BE. **Arch Ophthalmol** Prevalence of and risk factors for dry eye syndrome. 2000 Sep; (118) : 1264-1268

Moza AK, Mertsching H, Herden T, Bader A, Haverich A. **J Thorac Cardiovasc Surg** Heart valves from pigs and the porcine endogenous retrovirus: experimental and clinical data to assess the probability of porcine endogenous retrovirus infection in human subjects. 2001 Apr; (121) : 697-701

Murphy SV, Atala A. **Bioessays** Organ engineering - combining stem cells, biomaterials, and bioreactors to produce bioengineered organs for transplantation. 2012 Sep 20; :

Nagata S, Hanayama R, Kawane K. **Cell** Autoimmunity and the clearance of dead cells. 2010 Mar 5; (140) : 619-630

Nakajima T, Walkup RD, Tochigi A, Shearer TR, Azuma M. **Exp Eye Res** Establishment of an appropriate animal model for lacritin studies: cloning and

characterization of lacritin in monkey eyes. 2007 Nov; (85) : 651-658

Nakao K, Morita R, Saji Y, Ishida K, Tomita Y, Ogawa M, Saitoh M, Tomooka Y, Tsuji T. **Nat Methods** The development of a bioengineered organ germ method. 2007 Mar; (4) : 227-230

Obata H. **Cornea** Anatomy and histopathology of the human lacrimal gland. 2006 Dec; (25) : S82-9

Paulsson M. **Crit Rev Biochem Mol Biol** Basement membrane proteins: structure, assembly, and cellular interactions. 1992; (27) : 93-127

Perry HD. **Am J Manag Care** Dry eye disease: pathophysiology, classification, and diagnosis. 2008 Apr; (14) : S79-87

Pflugfelder SC, Jones D, Ji Z, Afonso A, Monroy D. **Curr Eye Res** Altered cytokine balance in the tear fluid and conjunctiva of patients with Sjogren's syndrome keratoconjunctivitis sicca. 1999 Sep; (19) : 201-211

Priya SG, Jungvid H, Kumar A. **Tissue Eng Part B Rev** Skin tissue engineering for tissue repair and regeneration. 2008 Mar; (14) : 105-118

Radisic M, Christman KL. **Mayo Clin Proc** Materials science and tissue engineering: repairing the heart. 2013 Aug; (88) : 884-898

Rahman S, Patel Y, Murray J, Patel KV, Sumathipala R, Sobel M, Wijelath ES. **BMC Cell Biol** Novel hepatocyte growth factor (HGF) binding domains on fibronectin and vitronectin coordinate a distinct and amplified Met-integrin induced signalling pathway in endothelial cells. 2005; (6) : 8

Raven PW, McCredie E, McAuley M, Vinson GP. **Cell Biochem Funct** Origins of the differences in function of rat adrenal zona glomerulosa cells incubated as intact tissue and as collagenase-prepared cell suspensions. 1983 Apr; (1) : 17-24

Raya-Rivera A, Esquiliano DR, Yoo JJ, Lopez-Bayghen E, Soker S, Atala A. **Lancet** Tissue-engineered autologous urethras for patients who need reconstruction: an observational study. 2011 Apr 2; (377) : 1175-1182

Roth M, Spaniol K, Kordes C, Schwarz S, Mertsch S, Häussinger D, Rotter N, Geerling G, Schrader S. **Invest Ophthalmol Vis Sci** The Influence of Oxygen on the Proliferative Capacity and Differentiation Potential of Lacrimal Gland-Derived Mesenchymal Stem Cells. 2015 Jul; (56) : 4741-4752

Schaumberg DA, Dana R, Buring JE, Sullivan DA. **Arch Ophthalmol** Prevalence of dry eye disease among US men: estimates from the Physicians' Health Studies. 2009 Jun; (127) : 763-768

Schaumberg DA, Sullivan DA, Buring JE, Dana MR. **Am J Ophthalmol** Prevalence of dry eye syndrome among US women. 2003 Aug; (136) : 318-326

Schechter J, Stevenson D, Chang D, Chang N, Pidgeon M, Nakamura T, Okamoto CT, Trousdale MD, Mircheff AK. **Exp Eye Res** Growth of purified lacrimal acinar cells in Matrigel raft cultures. 2002 Mar; (74) : 349-360

Schechter JE, Warren DW, Mircheff AK. **Ocul Surf** A lacrimal gland is a lacrimal gland, but rodent's and rabbit's are not human. 2010 Jul; (8) : 111-134

Schonthal AH, Warren DW, Stevenson D, Schecter JE, Azzarolo AM, Mircheff AK, Trousdale MD. **Exp Eye Res** Proliferation of lacrimal gland acinar cells in primary culture. Stimulation by extracellular matrix, EGF, and DHT. 2000 May; (70) : 639-649

Schrader S, Kremling C, Klinger M, Laqua H, Geerling G. **Br J Ophthalmol** Cultivation of lacrimal gland acinar cells in a microgravity environment. 2009 Aug; (93) : 1121-1125

Schrader S, Liu L, Kasper K, Geerling G. **Dev Ophthalmol** Generation of two- and three-dimensional lacrimal gland constructs. 2010; (45) : 49-56

Schrader S, Notara M, Beaconsfield M, Tuft D, Geerling G, Daniels JT. **Regen Med** Conjunctival epithelial cells maintain stem cell properties after long-term culture and cryopreservation. 2009 Sep; (4) : 677-87

Schrader S, Notara M, Tuft D, Beaconsfield M, Geerling G, Daniels JT. **Regen Med** Simulation of an in vitro niche environment that preserves conjunctival progenitor cells. 2010 Nov; (5) : 877-89

Schrader S, Wedel T, Kremling C, Laqua H, Geerling G. **Graefes Arch Clin Exp Ophthalmol** Amniotic membrane as a carrier for lacrimal gland acinar cells. 2007 Nov; (245) : 1699-1704

Selver OB, Barash A, Ahmed M, Wolosin JM. **Invest Ophthalmol Vis Sci** ABCG2-dependent dye exclusion activity and clonal potential in epithelial cells continuously growing for 1 month from limbal explants. 2011 Jun; (52) : 4330-4337

Shatos MA, Haugaard-Kedstrom L, Hodges RR, Dartt DA. **Invest Ophthalmol Vis Sci** Isolation and characterization of progenitor cells in uninjured, adult rat lacrimal gland. 2012 May; (53) : 2749-2759

Silverman WF, Krum JM, Mani N, Rosenstein JM. **Neuroscience** Vascular, glial and neuronal effects of vascular endothelial growth factor in mesencephalic explant

cultures. 1999; (90) : 1529-1541

Singh K, Masuda K, Thonar EJ, An HS, Cs-Szabo G. **Spine (Phila Pa 1976)** Age-related changes in the extracellular matrix of nucleus pulposus and anulus fibrosus of human intervertebral disc. 2009 Jan 1; (34) : 10-16

Spaniol K, Metzger M, Roth M, Greve B, Mertsch S, Geerling G, Schrader S. **Tissue Eng Part A** Engineering of a Secretory Active Three-Dimensional Lacrimal Gland Construct on the Basis of Decellularized Lacrimal Gland Tissue. 2015 Oct; (21) : 2605-2617

Tasman W, Jaeger EA (lww.com) **Duane's Ophthalmology** on DVD-ROM 2010 Edition 2010; Chapter 21.

Tiwari S, Ali MJ, Balla MM, Naik MN, Honavar SG, Reddy VA, Vemuganti GK. **PLoS One** Establishing human lacrimal gland cultures with secretory function. 2012; (7) : e29458

Tsai RJ, Li LM, Chen JK. **N Engl J Med** Reconstruction of damaged corneas by transplantation of autologous limbal epithelial cells. 2000 Jul 13; (343) : 86-93

Turley EA. **Differentiation** The control of adrenocortical cytodifferentiation by extracellular matrix. 1980; (17) : 93-103

Ueda Y, Karasawa Y, Satoh Y, Nishikawa S, Imaki J, Ito M. **Invest Ophthalmol Vis Sci** Purification and characterization of mouse lacrimal gland epithelial cells and reconstruction of an acinarlike structure in three-dimensional culture. 2009 May; (50) : 1978-1987

van Rijn LJ, van De Ven SJ, Krijnen JS, Jansen SM, Bakels AJ, Langenhorst AM. **Eur J Ophthalmol** Tendon elongation with bovine pericardium (Tutopatch(R)) when conventional strabismus surgery is not possible. 2016 Apr 12; (26) : 193-202

Voronov D, Gromova A, Liu D, Zoukhri D, Medvinsky A, Meech R, Makarenkova HP. **Invest Ophthalmol Vis Sci** Transcription factors Runx1 to 3 are expressed in the lacrimal gland epithelium and are involved in regulation of gland morphogenesis and regeneration. 2013 May; (54) : 3115-3125

Walters EM, Wolf E, Whyte JJ, Mao J, Renner S, Nagashima H, Kobayashi E, Zhao J, Wells KD, Critser JK, Riley LK, Prather RS. **BMC Med Genomics** Completion of the swine genome will simplify the production of swine as a large animal biomedical model. 2012; (5) : 55

Wilson PD, Dillingham MA, Breckon R, Anderson RJ (Am J Physiol) Defined human

renal tubular epithelia in culture: growth, characterization, and hormonal response. 1985 Mar; (248) : F436-43

Wu K, Jerdeva GV, da Costa SR, Sou E, Schechter JE, Hamm-Alvarez SF. **Exp Eye Res** Molecular mechanisms of lacrimal acinar secretory vesicle exocytosis. 2006 Jul; (83) : 84-96

Yamada KM, Olden K. **Nature** Fibronectins--adhesive glycoproteins of cell surface and blood. 1978 Sep 21; (275) : 179-184

Yoshino K. **Cornea** Establishment of a human lacrimal gland epithelial culture system with in vivo mimicry and its substrate modulation. 2000 May; (19) : S26-36

Yoshino K, Tseng SC, Pflugfelder SC. **Exp Cell Res** Substrate modulation of morphology, growth, and tear protein production by cultured human lacrimal gland epithelial cells. 1995 Sep; (220) : 138-151

You S, Kublin CL, Avidan O, Miyasaki D, Zoukhri D. **Invest Ophthalmol Vis Sci** Isolation and propagation of mesenchymal stem cells from the lacrimal gland. 2011 Apr; (52) : 2087-2094

Yurchenco PD. **Cold Spring Harb Perspect Biol** Basement membranes: cell scaffoldings and signaling platforms. 2011 Feb; (3) : 1-27

Zhang Y, McNeill E, Tian H, Soker S, Andersson KE, Yoo JJ, Atala A. **J Urol** Urine derived cells are a potential source for urological tissue reconstruction. 2008 Nov; (180) : 2226-2233

Zhu J, Clark RA. **J Invest Dermatol** Fibronectin at select sites binds multiple growth factors and enhances their activity: expansion of the collaborative ECM-GF paradigm. 2014 Apr; (134) : 895-901

Zoukhri D. **Ocul Surf** Mechanisms involved in injury and repair of the murine lacrimal gland: role of programmed cell death and mesenchymal stem cells. 2010 Apr; (8) : 60-69

Zoukhri D, Fix A, Alroy J, Kublin CL. **Invest Ophthalmol Vis Sci** Mechanisms of murine lacrimal gland repair after experimentally induced inflammation. 2008 Oct; (49) : 4399-4406

6.3 Declaration

Teile der Dissertationsarbeit mit dem Titel „Bio-engineering of porcine lacrimal gland tissue with secretory capacity" von Frau Dr. med. Kristina Spaniol wurden von der Autorin in der wissenschaftlichen Fachzeitschrift "Tissue Engineering Part A" unter dem Titel "Engineering of a Secretory Active Three-Dimensional Lacrimal Gland Construct on the Basis of Decellularized Lacrimal Gland Tissue" publiziert (1). Die Autorin hat hierbei die erforderlichen Gewebe (Tränendrüsen des Schweines) gewonnen und die Experimente sowie deren Dokumentation und Auswertung selbständig oder in Zusammenarbeit mit den Ko-Autoren durchgeführt. Frau Spaniol hat das Manuskript verfasst, als korrespondierende Autorin fungiert und die Revisionsarbeiten an dem Manuskript unter Mitwirkung der Ko-Autoren erstellt. Folgende Experimente wurden von anderen Personen oder in Zusammenarbeit mit diesen Personen durchgeführt:

- Gewebeschnitte für elektronenmikroskopische Aufnahmen und die elektronenmikroskopischen Aufnahmen wurden im Institut für Anatomie I der Heinrich-Heine-Universität Düsseldorf durch Herrn Dr. med. K. Zanger und Frau E. Wesbuer angefertigt.
- durchflusszytometrische Experimente erfolgten selbstständig durch die Autorin unter Anleitung von Herrn Dr. rer. nat. B. Greve, Westfälische Wilhems-Universität Münster.
- Proteinnachweise wurden in Zusammenarbeit mit Frau Dr. rer. nat. S. Mertsch, ehemals Westfälische Wilhems-Universität Münster, jetzt Heinrich-Heine-Universität Düsseldorf, durchgeführt.

Insgesamt hat die Autorin somit den hauptsächlichen Teil der Publikation eigenständig erbracht. Ich, Prof. G. Geerling, bestätige, dass diese Angaben korrekt sind.

Düsseldorf, den

Prof. Dr. med. G. Geerling
Direktor der Augenklinik

Referenz

1) Spaniol K, Metzger M, Roth M, Greve B, Mertsch S, Geerling G, Schrader S. **Tissue Eng Part A** Engineering of a Secretory Active Three-Dimensional Lacrimal Gland Construct on the Basis of Decellularized Lacrimal Gland Tissue. 2015 Oct; (21) : 2605-2617